

Tomislav Cernava BSc

Identification of volatile organic compounds from plant-associated bacteria

Master thesis

A thesis submitted in partial fulfillment of the requirements
for the degree of Master of Science (MSc)
in „Biochemie und Molekulare Biomedizin“



Institute of Environmental Biotechnology
Graz University of Technology

Supervisor: Univ.-Prof. Dipl.-Biol. Dr.rer.nat. Gabriele Berg

March 2012

EIDESSTATTLICHE ERKLÄRUNG

Ich erkläre an Eides statt, dass ich die vorliegende Arbeit selbstständig verfasst, andere als die angegebenen Quellen/Hilfsmittel nicht benutzt, und die den benutzten Quellen wörtlich und inhaltlich entnommene Stellen als solche kenntlich gemacht habe.

Graz, am
.....
(Unterschrift)

STATUTORY DECLARATION

I declare that I have authored this thesis independently, that I have not used other than the declared sources / resources, and that I have explicitly marked all material which has been quoted either literally or by content from the used sources.

.....
date

.....
(signature)

Acknowledgement

First of all I want to thank my supervisor Univ.-Prof. Dipl.-Biol. Dr.rer.nat. Gabriele Berg, she allowed me to get insight into fascinating fields of environmental biotechnology, molecular biology and microbial diversity. Furthermore I want to thank her for the provided intellectual support during all steps of my Master thesis.

I am also very thankful to my co-supervisor Univ.-Prof. Dr.rer.nat. Rudolf Bauer from the Institute of Pharmaceutical Sciences. He provided me help in general analytical questions and specific question regarding GC-MS techniques.

I am grateful for the excellent support from Dr. Stefan Liebming. It was both, an inspiring and successful project.

Dr. Massimiliano Cardinale helped me with the CLSM and gave me advises for statistical analysis. I want to express my gratitude for this.

The working atmosphere at the institute was always brilliant. Therefore I want to thank DI Armin Erlacher for his encouragement in many situations, Martina Köberl MSc for her Egyptian isolates, Mag. Michael Fürnkranz for his oil pumpkin isolates and the whole Institute of Environmental Biotechnology for the great time.

Special thanks go to the RCPE and the industrial partners Ortner and Dastex for enabling the outstanding project.

Finally I want to thank my parents for the awesome support they offered me during my whole studies and especially during my Master thesis.



Abstract

Plant-associated microorganisms with antagonistic properties towards pathogens provide a rich source for biocontrol agents, which can be used for sustainable plant protection. In the context of this Master thesis, we demonstrated that some of those plant-associated microorganisms have also remarkable antagonistic potential against opportunistic human pathogens targeting bacterial as well as fungal species. The concept of naturally occurring antagonists to control plant pathogens was transferred to human pathogens. Possible applications were found in clean rooms and clinical environments. Our focus lies on volatile organic compounds (VOCs), which are produced by bacterial antagonists and inhibit the growth of human pathogens, e.g. MRSA (methicillin-resistant *Staphylococcus aureus*), *Stenotrophomonas maltophilia* and *Pseudomonas aeruginosa*. GC-MS headspace SPME analysis allowed a specific identification of several antimicrobial VOCs of various bacterial plant-associated species, e.g. *Pseudomonas* and *Paenibacillus* strains. The volatiles of *Pseudomonas chlororaphis* consist of different unspecific toxic sulfuric compounds like methanethiol and dimethyldisulfide as well as 1-undecene. In contrast, *Paenibacillus polymyxa* isolates secreted distinctive amounts of different specific pyrazines into the gas phase. Additionally we could prove that certain synthetic pyrazines show inhibitory effects towards Gram-negative pathogenic bacteria as well as fungal species.

Kurzfassung

Pflanzen-assoziierte Mikroorganismen mit antagonistischer Aktivität gegenüber Pathogenen stellen eine wichtige Quelle für die biologische Kontrolle im nachhaltigen Pflanzenschutz dar. Im Rahmen dieser Masterarbeit konnten wir zeigen, dass einige dieser Pflanzen-assoziierten Mikroorganismen gleichzeitig eine beachtliche antagonistische Wirkung gegenüber opportunistischen Humanpathogenen haben, wobei sowohl bakterielle als auch fungale Pathogene betroffen sind. In der Arbeit wurde das Prinzip der natürlich vorkommenden und zum Schutz vor Pflanzenpathogenen eingesetzten Antagonisten auf Humanpathogene übertragen. Mögliche Anwendungen dieser Antagonisten könnte man unter anderem im klinischen Bereich sowie in Reinräumen finden. Der Schwerpunkt wurde auf flüchtige organische Verbindungen (VOCs) gesetzt, die von bakteriellen Antagonisten produziert werden und Humanpathogene wie MRSA (Methicillin-resistenter *Staphylococcus aureus*), *Stenotrophomonas maltophilia*, und *Pseudomonas aeruginosa* inhibieren konnten. Eine durchgeführte Analyse mittels GC-MS headspace SPME ermöglichte die Identifizierung unterschiedlicher antimikrobieller VOCs, die von verschiedenen Pflanzen-assoziierten Bakterien wie zum Beispiel *Pseudomonas* und *Paenibacillus* Stämmen sekretiert werden. Verschiedene flüchtige toxische Schwefelverbindungen wie Methanethiol und Dimethyldisulfid konnten im Fall von *Pseudomonas chlororaphis* nachgewiesen werden, aber auch 1-Undecen. Im Gegensatz dazu ließen *Paenibacillus polymyxa* Stämme darauf schließen, dass sie bestimmte Pyrazinverbindungen in charakteristischen Ausmaßen in den Gasraum sekretieren. Zusätzlich konnten wir zeigen, dass auch bestimmte synthetische Pyrazine eine inhibitorische Wirkung gegenüber bestimmten gramnegativen Bakterien und fungalen Spezies aufweisen.

List of contents

1 Introduction.....	1
1.1 Innovative concepts for clean room technology	1
1.2 Plant-associated bacteria and biocontrol of pathogens.....	2
1.2.1 <i>Pseudomonas chlororaphis</i>	3
1.2.2 <i>Paenibacillus polymyxa</i>	3
1.2.3 <i>Lysobacter</i> spp.	4
1.2.4 Volatile organic compounds (VOCs) and bacteria.....	5
1.2.5 Specific bacterial metabolites	5
1.3 Human-associated opportunistic pathogens	7
1.4 Objectives	8
2 Material and Methods	10
2.1 Material	10
2.1.1 Manufacturing certificate	10
2.1.2 Nutrient media.....	10
2.1.3 Chemicals	12
2.1.4 Pathogen model organisms	13
2.1.5 Antagonistic bacteria strains	13
2.1.6 Clean room textiles.....	14
2.1.7 Confocal laser-scanning microscopy (CLSM)	15
2.1.8 LIVE/DEAD® Bacterial Viability Kit (BacLight™)	15
2.1.9 EZ-Tn5™ <KAN-2>Tnp Transposome™ Kit.....	16
2.1.10 Gas chromatography–mass spectrometry.....	17
2.2 Methods	18
2.2.1 VOCs dual-culture test.....	18
2.2.2 Standard high-throughput VOCs assay	19

2.2.3 High-throughput VOCs assay for weak antagonists	19
2.2.4 High-throughput VOCs assay for synthetic compounds.....	20
2.2.5 Modified high-throughput VOCs assay.....	20
2.2.3 Microbial viability test	21
2.2.4 GC-MS analysis of bacterial VOCs.....	21
2.2.5 GC-MS analysis of co-cultivated bacteria.....	22
2.2.4 GC-MS analysis of synthetic VOCs	23
2.2.5 Preparation of electrocompetent <i>Pseudomonas chlororaphis</i> cells.....	24
2.2.6 Electroporation of electrocompetent <i>Pseudomonas chlororaphis</i> cells	24
2.2.7 Statistical analysis	25
3 Results.....	26
3.1 Supplemental VOCs dual-culture tests	26
3.1.1 Utilization of different textiles	26
3.1.2 VOCs dual-culture tests with <i>C. albicans</i>	27
3.1.3 VOCs dual-culture tests with <i>P. aeruginosa</i>	29
3.1.4 VOCs dual-culture tests with <i>S. aureus</i>	31
3.1.5 VOCs dual-culture tests with <i>S. epidermidis</i>	33
3.1.6 VOCs dual-culture tests with <i>S. maltophilia</i>	35
3.1.7 Time-dependent VOCs dual-culture tests.....	37
3.2 High-throughput VOCs assays	41
3.2.1 <i>Pseudomonas chlororaphis</i> strains.....	41
3.2.2 <i>Paenibacillus polymyxa</i> strains.....	44
3.2.3 Synthetic pyrazines I	47
3.2.4 Synthetic pyrazines II	51
3.3 GC-MS identification and characterization of bacterial VOCs	53
3.3.1 Comparison of different GC-MS headspace SPME fibers and methods	53
3.3.2 Identification of VOCs originating from LB-agar and GC-column	55
3.3.3 Identification of VOCs from <i>Pseudomonas chlororaphis</i> strains.....	56

3.3.4 Identification of VOCs from <i>Paenibacillus polymyxa</i> strains.....	58
3.3.5 Comparison of pyrazine production between different <i>Paenibacillus spp.</i>	61
3.3.6 GC-MS quantification of volatile pyrazines.....	62
3.3.7 Co-cultivation experiments with <i>Paenibacillus polymyxa</i> GnDWu39	63
3.4 Random mutagenesis of <i>Pseudomonas chlororaphis</i> P28.....	64
4 Discussion	66
4.1 First evaluation of antagonistic efficacy in CLSM approaches	66
4.2 Re-evaluation of antagonistic activity.....	67
4.3 Identification of novel bacteria-derived VOCs.....	67
4.4 Antimicrobial effects of synthetic pyrazines	69
4.5 High efficiency <i>Pseudomonas chlororaphis</i> P28 mutation	69
5 Conclusions	70
6 References	71
7 List of abbreviations	80
8 List of figures	82
9 List of tables.....	88

1 Introduction

1.1 Innovative concepts for clean room technology

Modern clean rooms and clinical environments have to deal with a rising emergence of highly resistant microbial inhabitants. Bacterial communities which can be found in e.g. spacecraft assembly facilities harbor amongst others extremophilic and extremotolerant species. These bacteria could colonize extraterrestrial sites and are considered as a risk factor therefore (La Duc et al., 2007). Air filtration can decrease the amount of pathogens entering such areas, but they still cannot be avoided completely (Boswell and Fox, 2006). The importance to remove opportunistic pathogens from clinical environments is illustrated by the fact that nowadays infections at surgical-sites are the most common complications after surgery. However it is not fully clarified if most pathogens that cause such complications originate from natural skin-flora of patients and medical personnel or if airborne pathogens also play an important role. Therefore different clean room industry standards are transferred continuously to hospitals and the effects are observed (Daran and Pittet 2002). During a 6-year study covering 173 intensive care units and 155,358 patients in Latin America, Asia, Africa, and Europe the incidence of distinctive nosocomial infections was documented. Device-associated infections (central venous and urinary tract catheters) were observed in 13.9 cases per 1000 catheter-days, while ventilator-associated pneumonia accounted for 13.6 infections in 1000 ventilator-days. The frequencies for resistant microbes were between 46.3% for *Acinetobacter baumannii* and 84.1% for MRSA (Rosenthal et al., 2010). Although those microorganisms can be fought with various chemical substances and irradiation, little is known about biological control of these inhabitants. Uprising resistance against applied antimicrobial substances e.g. silver (reviewed in Percival et al., 2005) and conventional antibiotics (Barbosa and Levy, 2000) requires advanced strategies to control unwanted inhabitants.

Transferring the observed effects of plant-associated antagonists to such areas could open alternative doors to novel approaches in clean room and clinical

environments. Whole cell systems could be implemented into artificial environments to control microbial communities by reducing the fraction of resistant microbes. Assuming that plant-associated antagonists would colonize such areas, a competition for nutrition and space would be a natural progression. Another non-cultivation dependent strategy involves the implementation of purified bacterial metabolites e.g. VOCs. However these VOCs need to be identified and evaluated regarding their efficacy and their safe application in new environments. Dual-culture tests (Liebminger et al., 2011) together with GC-MS headspace SPME analysis (Verginer et al., 2010) are practical tools for a first pre-screening attempt of different isolates.

1.2 Plant-associated bacteria and biocontrol of pathogens

Biocontrol using plant-associated bacteria is an innovative concept with several benefits, e.g. the reduction of chemical pesticides in agriculture or specific inhibition of phytopathogenic organisms. Plant growth can be stimulated by certain bacteria directly due to increased hormonal levels and improved nutrient acquisition. Plant health on the other hand is enhanced by various indirect mechanisms. Antagonistic potential of plant pathogens can be carried out through toxins and biosurfactants, competition for nutrients and colonization sites and also by diffusible antibiotics and volatile organic compounds (VOCs; reviewed in Berg, 2009). Bacteria-derived VOCs can carry out both, stimulating and inhibiting effects on plant pathogens. These interactions were demonstrated with a wide range of soil bacteria and fungi (Wheatley, 2002). Further acyl-homoserine lactones were identified as common quorum-sensing molecules of Gram-negative plant-associated bacteria which can regulate population density and other colonization factors (Cha et al., 1998). Pierson et al. (1998) suggested that acyl-homoserine lactones also play a role in the bacterial interaction with the eukaryotic host. Plant associated bacteria can receive signals from the host plant by expressing specific receptors that interact with small plant-produced molecules. Changes in the bacterial gene expression can result in higher nitrogen fixation which has positive effects on the host plant. *In vitro* experiments with beneficial plant-associated isolates can be utilized to prove their antagonistic effect against various soil-borne pathogens (Fürnkranz et al., 2011), as well as field experiments (Johnsson et al.,

1998). Positive effects of Gram-positive plant-associated bacteria have been observed with *Bacillus* and *Streptomyces* species. Their ability of spore formation allows an easier application in biocontrol attempts due to their enhanced resistance during formulation (reviewed in Emmert and Handelsman, 1999). However plant-associated bacteria always need an extensive evaluation before a biocontrol attempt can be considered. *Stenotrophomonas maltophilia* can cause serious diseases in immunocompromised patients. Despite this bias, specific strains were implemented in different biotechnological fields like biocontrol of plant-associated pathogens and bioremediation (Berg et al., 1999).

1.2.1 *Pseudomonas chlororaphis*

Pseudomonas chlororaphis is a well-studied Gram-negative bacterium that was already successfully introduced into large scale biocontrol applications (Johnsson et al., 1998; Weller et al., 2007). Colonization patterns were studied on seeds to identify the most efficient application method. The results with a gfp-tagged *Pseudomonas chlororaphis* MA 342 strain proved epiphytic plant colonization (Tombolini et al., 1999). Endophytic *Pseudomonas chlororaphis* strains were isolated from the Styrian oil pumpkin (Fürnkranz et al., 2011). These and several other strains found in different screening assays showed high antifungal activity (Fürnkranz et al., 2011; Thomas F. C. Chin-A-Woeng et al., 1998) but also remarkable antibacterial properties (Fürnkranz et al., 2011; Liebming et al., 2011). The main advantage of this bacterium is a broad spectrum of affected pathogens which makes it a promising agent in biological control (Johnsson et al., 1998). Phenazines and phloroglucinols produced by *Pseudomonas* spp. in volatile/diffusible form are responsible for the observed antifungal activity (Haas and Keel, 2003; Chin-A-Woeng et al., 2003), while less is known about the antibacterial activity of volatile metabolites. However many of the newly discovered strains need further evaluation to find their way into large scale applications.

1.2.2 *Paenibacillus polymyxa*

The Gram-positive genus *Paenibacillus* contains very interesting species. *Paenibacillus vortex* exhibits a complex colonization behavior when plated out on

agar plates with differing nutrient concentrations. The swarming motility was described as flagellum-driven social form of surface locomotion by Sirota-Madi et al. (2010). Other *Paenibacillus* species showed to have an impact on fruit flavor of grapes cultivated on different vineyards in Austria (Verginer et al., 2010). *Paenibacillus polymyxa* presents the most interesting species for biological control agents. Different endophytic isolates from the Styrian oil pumpkin inhibited fungal and bacterial pathogens associated with different pumpkin diseases (Fürnkranz et al., 2011). Mageshwaran et al. (2010) proved that metabolite extracts of plant-associated *Paenibacillus polymyxa* HKA-15 could inhibit the growth of different plant pathogens. They suggested a peptide-based inhibition of bacteria which was lost after pepsin treatment of the extract. Colistin A and B were identified as inhibitors of Gram-negative bacteria (Naghmouchi et al., 2011), while lipopeptides and polyketides carry out the antifungal activity (Niu et al., 2011). Moreover volatiles originating from *Paenibacillus* spp. inhibited growth of different soil-borne plant pathogens (Wei-wei et al., 2008; Li-jing et al., 2011). Those pathogens include in the first instance fungal species, while little is known about effects on bacterial species. A complex mixture of pyrazine metabolites was found in the polymyxin biosynthesis of *Paenibacillus polymyxa*. However the function of these metabolites is not fully resolved although it is known that pyrazines are involved in bactericidal and chemoprotective activities (Beck et al., 2003).

1.2.3 *Lysobacter* spp.

Lysobacter species are ubiquitous Gram-negative plant-associated bacteria and a dominant component of the plant microbiome (Hayward et al., 2009). They are able to produce biofilms which influence both, the host plant and other colonizing microbial species (reviewed in Danhorn and Fuqua, 2007). Biocontrol attempts with rice showed that *Lysobacter antibioticus* strains can significantly decrease plant diseases caused by bacterial pathogens. Further, pathogen suppression was observed with cell free supernatants of liquid cultures, suggesting that antibacterial substances are secreted into the media during cultivation (Ji et al., 2008). Other greenhouse experiments with wheat and cucumber plants showed that *Lysobacter enzymogenes* strains can inhibit fungal pathogens causing destructive diseases. The severity of observable infestation was reduced drastically after application of

the antagonist (Jochum et al., 2006; Postma et al., 2009). Endophytic *Lysobacter* spp. reduced the growth of different bacterial pathogens in VOCs dual-culture tests (Liebminger et al., 2011). These observations make *Lysobacter* spp. an even more considerable agent for biological control.

1.2.4 Volatile organic compounds (VOCs) and bacteria

VOCs are defined as organic compounds that have a boiling point ≤ 100 °C and/or a vapor pressure >1 mm Hg at 25 °C (Golfinopoulos et al., 2001). They can originate from natural products (Radovic et al., 2001) but also from artificial products like fuels, solvents, paints, adhesives, deodorants and refrigerants (Golfinopoulos et al., 2001). Qualitative and quantitative analysis can be done using headspace solid phase micro extraction and gas chromatography coupled with mass-spectrometry (Zhang and Pawliszyn, 1993). Different bacterial and yeast species were identified as efficient VOCs producers. While some of them contribute to food flavoring (Verginer et al., 2010) others showed remarkable antifungal effects towards various plant-associated pathogens (Fernando et al., 2005). Kai et al. (2006) observed that various bacterial-emitted VOCs could reduce the growth of *Rhizoctonia solani* significantly. Furthermore they could identify different substances e.g. benzyl nitrile, dimethyl trisulfide, undecene and benzyloxybenzotrile produced by these antagonists with a specifically designed GC-MS method.

1.2.5 Specific bacterial metabolites

Pyrazines are heterocyclic aromatic compounds with variable side chains on the four carbon atoms. Often one or more of these positions are occupied with a hydrogen atom, while the other positions can be substituted with alkyl, carboxyl and other groups. Common pyrazine structures are fluid at room temperature. Nevertheless an undefined fraction can be detected in the gas phase simultaneously with analytical methods e.g. GC-MS headspace SPME analysis. Different naturally occurring pyrazines were found in plants (Murray et al., 1970; Zhang et al., 2003), lower eukaryotes (Larsen et al., 1995) and also in bacteria (Beck et al., 2003; Schulz et al., 2007). Alkylpyrazines are produced by insects as

a compound of defensive sprays (Dossey et al., 2009) or ant trail pheromones (Cross et al., 1979). The metabolism of pyrazines is not entirely explored. Earlier studies could find indicators that the bacterial biosynthesis of alkyl-substituted pyrazines undergoes an amino acid amidation, followed by a condensation reaction where the ring structure is formed (1965; Murray et al., 1970; Cheng et al., 1991). Demain et al. (1967) could limit the biosynthetically utilized amino acids to valine, leucine and isoleucine without losing the ability of a *Corneibacterium glutamicum* mutant to produce distinctive pyrazines. The latest studies used deletion mutants and distinctive isotopes to get a deeper insight into the biosynthetic pathways. Branched amino acids and acetoin as early precursor of the pyrazine synthesis were essential in the case of *Corneibacterium glutanicum* (Dickschat et al., 2010). Pyrazines can also be synthetically produced by utilizing different substrates and catalysts (Masuda and Mihara, 1986; Anand et al., 2002). Furthermore pyrazines can be found in different foods, where they contribute to nutty, roasted cocoa and popcorn-like aromas (Burdock et al., 2008; Adams et al. 2002). A FDA evaluation of pyrazines has shown that specified derivatives are consumed together with food in μg range (Adams et al., 2002). This is an indicator that various pyrazines are harmless in low dose consumption. There is evidence that different pyrazine complexes with structural metal ions (Yesilel et al., 2010) and also more distant substances like phenazines (Raio et al., 2011) show antimicrobial effects. Furthermore antagonistic effects against soil-borne plant pathogens were observed with different *Bacillus* sp. and *Paenibacillus* sp. (Weiwei et al., 2008) which are known to produce different pyrazines (Beck et al., 2003). However there is no data available describing the effect of volatile pyrazines on human associated opportunistic pathogens.

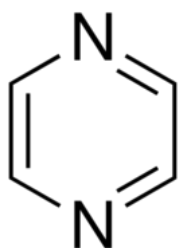


Figure 1.1 – Pyrazine compounds always contain a heterocyclic aromatic ring as main building block. The four carbon atoms can be substituted with a great variety of side chains. Source: www.sigmaaldrich.com

1.3 Human-associated opportunistic pathogens

An opportunistic pathogen is defined as an organism that is capable of causing disease only when the host's resistance is lowered, by other diseases or drugs (www.medilexicon.com, February 2012). Infections are often followed by a sepsis with a high mortality rate. Adequate antibiotic therapy of infected patients is an essential approach in such cases (MacArthur et al., 2003). Uprising occurrence of resistant microbes was observed in the last decades. The first European isolate of methicillin-resistant *Staphylococcus aureus* (MRSA) was detected in 1960. MRSA has become one of the leading causes for nosocomial infections worldwide. A high number of virulence factors and the ability to survive in a wide range of environments contribute to a notable assertion in hospitals (reviewed in Oliveira et al., 2003). The persistence of staphylococci is assisted by the ability to form biofilms on native tissues and biomaterials e.g. catheters (Götz, 2002). Antibiotic-resistant *Staphylococcus epidermidis* can cause life-threatening bloodstream infections after colonization of intravascular devices (Christensen et al., 1982). The list of common opportunistic pathogens is supplemented by Gram-negative bacteria with increasing resistance against cephalosporins and penicillins (Burwen et al., 1993). Resistant strains of *Klebsiella pneumoniae*, *Pseudomonas aeruginosa* and *Stenotrophomonas maltophilia* were enriched in clinical environments linked to prior treatment with a third-generation cephalosporin (reviewed in Quinn, 1998). *Candida albicans* is a fungal opportunistic pathogen that can cause nosocomial infections. While healthy carriers of *C. albicans* remain asymptomatic, immunocompromised patients suffering from AIDS or undergoing chemotherapy are susceptible to candidiasis. Resistant strains of the pathogen are known and severe side effects are associated with therapeutic agents (Lemar et al., 2003). Interestingly the plant rhizosphere showed to be a reservoir for bacterial opportunistic pathogens showing antibiotic-resistance. Competition for colonization sites, nutrients and minerals together with naturally occurring antibiotics contributes to the selection of resistant species (Berg et al., 2005). However the rhizosphere also harbors antagonists of such resistant microbes and they may apply undiscovered strategies to survive which could be adopted for artificial habitats.

1.4 Objectives

Plants harbor an enormous, plant species-specific diversity including antagonistic strains (Berg and Smalla, 2009), which can be used for alternative solutions in clean room technology. For example, different genera and species of plant-associated endophytic bacteria have been isolated during several sampling approaches on Styrian pumpkin fields. Another source for plant-associated isolates was found on various agricultural lands and desert soil, both located in Sekem/Egypt. These bacteria were tested regarding their antagonistic activity against plant pathogens like bacteria, oomycetes, fungi and nematodes (Fürnkranz et al., 2011; Köberl et al., 2011). Some of the positively tested isolates belong to *Paenibacillus* spp., *Pseudomonas* spp. and *Lysobacter* spp. and could be therefore applicable tools for biocontrol implementation. Available strains were further differentiated by BOX PCR, SSCP and 454-pyrosequencing. Both, the different bacterial species but also the in-house strains have shown differences in their antagonistic potential by targeting varying pathogens, or affecting them with diverse severity (Liebminger et al., 2011; Fürnkranz et al., 2011; Köberl et al., 2011). The pathogen coverage has been extended to human-associated opportunistic pathogens, without losing the antagonistic effect of the tested isolates. Interestingly the antagonistic potential was not just observable in classic testing methods like dual-culture tests, but also in a novel textile-based approach. This approach showed that some plant-associated bacteria are able to produce highly effective volatile organic compounds (VOCs) that can inhibit pathogen growth on textile surfaces (Liebminger et al., 2011).

A deeper insight into the antagonistic potential of known plant-associated antagonists should be achieved by utilization of optimized dual-culture tests and CLSM methods. Furthermore an adequate workflow needs to be developed for high-throughput screening of new antagonists, followed by the identification of active VOCs. This requires development of adapted GC-MS headspace SPME methods and high resolution profiles of volatile metabolites. Identified VOCs should be characterized regarding their applicability in further experiments. Their efficacy must be proved by utilization of pure synthetic substances in high-throughput VOCs assays. Finally defined bacterial VOCs should be quantified and

the effect of pathogens on the produced quantity should be investigated in co-cultivation experiments.

2 Material and Methods

2.1 Material

All used media, media components and surfaces (e.g. clean room textiles) were autoclaved (121 °C and 15 min holding time) or filtered using a 0.20 µm filter if the substances were in solution and had a low thermostability. The media was always prepared with deionized water, while double distilled water was used for different dilution approaches. Petri dishes and micro well plates were obtained sterile in sealed packages.

2.1.1 Manufacturing certificate

If not specifically mentioned otherwise, all chemicals, culture media, ready-for-use kits and hardware were obtained from the following companies: Agilent (Santa Clara, USA), Dastex (Muggenstum, Germany), Epicentre (Madison, USA), Eppendorf (Hamburg, Germany), Greiner Bio-One (Kremsmünster, Austria), Fluka (Buchs, Switzerland), Invitrogen (Lofer, Austria), Lactan (Graz, Austria), Leica Microsystems (Wetzlar, Germany), Merck (Darmstadt, Germany), MP Biomedicals (Eschwege, Germany), Sarstedt (Nümbrecht, Germany), Sifin (Berlin, Germany), Roth (Karlsruhe, Germany), Sigma-Aldrich (St. Louis, USA), Sorvall (Buckinghamshire, England).

2.1.2 Nutrient media

Fluid media: 2xTY media
 16 g/L Pepton from casein
 10 g/L Beef extract
 5 g/L NaCl

 Caso media (TSB)
 30 g/L Caso media

LB media

25 g/L LB media

SOC media

20 g/L Trypton

5 g/L Yeast Extract

0.6 g/L NaCl

0.18 g/L KCl

2.04 g/L MgCl₂

2.46 g/L MgSO₄

3.6 g/L Glucose

Solid media: Caso media

30 g/L Caso media

15 g/L agar

LB media

25 g/L LB media

15 g/L agar

LB media for *Pseudomonas chlororaphis* strains

25 g/L LB media

0.5 g/L Dextrose

15 g/L agar

Selective LB media

25 g/L LB media

25 µg/mL Kanamycin

Nutrient Agar (NA)

4.0 g/L Peptone

2.4 g/L Beef Extract

15.0 g/L agar

2.1.3 Chemicals

Solutions: NaCl Solution 0.9%
9 g/L NaCl

PBS Buffer
3.0 g/L KH_2PO_4
4.0 g/L NaCl
7.0 g/L Na_2HPO_4
pH 7.1 ± 0.2

Synthetic pyrazines: 2,3-dimethyl-5-(1-methylpropyl)-pyrazine 97%
2,3-dimethyl-5-(2-methylpropyl)-pyrazine 97%

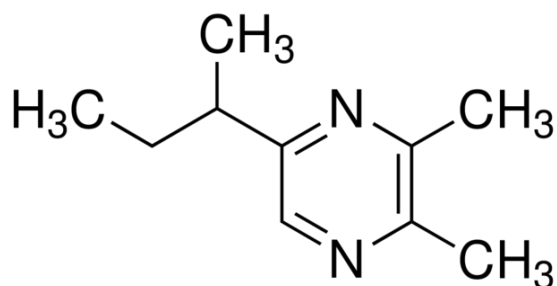


Figure 2.1 – The molecular structure of 2,3-dimethyl-5-(1-methylpropyl)-pyrazine is shown. One common synonym used for this structure is 5-sec-butyl-2,3-dimethylpyrazine. Source: www.sigmaaldrich.com

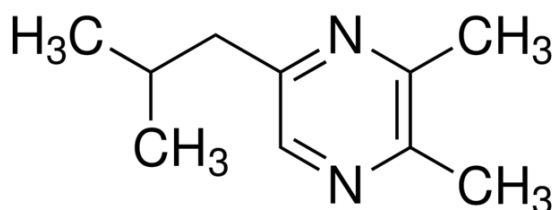


Figure 2.2 – The molecular structure of 2,3-dimethyl-5-(2-methylpropyl)-pyrazine is shown. One common synonym used for this structure is 5-isobutyl-2,3-dimethylpyrazine. Source: www.sigmaaldrich.com

2.1.4 Pathogen model organisms

Gram-positive: *Staphylococcus aureus* ATCC 25923
Staphylococcus epidermididis ATCC 14990
Pseudomonas aerugionosa QC 14-3-8

Gram-negative: *Klebsiella pneumoniae*
Stenotrophomonas maltophilia DSM 50170

Fungal: *Candida albicans* H5

All pathogen model organisms were inoculated in 100 mL flasks and 20 mL fluid LB media for an ONC. The ONC was incubated at 37 °C under agitation (120 rpm). On the next day the cultures were grown to an OD₆₀₀ of 0.4–0.7 which assured that they were in the exponential growth phase.

2.1.5 Antagonistic bacteria strains

Paenibacillus species: *Paenibacillus pabuli* Bint1
Paenibacillus amylyticus Eint1a
Paenibacillus polymyxa GnDWu39
Paenibacillus polymyxa GnMWu33/2
Paenibacillus polymyxa GnOeWu11
Paenibacillus brasilensis Mc2-9
Paenibacillus brasilensis Mc2Re-16
Paenibacillus polymyxa Mc5Re-14
Paenibacillus polymyxa PB71
Paenibacillus kribbensis Sb3-1
Paenibacillus brasilensis Sd5Re-24
Paenibacillus polymyxa Wb2-3

Pseudomonas species: *Pseudomonas chlororaphis* OeWuP28
Pseudomonas chlororaphis OeWuP34
Pseudomonas chlororaphis OeWu259

Lysobacter species: *Lysobacter* sp. MWu227

2.1.6 Clean room textiles

The clean room textiles (Fig. 2.3) were obtained as bulk stock (Dastex - Muggensturm/Germany) and trimmed into smaller pieces to enable utilization in different experimental approaches. Further the autoclaving step was always performed after finishing the assembly of textile based assemblies like “flags” in the bacterial co-cultivation experiments.


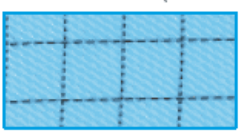
Criterion	ION-NOSTAT VI.2	
Fabric	HA	98 % Polyester + 2 % Carbon
Dispersion of the conductive fibre	HA	warp & weft by intervals of 5 mm
Conductive material / yarn	HA	Carbon-Fibre in “Sandwich-Construction” Carbon interim  Polyester fibre
Weave	HA	Twill 3/2 (Scale of 2:1) 
Weight	ITV	approx. 113 g/m ²
Air permeability (DIN 53887) at 200 Pa (l/min x dm²)	ITV	29.2
Water vapour diffusion resistance (35°C 40 % r.F. 10⁻³ m² mbar/V)	FIH	28.3
As a result the wearing comfort is		very good
Particle retention capacity for airborne particles Duration: 60 min Crude gas concentration: 25 mg/m ³	ITV	0.5 µm, approx. 97 % 5.0 µm, approx. 98 %
Electrostatic behaviour a) Charge tendency (valuation) b) Discharge velocity (valuation)	ITV	in warp & weft direction: low in warp & weft direction: very high
Surface resistance (DIN 54345)	HA	10 ⁷ – 10 ⁹ Ohms
Abrasion tendency Test method Martindale (valuation)	ITV	good to very good

Figure 2.3 - Specifications of the used ION-NOSTAT VI.2 textile are shown above.

Source: www.dastex.de

2.1.7 Confocal laser-scanning microscopy (CLSM)

Confocal laser-scanning microscopy enables the examination of biological samples like tissues or single cells. It is important to apply adequate hardware as well as an appropriate method to achieve the best results (Pawley et al., 2006). We utilized a Leica TCS SPE confocal laser-scanning microscope (Leica Microsystems, Wetzlar, Germany) within this Master thesis to examine bacteria inoculated textile samples after exposure to different antagonists. Solid state laser excitation was used together with a Bacterial Viability Kit in two different channels. The excitation and detection wavelengths have been adjusted according the fluorophore manufacturer's fact sheet. A third channel was excited with a UV laser and the textile's autofluorescence was detected to gain a good overview of the surface. The resulting overlap of all channels was used to observe both, position and viability of examined bacteria.

2.1.8 LIVE/DEAD[®] Bacterial Viability Kit (BacLight[™])

Staining of pathogen inoculated textile surfaces with the LIVE/DEAD[®] Bacterial Viability Kit (BacLight[™]) allows differentiation between vital and dead cells. The kit is based on two different fluorophores that are applied simultaneously to the examined sample. SYTO[®] 9 nucleic-acid green fluorescent dye can penetrate both living and dead cells, while propidium iodide nucleic-acid red fluorescent dye can only penetrate dead cells with a damaged membrane. By using CLSM the samples can be excited in different channels with distinctive wavelengths, SYTO[®] 9 has an extinction maximum at 480 nm and propidium iodide at 490 nm. The detectable emission maxima are at 530 nm for SYTO[®] 9 and at 630 nm for propidium iodide (Molecular Probes[®] – www.invitrogen.com, 2008). Additionally an adapted evaluation scale was developed to allow interpretation of the gained CLSM pictures (Fig. 2.4).

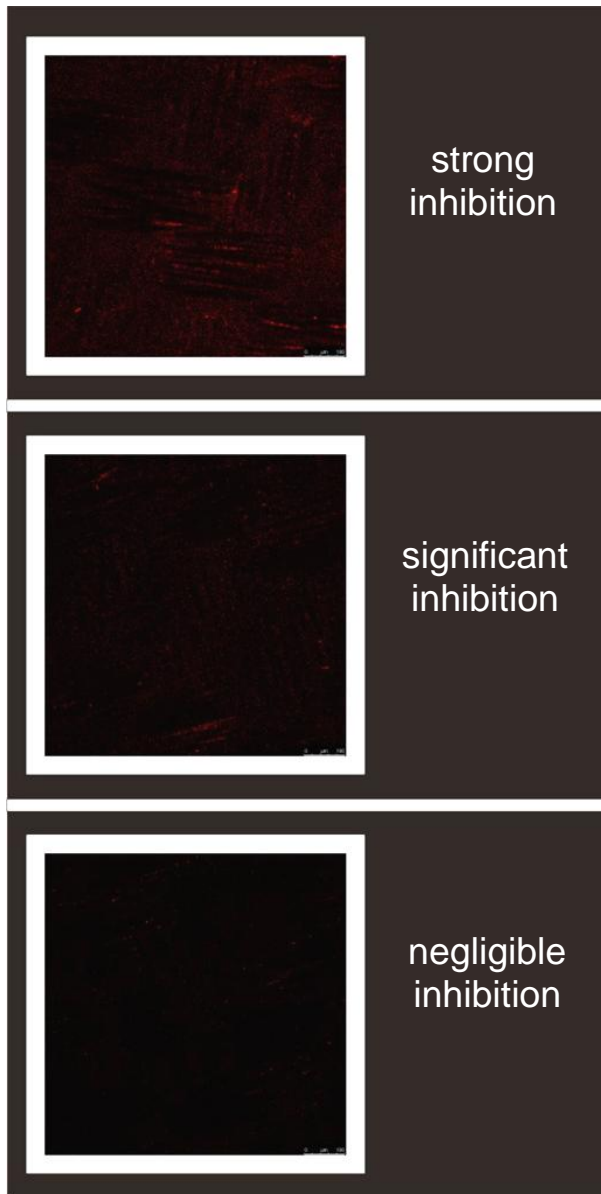


Figure 2.4 – Visual analysis of all pathogen inoculated textiles was performed with an adapted evaluation scale. The effects have been classified in strong inhibition, significant inhibition and negligible inhibition like shown above.

2.1.9 EZ-Tn5TM <KAN-2>Tnp TransposomeTM Kit

The EZ-Tn5TM <KAN-2>Tnp TransposomeTM Kit allows random insertion of a Tn903 kanamycin resistance gene into the host organism. During electroporation of adequate bacterial cells, the stable complex containing a transposase (enzyme) and a transposome (gene region) can be transferred into the cytoplasm. The transformation efficiency for *Pseudomonas* species is $>10^2$ cfu/ μ L of EZ-Tn5TM <KAN-2>Tnp TransposomeTM. This kit is suitable for creating gene-knockout

mutants with disruptions in unspecified gene regions. These mutants can be isolated by using selective media with distinctive kanamycin concentrations (25 - 50 µg/mL). Additionally the kit contains specific primers that can be used to amplify and sequence the disrupted gene regions (Epicentre – www.EpiBio.com).

2.1.10 Gas chromatography–mass spectrometry

Headspace SPME analysis of living bacteria samples allows identification of formed volatile organic compounds in the gas phase. The substances are adsorbed during the extraction phase by the fiber coating and desorbed during a desorption phase conditioned by a temperature rise. After separation in the GC column, the mass to charge (m/z) is filtered by a quadrupole and a software based analysis can be done by comparison with a spectral library.

Gas chromatography: Agilent 7890A GC with CombiPAL – Headspace and SPME option

Carrier gas: helium

Column: HP-5MS (30 m x 0.250 mm x 0.25 µm)

Mass spectrometry: Agilent 5975C MSD

Ion Source: EI, positive

Energy: 70eV

Mass filter: Quadrupole

Mass range: 1.6-1050 u

Temperature limits: Source: 250°C, Quadrupole: 200°C

Detector: Triple-Axis-HED-EM

Pump type: Diffusion pump

Library: NIST 2008

Fibres: **SPME headspace fibre** – 50/30 µm Divinylbenzen/CarboxenTM/
Polydimethylsiloxane (PDMS) 1 cm Stableflex/SS

SPME headspace fibre – 50/30 µm Divinylbenzen/CarboxenTM/
Polydimethylsiloxane (PDMS) 2 cm Stableflex/SS

SPME headspace fibre – 85 µm Carboxen[™]/Polydimethylsiloxane (PDMS) 1 cm Stableflex/SS

2.2 Methods

2.2.1 VOCs dual-culture test

The VOCs dual-culture test is based on two compartment petri dishes. One side contains solid media, while the other side is used for 1 x 1 cm textile pieces. Depending on the antagonist species solid LB media (*Pseudomonas* and *Paenibacillus species*) and solid NA media (*Lysobacter species*) was used. In the first step the antagonists were cultivated and plated on the agar side of the petri dishes. The antagonists were inoculated in 20 mL of LB media (*Pseudomonas* and *Paenibacillus species*) or 20 mL Caso media (*Lysobacter species*) for an ONC under agitation (120 rpm) at 37 °C (*Paenibacillus polymyxa*,) or 30°C (*Lysobacter species* and *Pseudomonas species*). On the next day strains of *Paenibacillus polymyxa*, *Pseudomonas chlororaphis* and *Lysobacter sp.* were inoculated to an OD₆₀₀ = 0,6-0,9 in the same media and were incubated at 37 °C or 30° C under agitation (120 rpm) until an OD₆₀₀ = 1,3-2 was reached. After this step 50 µL of the suspensions were plated out on the nutrient agar side of the petri dishes. Finally the strains were incubated at 30°C for 20-24 hours.

The pathogen models were grown to an OD₆₀₀ of 0.4-0.7 in Caso media. Thereon 3 µL of these suspensions were pipetted on 1x1 cm textile pieces and placed into the empty compartment of the petri dishes. Parafilm was used to seal the petri dishes. This allows a better accumulation of effective VOCs in the gas phase. The plates were incubated for 20-24 h at 30 °C. In the time dependent experiment the temperature was maintained, but the incubation times were varied in the range of 13-21 h.

CLSM was used to monitor the effect of the volatile antimicrobials on the pathogens. Textile pieces containing bacterial samples were stained with the LIVE/DEAD® BacLight[™] kit. Therefore 15 µL of propidium iodide were mixed with 15 µL of Syto[®] 9. From this mixture 3 µL were diluted into 1 mL PBS. Caps of 15

mL Greiner vials were used to stain textile samples in 150 μ L of this solution for about five minutes. The samples were immediately investigated by CLSM microscopy with a 10 x objective (NA= 0.25).

2.2.2 Standard high-throughput VOCs assay

The standard screening assay is based on two multiwell plates (48 well plates), one filled with 300 μ L 15% LB-agar + 0.5 g/L dextrose per well and the other filled with 300 μ L 15% Caso-agar per well (Fig. 2.5). Dextrose was added as a supplement to avoid lysis of agar by *Pseudomonas chlororaphis* strains (Rogul et al., 1974). The wells containing LB-agar were always inoculated with a tooth pick and a single antagonist colony put down twice on the agar for each well. After incubation times of 20–24 hours at 37 °C a pathogen strain was grown in a liquid culture to a density of $OD_{600} = 0.4–0.7$. Then 5 μ L of this suspension were transferred into each well of the Caso-agar plates and the two different plates were clamped together with a perforated (1 hole for each well) silicone foil between them. It is very important that the plates are close by in order to allow the interaction of just one well with another. After a second incubation time of 20–24 hours the Caso-agar plates were checked for spots showing growth inhibition.

2.2.3 High-throughput VOCs assay for weak antagonists

The screening assay for weaker antagonists (e.g. *Paenibacillus* strains) is based on two multiwell plates (12 well plates), one filled with 1 mL 15% LB-agar per well and the other filled with 1 mL 15% Caso-agar per well. The wells containing LB-agar were always inoculated with an inoculating loop by streaking a single antagonist colony 5 times on the agar for each well. After incubation times of 20–24 hours at 37 °C a pathogen strain was grown in a liquid culture to a density of $OD_{600} = 0.4–0.7$. Then 5 μ L of this suspension were transferred into each well of the Caso-agar plates and the two different plates were clamped together with a perforated (3 holes for each well) silicone foil between them. It is very important that the plates are close by in order to allow the interaction of just one well with another. After a second incubation time of 44–48 hours the Caso-agar plates were checked for spots showing growth inhibition.

2.2.4 High-throughput VOCs assay for synthetic compounds

The assay for synthetic VOCs is based on two multiwell plates (12 well plates), one filled with 1 mL 15% LB-agar dextrose per well and the other filled with 1 mL 15% Caso-agar per well. The wells containing Caso-agar were always inoculated with 5 μ L bacterial suspension grown in liquid LB-medium to a recorded OD₆₀₀ value in the range of 0.4–0.7. At the same time different dilutions of the synthetic pyrazine fluid were prepared with a dilution rate of 10 respectively. Then 5 μ L of these dilutions were transferred into each well of the LB-agar plates and the two different plates were clamped together with a perforated (3 holes for each well) silicone foil between them. It is very important that the plates are close by in order to allow the interaction of just one well with another. After an incubation time of 44–48 hours the Caso-agar plates were checked for spots showing growth inhibition.

2.2.5 Modified high-throughput VOCs assay

A modified VOCs Assay was developed for simulation of pathogen growth under harsh conditions. It is based on two multiwell plates (12 well plates), one filled with 1 mL 15% LB-agar dextrose per well and a second plate without growth media. The wells containing LB-agar were always inoculated with an inoculating loop by streaking a single antagonist colony 5 times on the agar for each well. After 20-24 hours incubation at 37 °C the empty wells were inoculated with 5 μ L bacterial suspension grown in liquid LB-medium to a recorded OD₆₀₀ value in the range of 0.4–0.7. The two different plates were clamped together with a perforated (3 holes for each well) silicone foil between them. It is very important that the plates are close by in order to allow the interaction of just one well with another. After an incubation time of 44–48 hours a viability test was performed with the partly dried out cells.

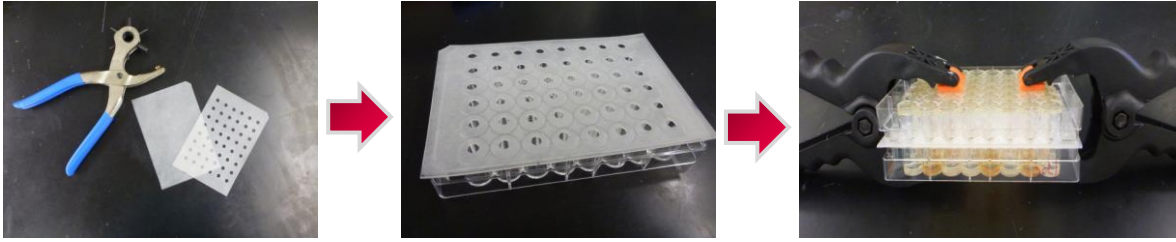


Figure 2.5 - The particular steps of the VOCs assay assembly are shown together with important components. A perforated silicone foil serves as seal between nearby wells and therefore only allows VOCs exchange between joining wells. Ordinary clamps were utilized to hold two multi-well plates together.

2.2.3 Microbial viability test

The microbial viability test is an additional method to combine the VOCs screening assay in order to analyze the effect of all antagonists. In the first step all pathogen containing wells are filled with 500 μL LB-Media (48 well plates) and 3 mL LB-media (12 well plates). The plates are incubated under agitation (120 rpm) at 37 $^{\circ}\text{C}$ for 1-2 h in the following step. After incubation in 48 well plates 50 μL of the suspension are removed from each well and diluted to 500 μL end volume with sterile LB-media. In the case of 12 well plates 500 μL are directly removed from each well. In the last step the OD_{600} value is determined for each sample and compared with a negative control (pathogen without antagonists in the same gas phase).

2.2.4 GC-MS analysis of bacterial VOCs

The utilized GC-MS SPME headspace method was adapted with slight changes from Verginer et al. (2010). In order to detect all bacterial VOCs the antagonists were placed with an inoculating loop on 10 mL 15% LB slope agar in 20 mL headspace vials (75.5 x 22.5 mm). The antagonists were always streaked out in 3 parallel lanes to ensure similar bacterial lawn density after incubation. After 20–24 hours of incubation at 37 $^{\circ}\text{C}$ and additional 20-24 hours incubation 30 $^{\circ}\text{C}$ the vials were sealed with adequate crimp seals and placed after another 2 hours into the tempered (30 $^{\circ}\text{C}$) GC-MS tray (agitator). The GC-MS analysis was started

immediately after that. Serial analysis was done with up to 15 samples and a cycle length of 46 min.

Settings: The extraction time with different headspace SPME fibers was always 10 min to ensure good adsorption of both, high and low abundant VOCs. In order to achieve a good desorption yield the inlet temperature was adjusted to the maximum (270 °C). The GC column temperature was kept at 40 °C for 2 min, raised to 110 °C at a rate of 5 °C/min, then up to 280 °C at 10 °C/min and finally maintained at 280 °C for 3 min. Furthermore the helium flow rate was set to 1.2 mL/min and kept at this value during the whole cycle (Fig. 2.6). The GC settings were adapted with slight changes from Buzzini et al. (2003).



Figure 2.6 – The diagram shows the adjusted temperature gradient in the GC oven. Additionally the carrier gas (Helium) flow is shown, which remains constant while the pressure rises conditioned by the temperature changes.

2.2.5 GC-MS analysis of co-cultivated bacteria

In order to detect changes in the antagonistic VOCs production, when pathogens are present in the same gas phase, the method from Verginer et al. (2010) was further adapted. The antagonists were placed with an inoculating loop on 10 mL 15% LB slope agar in 20 mL headspace vials (75.5 x 22.5 mm). The antagonists were always streaked out in 3 parallel lanes to ensure similar bacterial lawn density after incubation. After 20-24 hours of incubation at 37 °C small “flags” consisting of a glass capillary and a 1x1 cm clean room garment piece were stuck into the agar inside the headspace vials. The clean room garment part was inoculated with 5 µL of a pathogen culture grown to an $OD_{600} = 0.4-0.7$. This

allows a contact-free setup while the gas phase is shared (Fig. 2.7). After a second incubation time of 20–24 hours and 30 °C the vials were sealed with adequate crimp seals and placed after another 2 hours into the tempered (30 °C) GC-MS tray (agitator). The GC-MS analysis was started immediately after that. Serial analysis was done with up to 10 samples and a cycle length of 41 min.

Settings: The settings were not changed in comparison with the standard GC-MS analysis of bacterial VOCs beside the extraction time. It was lowered to 5 min in order to avoid saturation of the SPME fiber and therefore allow better quantification.

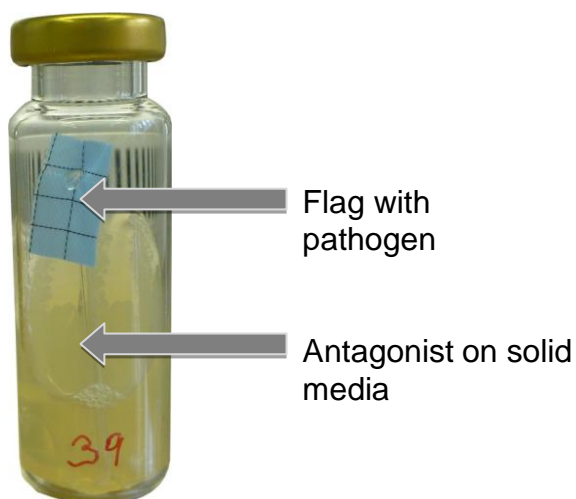


Figure 2.7 – The assembly of the GC-MS co-cultivation experiment allows VOCs detection from antagonists that were sharing the same gas phase with particular pathogens. It is important to avoid contamination of the solid media (15% LB-agar) with the applied pathogen.

2.2.4 GC-MS analysis of synthetic VOCs

The analysis of synthetic VOCs was done with additional changes in the utilized methods for VOCs analysis of living bacteria. First dilutions of the fluid chemicals were prepared with ddH₂O. Subsequently 5 µL of these dilutions were transferred on 10 mL 15% LB slope agar in 20 mL headspace vials (75.5 x 22.5 mm). The vials were immediately sealed with adequate crimp seals and incubated at 30 °C. This allows VOCs formation due to the vapor pressure of used chemicals. Finally

the vials were placed into the tempered (30 °C) GC-MS tray (agitator) and the GC-MS analysis was started (each cycle lasts 46 min).

Settings: To allow comparison with bacterial VOCs production the same GC-MS settings were applied without any changes.

2.2.5 Preparation of electrocompetent *Pseudomonas chlororaphis* cells

An ONC in 20 mL 2xTY media with a single *Pseudomonas chlororaphis* colony was prepared. On the next day a 500 mL flask with 100 mL 2xTY media was inoculated to an OD₆₀₀ = 0.1 – 0.2 and grown under agitation (120 rpm) and 37 °C to an OD₆₀₀ = 0.5 – 0.7. The suspension was portioned into 2 Sarstedt tubes and cooled for 30 min on ice. In the following step the tubes were centrifuged at 4500 rpm (Sorvall RC-5B centrifuge – F13S rotor) and 4 °C for 10 min. The pellets were resuspended in 50 mL 10% glycerin solution and centrifuged. This procedure was repeated with 20 mL 10% glycerin solution and 10 mL 10% glycerin solution. Prior to the last centrifugation step the pellets were pooled and resuspended in 10 mL 10% glycerin solution. In the last step the pellet was resuspended in 2 mL 10% glycerin solution and portioned into 1.5 mL Eppendorf tubes. The tubes were shock frozen in fluid nitrogen and stored at -70 °C until their utilization.

2.2.6 Electroporation of electrocompetent *Pseudomonas chlororaphis* cells

The Eppendorf tubes with electrocompetent cells were placed in an ice box for thawing. Precooled 0.1 cm cuvettes were used to mix 50 µL cell suspension with 1 µL EZ::TN <KAN-2> Tnp Transposome. Additionally a negative control containing 50 µL cell suspension without EZ::TN <KAN-2> Tnp Transposome was prepared. The cuvettes were electroporated using the “EC2” channel (2.5 kV) and immediately recovered in 1 mL SOC media (37 °C). After 1 h recovery time at 37 °C and agitation (120 rpm) 100 µL aliquots of undiluted and diluted (1:10) cell suspension were plated out on selective LB media (25 µg/mL kanamycin). The plates were incubated at 30 °C for 48 h and checked for bacterial growth.

2.2.7 Statistical analysis

All suitable data obtained in VOCs high-throughput assays was analyzed by using PASW Statistics 18 software (SPSS Inc). First the data was checked for Normal distribution and Homogeneity of variance. After this an ANOVA analysis was performed with data that follows a Normal distribution. Furthermore a Post Hoc test was applied depending on the Homogeneity of variance index. Homogenous data with a variance $P > 0.05$ was subjected to a Tukey analysis, while not homogenous data with a variance $P < 0.05$ was subjected to a Games-Howell analysis. Figures containing analyzed data were labeled with letters corresponding to the associated group. Furthermore a T-test was applied for comparison of two individual data sets.

3 Results

3.1 Supplemental VOCs dual-culture tests

The VOCs dual-culture test was efficiently used to evaluate the impact of bacterial VOCs on various pathogenic microorganisms (Liebminger et al., 2011). In additional approaches the quality of gained pictures was shown to be considerably dependent on the used textile surface. Unspecific signals can be reduced by utilization of the same fabric but different pre-staining. Various antagonist-pathogen combinations were observed with selected textiles and optimized settings. Furthermore a time-dependent experiment with *Staphylococcus aureus* was done to identify critical time points and therefore allowing a better evaluation of the antagonistic effects.

3.1.1 Utilization of different textiles

Two different fabrics were compared after a standard staining procedure with the LIVE/DEAD[®] Bacterial Viability Kit. Both textile pieces were not inoculated with bacterial samples, for this reason the visible fluorescence has always an unspecific character and should be avoided. The blue stained ION-NOSTAT VI.2 fabric showed high unspecific fluorescence, especially in the propidium iodide channel. This leads also to an altered color in the overlay channel. White stained textiles proved to be more suitable for the VOCs dual-culture test since the unspecific signal was minimal and did not lead to interference in the overlay channel. However the signal difference in the green channel was negligible. A comparison with same detection settings in all channels showed that the white ION-NOSTAT VI.2 fabric has significant advantages. It can be used as a neutral carrier for pathogen samples and it prevents misinterpretation of the VOCs effect due to a low interaction with utilized fluorescent dyes (Fig. 3.1).

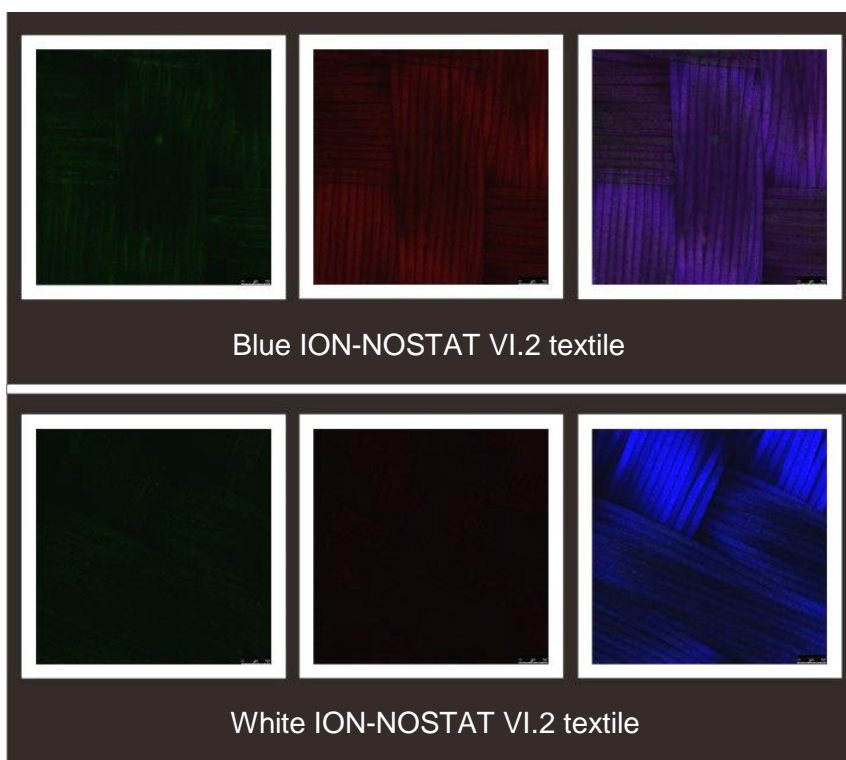


Figure 3.1 – CLSM pictures of two different fabrics stained with LIVE/DEAD[®] Bacterial Viability Kit. The samples were not inoculated with bacteria. White ION-NOSTAT VI.2 fabrics showed better applicability for VOCs dual-culture tests. The differences in the SYTO[®] 9 channel were negligible while the blue textile showed a high unspecific signal in the propidium iodide channel.

3.1.2 VOCs dual-culture tests with *C. albicans*

Candida albicans was exposed to three different antagonists in dual-culture tests. Thereof two antagonists showed to be able to inhibit the pathogen with high efficacy. *Paenibacillus polymyxa* GnDWu39 reduced the growth significantly and also caused an increase of dead cells which was visible in the propidium iodide channel (Fig. 3.2). *Lysobacter* sp. MWu228 could not reduce the growth of *C. albicans* and a low number of dead cells was visible at the same time (Fig. 3.3). A remarkable growth inhibition by *Pseudomonas chlororaphis* OeWuP28 was observed expressed by the high number of dead cells (Fig. 3.4).

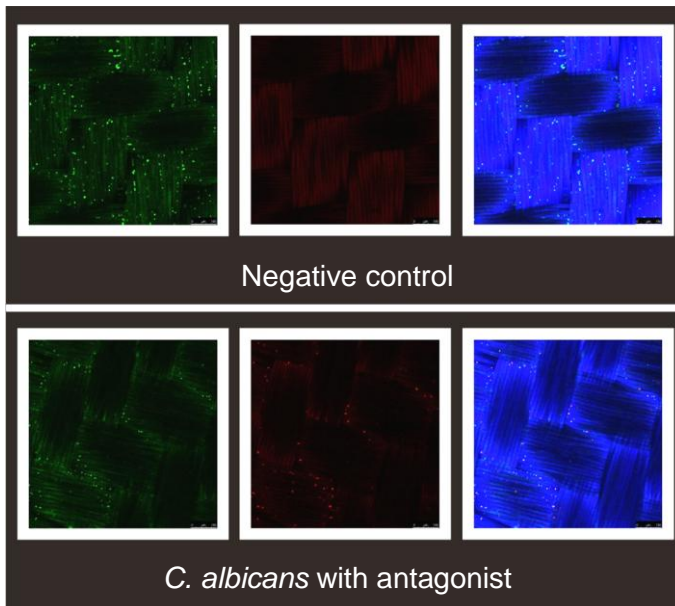


Figure 3.2 – CLSM pictures of *C. albicans* negative control and VOCs dual-culture test with antagonist after 44-48 h co-incubation. BacLight™ staining allows visualization of living cells (green) and dead cells (red). A decrease in growth of *C. albicans* and increase of dead cells can be observed after incubation with *Paenibacillus polymyxa* GndWu39.

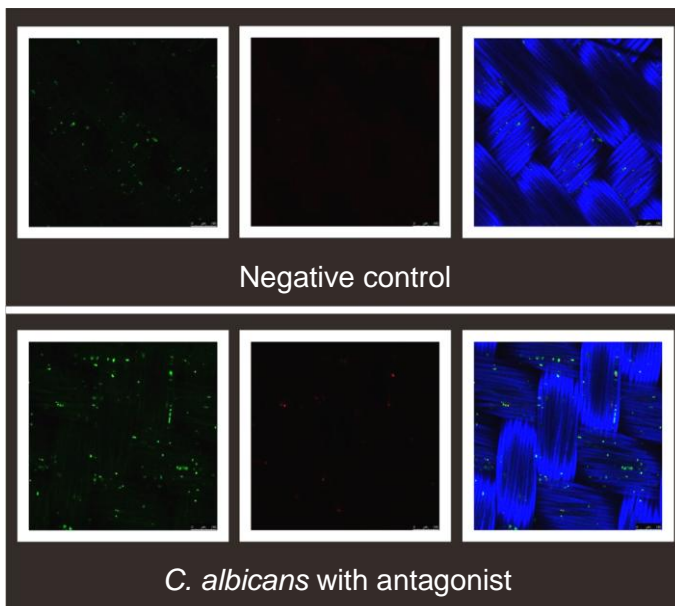


Figure 3.3 – CLSM pictures of *C. albicans* negative control and VOCs dual-culture test with antagonist after 44-48 h co-incubation. BacLight™ staining allows visualization of living cells (green) and dead cells (red). The growth inhibiting effect of *Lysobacter* sp. MWu228 on *C. albicans* was negligible expressed by the number of dead cells.

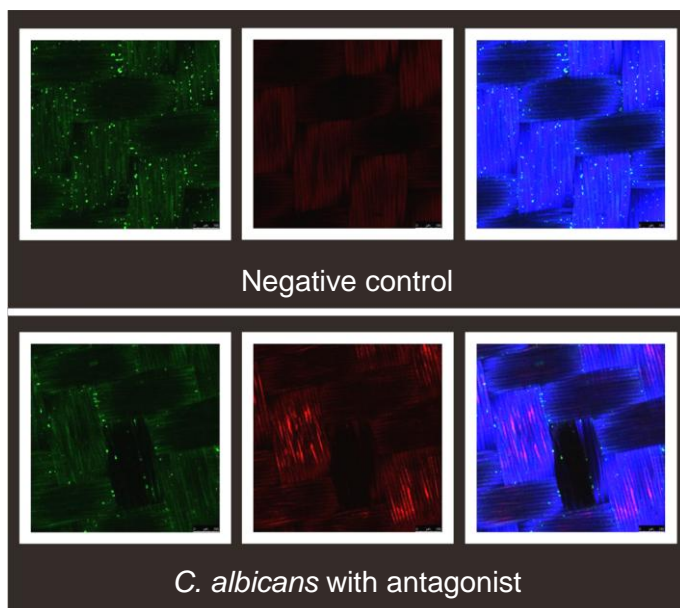


Figure 3.4 – CLSM pictures of *C. albicans* negative control and VOCs dual-culture test with antagonist after 44-48 h co-incubation. BacLight™ staining allows visualization of living cells (green) and dead cells (red). *Pseudomonas chlororaphis* OeWuP28 reduced the growth of *C. albicans* and led to a high number of dead cells simultaneously.

3.1.3 VOCs dual-culture tests with *P. aeruginosa*

Pseudomonas aeruginosa was subjected to three antagonists in the VOCs dual-culture test. *Paenibacillus polymyxa* GnDWu39 and *Lysobacter* sp. MWu227 could not decrease the pathogen growth and the amount of dead cells was low (Fig. 3.5 and Fig. 3.6). In contrast *Pseudomonas chlororaphis* OeWuP28 led to a reduction of living cells together with a high signal increase in the propidium iodide channel correlating with pathogen death (Fig. 3.7).

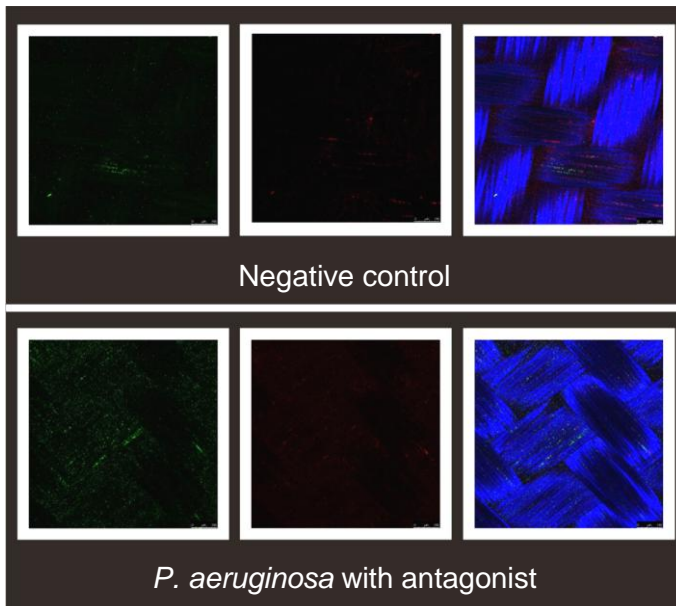


Figure 3.5 – CLSM pictures of *P. aeruginosa* negative control and VOCs dual-culture test with antagonist after 44-48 h co-incubation. BacLight™ staining allows visualization of living cells (green) and dead cells (red). The growth of *P. aeruginosa* was not affected by *Paenibacillus polymyxa* GnDWU39 and there was no difference in the amount of dead cells compared to the negative control.

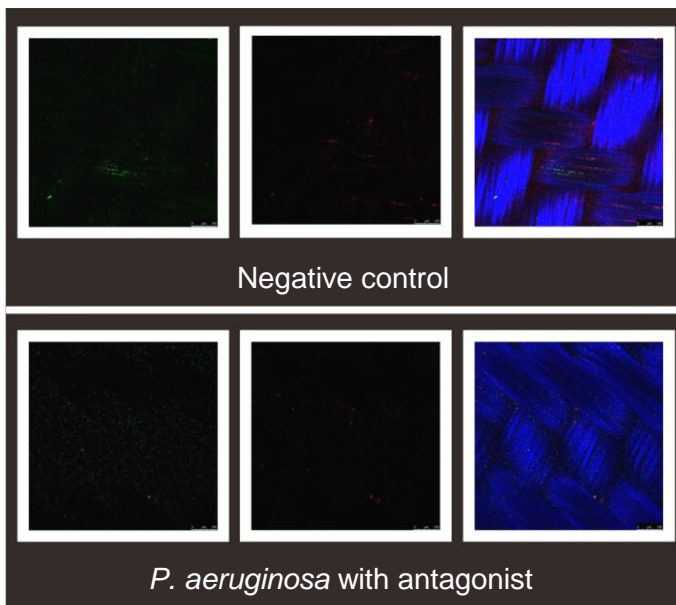


Figure 3.6 – CLSM pictures of *P. aeruginosa* negative control and VOCs dual-culture test with antagonist after 44-48 h co-incubation. BacLight™ staining allows visualization of living cells (green) and dead cells (red). *Lysobacter* sp. MWu227 did not show a reduction of viable pathogens and a low number of dead *P. aeruginosa* cells.

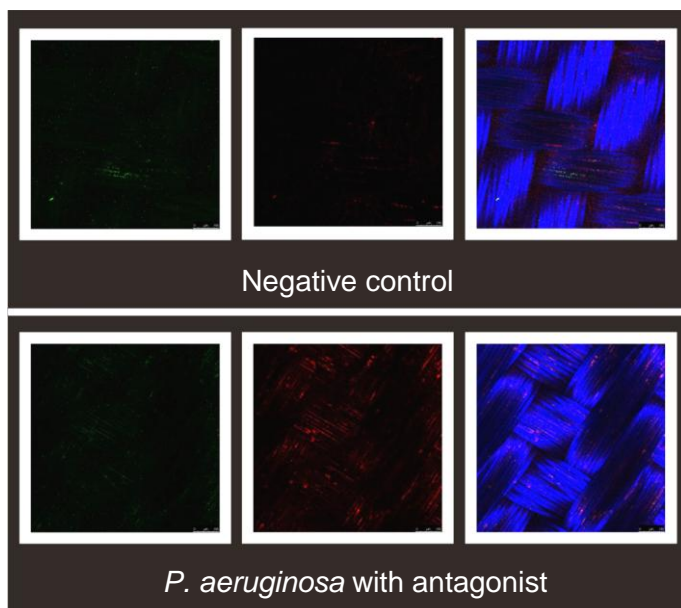


Figure 3.7 – CLSM pictures of *P. aeruginosa* negative control and VOCs dual-culture test with antagonist after 44-48 h co-incubation. BacLight™ staining allows visualization of living cells (green) and dead cells (red). *Pseudomonas chlororaphis* OeWuP28 showed a decrease of viable *P. aeruginosa* cells together with a high amount of dead cells in the propidium iodide channel.

3.1.4 VOCs dual-culture tests with *S. aureus*

S. aureus was incubated together with three different antagonistic isolates. *Paenibacillus polymyxa* GnDWu39 and *Lysobacter* sp. MWu228 could not decrease the pathogen growth and the amount of dead cells was low (Fig. 3.8 and Fig. 3.9). Incubation with *Pseudomonas chlororaphis* OeWuP28 led to a decrease of viable pathogens in the SYTO® 9 channel and also to an increase of dead cells in the propidium iodide channel (Fig. 3.10).

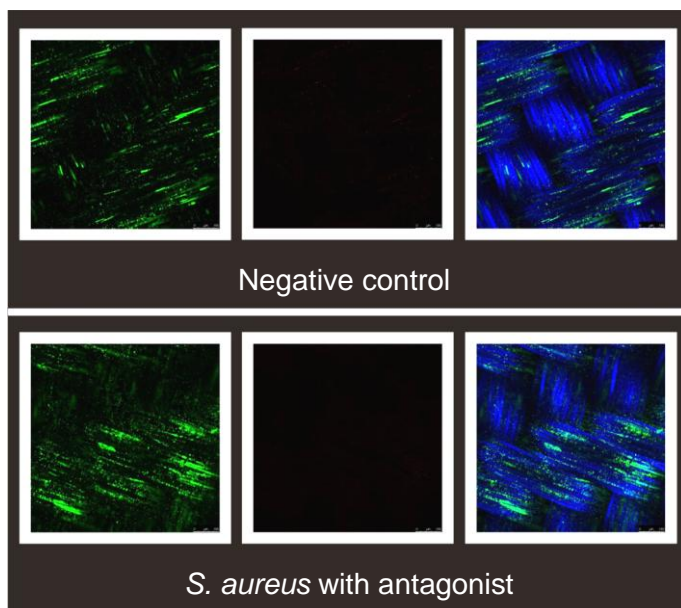


Figure 3.8 – CLSM pictures of *S. aureus* negative control and VOCs dual-culture test with antagonist after 44-48 h co-incubation. BacLight™ staining allows visualization of living cells (green) and dead cells (red). A growth inhibiting effect of *Paenibacillus polymyxa* GnDWu39 on *S. aureus* was not given. Therefore no dead cells could be detected after incubation.

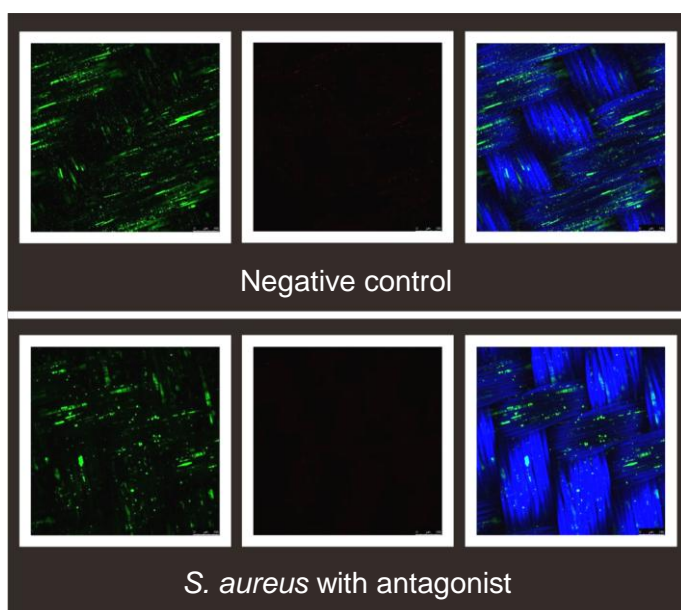


Figure 3.9 – CLSM pictures of *S. aureus* negative control and VOCs dual-culture test with antagonist after 44-48 h co-incubation. BacLight™ staining allows visualization of living cells (green) and dead cells (red). *S. aureus* could not be inhibited after incubation with *Lysobacter* sp. MWu228 in the dual-culture test.

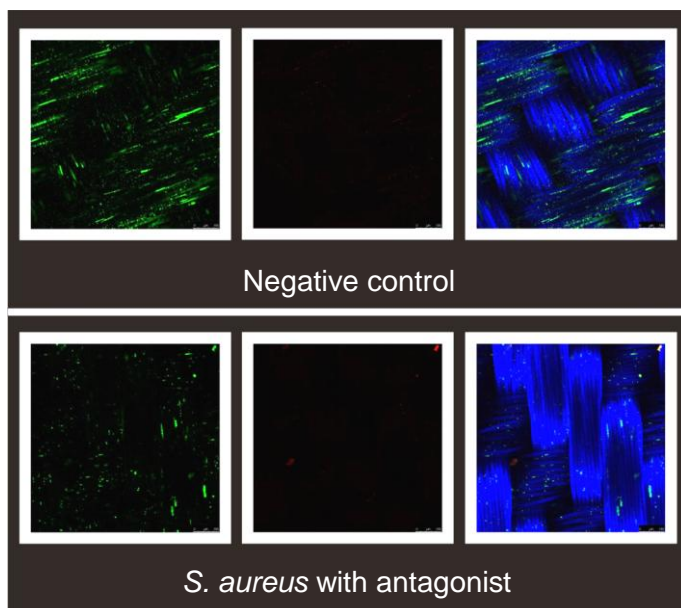


Figure 3.10 – CLSM pictures of *S. aureus* negative control and VOCs dual-culture test with antagonist after 44-48 h co-incubation. BacLight™ staining allows visualization of living cells (green) and dead cells (red). The growth of *S. aureus* was reduced by *Pseudomonas chlororaphis* OeWuP28 expressed by an increase of dead pathogens.

3.1.5 VOCs dual-culture tests with *S. epidermidis*

None of the three applied antagonists could inhibit *Staphylococcus epidermidis* significantly. *Paenibacillus polymyxa* GnDWu39 and *Pseudomonas chlororaphis* OeWUP28 did not show any increase in dead pathogen cells (Fig. 3.11 and Fig. 3.13), while *Lysobacter* sp. MWu228 led to an insignificant increase of the amount of dead pathogens which was seen in the propidium iodide channel (Fig. 3.12). The amount of living *S. epidermidis* cells was comparable to the one of the negative control.

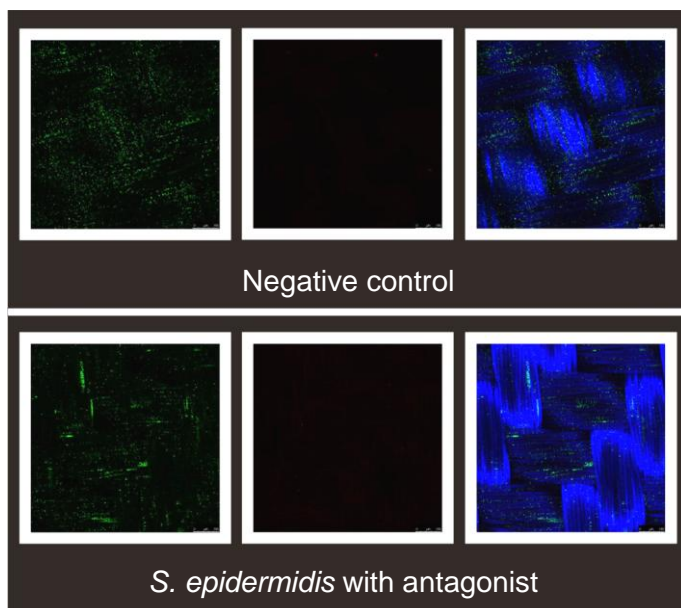


Figure 3.11 – CLSM pictures of *S. epidermidis* negative control and VOCs dual-culture test with antagonist after 44-48 h co-incubation. BacLight™ staining allows visualization of living cells (green) and dead cells (red). *S. epidermidis* was not affected by *Paenibacillus polymyxa* GnDWu39, no growth inhibiting effect could be observed after the incubation.

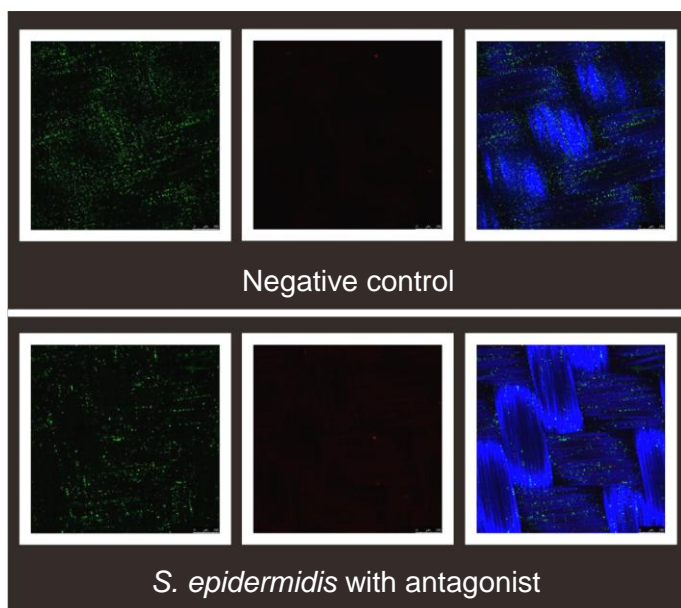


Figure 3.12 – CLSM pictures of *S. epidermidis* negative control and VOCs dual-culture test with antagonist after 44-48 h co-incubation. BacLight™ staining allows visualization of living cells (green) and dead cells (red). *Lysobacter* sp. Mw228 did not affect the growth of *S. epidermidis* expressed by the number of dead cells.

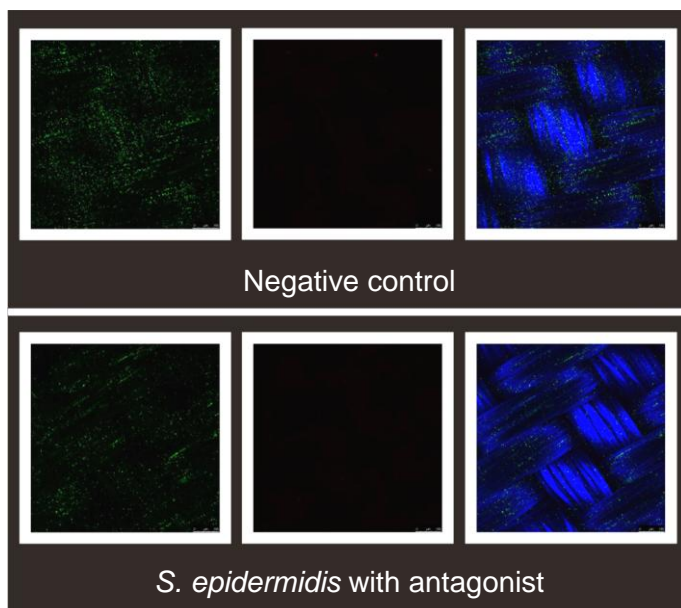


Figure 3.13 – CLSM pictures of *S. epidermidis* negative control and VOCs dual-culture test with antagonist after 44-48 h co-incubation. BacLight™ staining allows visualization of living cells (green) and dead cells (red). A growth inhibiting effect of *Pseudomonas chlororaphis* OEWuP28 on *S. epidermidis* was not detectable after incubation in the dual-culture test.

3.1.6 VOCs dual-culture tests with *S. maltophilia*

All three antagonists reduced the growth of *S. maltophilia* compared to the negative control. A significant increase of dead cells was observed with *Paenibacillus polymxya* GnDWu39 (Fig. 3.14). *Lysobacter* sp. MWu228 and *Pseudomonas chlororaphis* OeWuP28 did not show an increased amount of dead cells due to an early initiation of the growth inhibition. The pathogen growth was strongly decreased compared to the negative control. This resulted in a low number of detectable dead pathogens (Fig. 3.15 and Fig. 3.16).

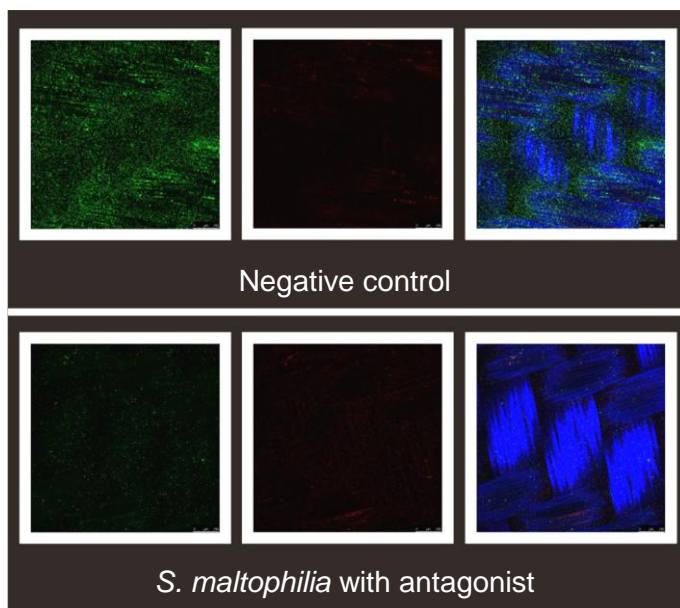


Figure 3.14 – CLSM pictures of *S. maltophilia* negative control and VOCs dual-culture test with antagonist after 44-48 h co-incubation. BacLight™ staining allows visualization of living cells (green) and dead cells (red). *S. maltophilia* was significantly inhibited by *Paenibacillus polymyxa* GnDWu39. The pathogen growth was decreased while the number of dead cells increased.

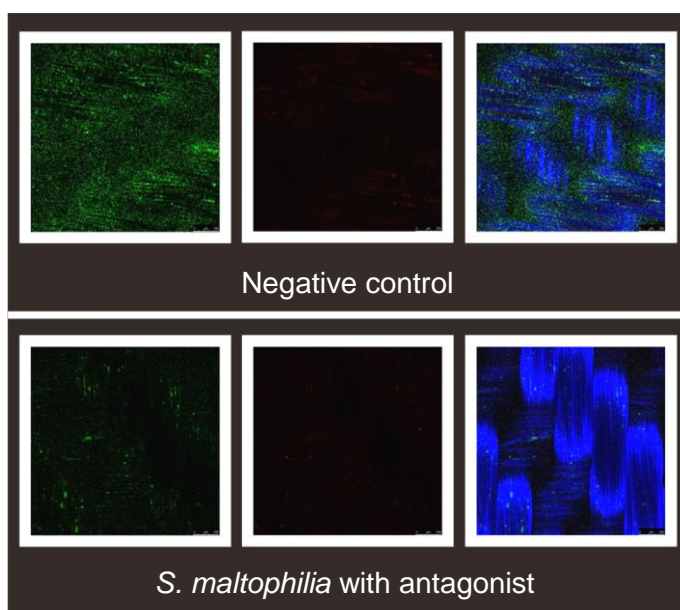


Figure 3.15 – CLSM pictures of *S. maltophilia* negative control and VOCs dual-culture test with antagonist after 44-48 h co-incubation. BacLight™ staining allows visualization of living cells (green) and dead cells (red). *Lysobacter* sp. MWu228 reduced the growth of *S. maltophilia* significantly, but an increase of dead pathogens could not be observed.

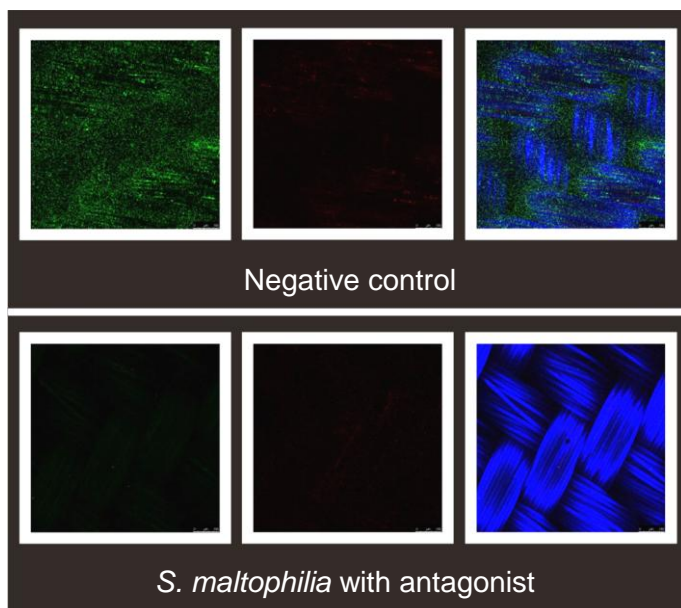


Figure 3.16 – CLSM pictures of *S. maltophilia* negative control and VOCs dual-culture test with antagonist after 44-48 h co-incubation. BacLight™ staining allows visualization of living cells (green) and dead cells (red). The growth of *S. maltophilia* was reduced by *Pseudomonas chlororaphis* OeWuP28, while a gain of dead cells was not observed.

3.1.7 Time-dependent VOCs dual-culture tests

A time-dependent test was done to get a better insight into the antagonistic properties of two different isolates. Samples that were evaluated at defined times showed the progress of *S. aureus* growth without an antagonist in the same gas phase (Fig. 3.17). In contrast the pathogen growth was evaluated with two antagonists, sharing one gas phase,. *Paenibacillus polymyxa* GnDWu39 did not affect the pathogen growth and an increase of dead cells of *S. aureus* could not be observed during the whole incubation time (Fig. 3.18). *Pseudomonas chlororaphis* OeWuP28 showed an early reduction of living pathogens within 13-17 h of co-incubation. The number of viable cells in the SYTO® 9 channel was significantly lower than in the negative control. However the first dead cells were detectable after 21 h of incubation (Fig. 3.19).

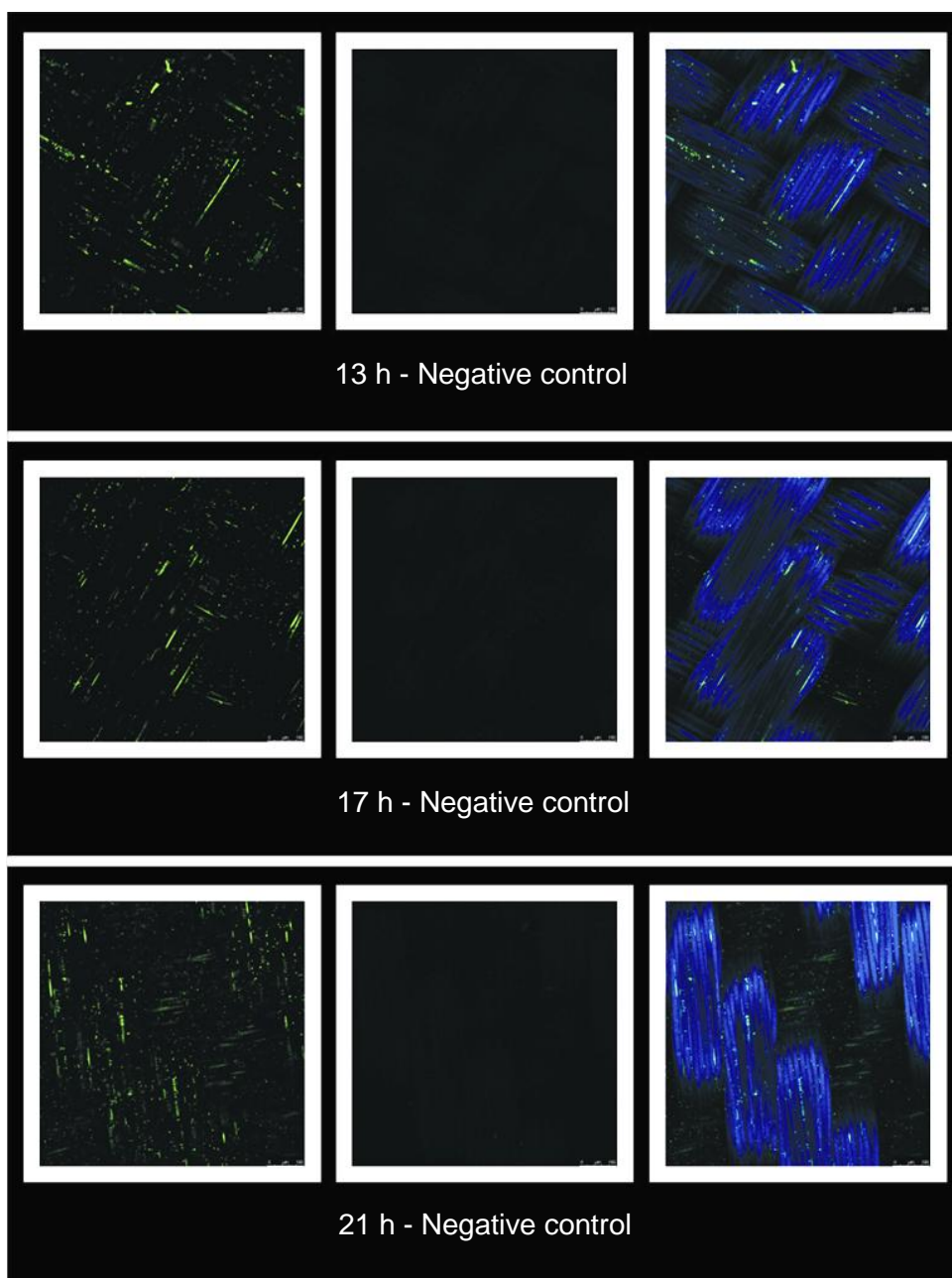


Figure 3.17 – CLSM pictures of negative controls 13 h, 17 h and 21 h after incubation of *S. aureus* on ION-NOSTAT VI.2 textile without antagonist. BacLight™ staining allows visualization of living cells (green) and dead cells (red). Constant bacterial growth was observed on the textile surface during the whole experiment.

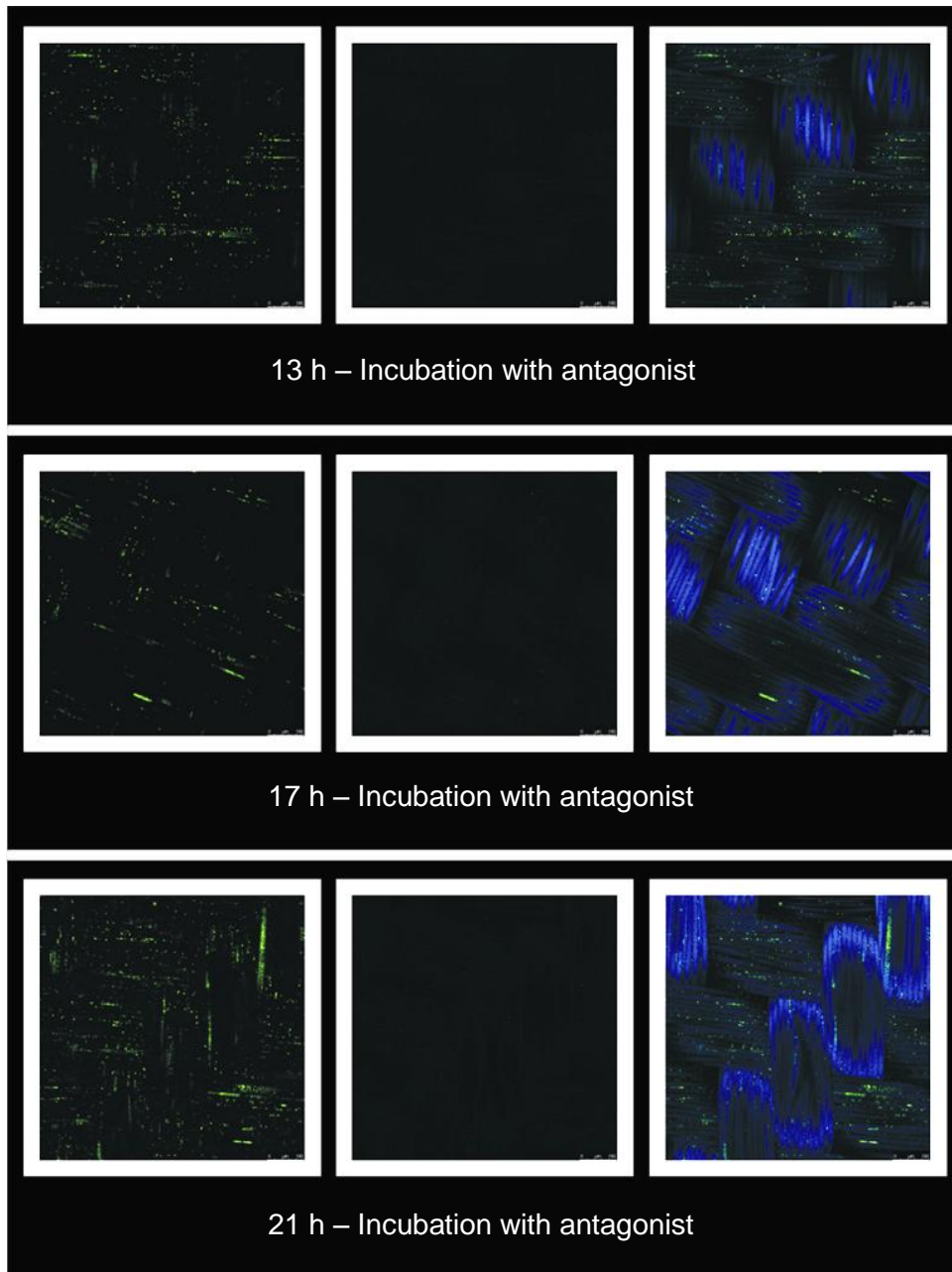


Figure 3.18 – CLSM pictures of *S. aureus* co-incubated on ION-NOSTAT VI.2 textile with *Paenibacillus polymyxa* GndWu39. Samples were taken after 13 h, 17 h and 21 h incubation. BacLight™ staining allows visualization of living cells (green) and dead cells (red). The growth process was not significantly hindered and an occurrence of dead cells could not be observed during the whole experiment.

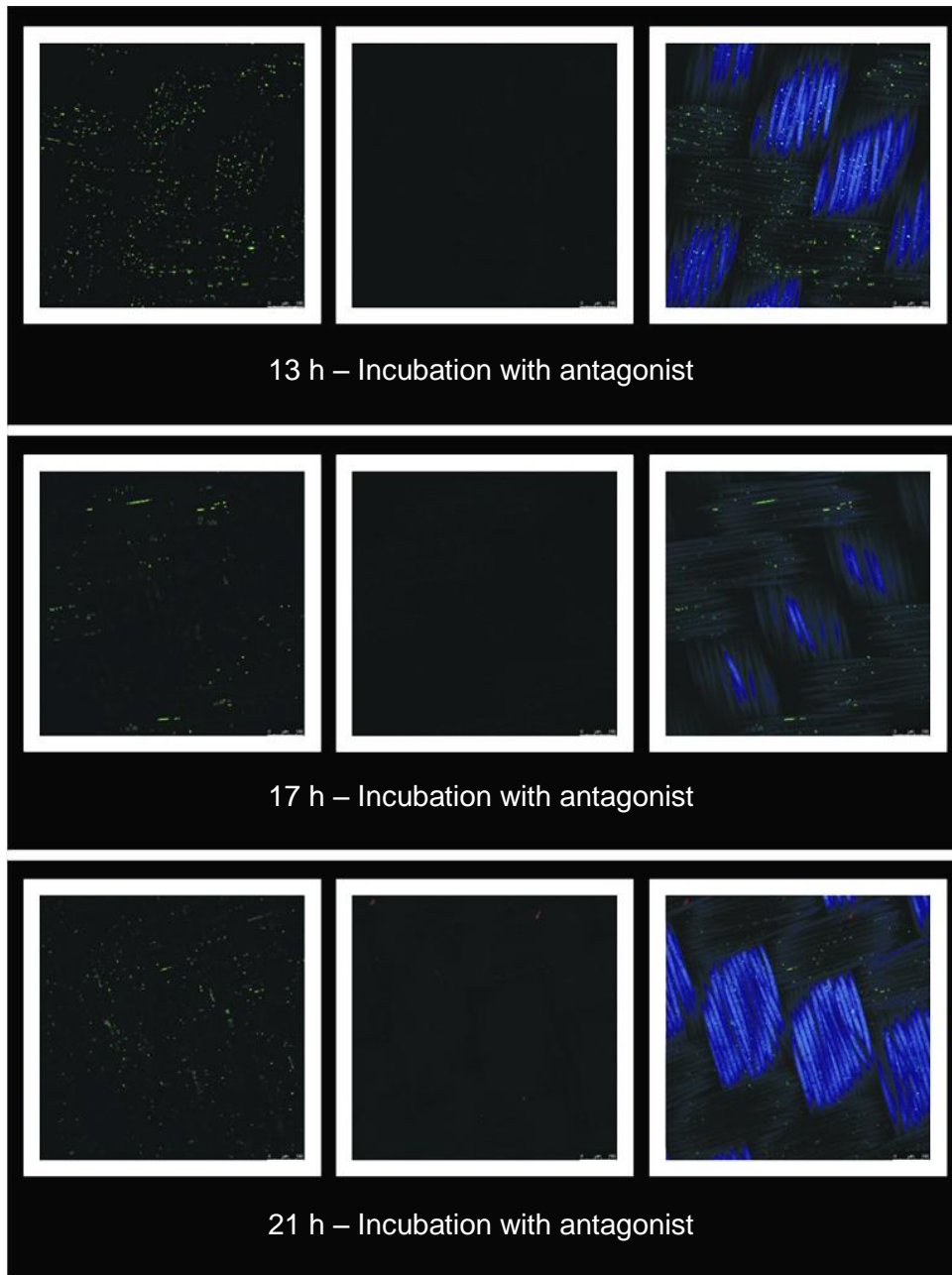


Figure 3.19 – CLSM pictures of *S. aureus* co-incubated on ION-NOSTAT VI.2 textile with *Pseudomonas chlororaphis* OeWuP28. Samples were taken after 13 h, 17 h and 21 h incubation. BacLight™ staining allows visualization of living cells (green) and dead cells (red). A growth deficiency was observed at early growth stages and the first dead cells appeared after 21 h incubation.

3.2 High-throughput VOCs assays

A high-throughput VOCs assay was newly developed and applied for the detection of gaseous antimicrobials produced by plant-associated antagonists. Different strains of *Paenibacillus polymyxa* and *Pseudomonas chlororaphis* were used to evaluate their antagonistic potential. Together with the combined viability test this approach allowed a qualification of the antagonistic potential and a direct comparison between different species and strains. Additionally this assay was used for the analysis of synthetic substances, to confirm their antimicrobial effects carried out through the gas phase.

3.2.1 *Pseudomonas chlororaphis* strains

All tested opportunistic pathogens were inhibited by *Pseudomonas chlororaphis* strains in the high-throughput VOCs assay. However there were significant differences regarding the inhibition intensity of different pathogens, but also between the different *Pseudomonas chlororaphis* strains. *S. aureus* was inhibited strongly and the effect was observable using micro-well plates. All wells without inhibition show milky nontransparent spots, which can be interpreted as growth of the pathogen, while wells with strong inhibition became clear (Fig. 3.20).

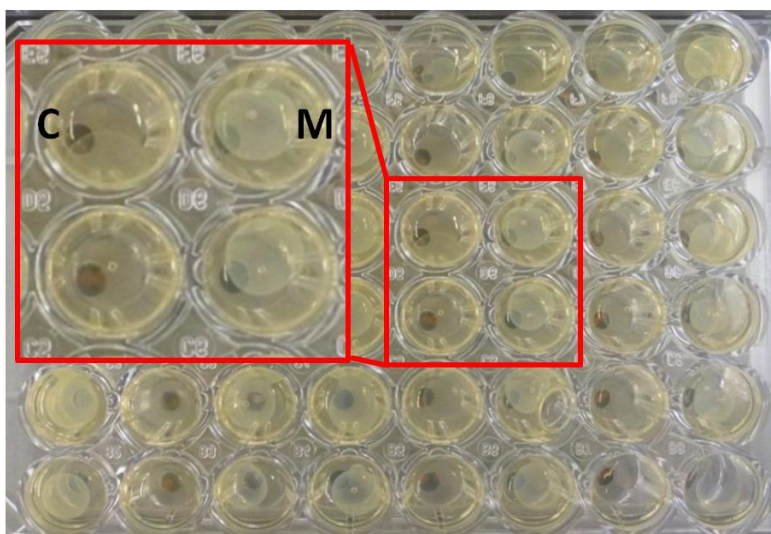


Figure 3.20 – Treatment of *S. aureus* with *Pseudomonas chlororaphis* OeWuP34 resulted in clear spots (C), while the negative controls became milky and nontransparent (M).

S. aureus showed always strong inhibition by all *Pseudomonas chlororaphis* strains. The differences relating pathogen growth between the standard VOCs high-throughput assay (Fig. 3.21) and the modified VOCs high-throughput assay with media limitation (Fig. 3.22) are negligible.

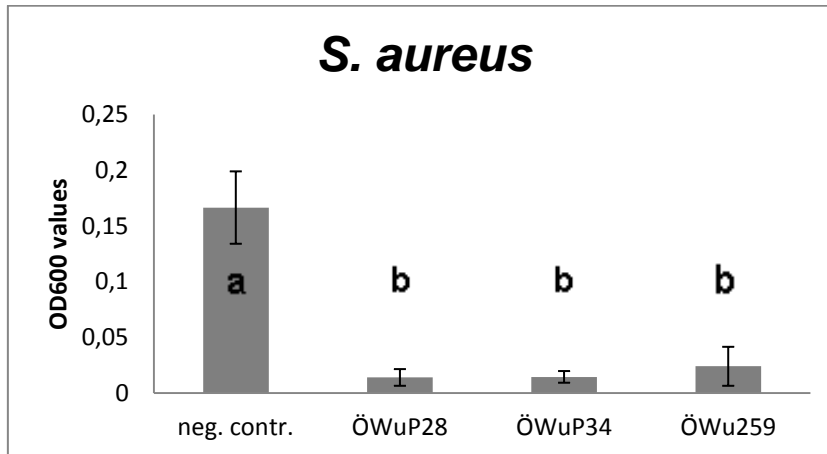


Figure 3.21 – All *Pseudomonas chlororaphis* strains inhibited the growth of *S. aureus* in the standard VOCs high-throughput assay. Different letters represent significant differences between respective mean values (ANOVA, Tukey-HSD, $P \leq 0.05$).

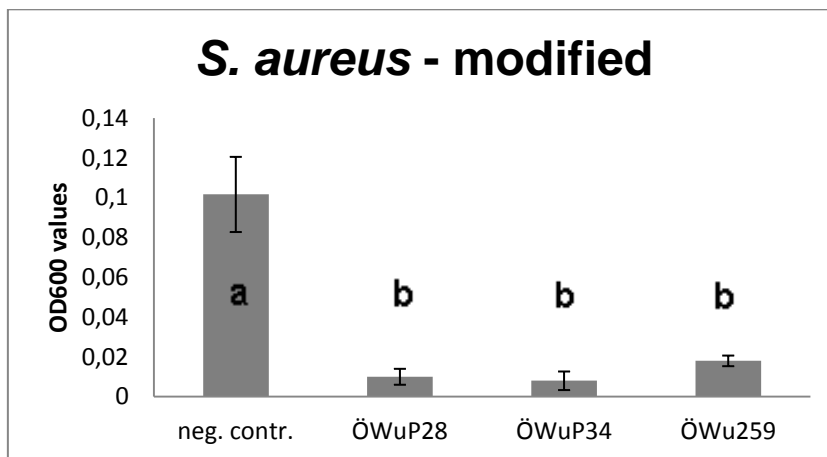


Figure 3.22 – The modified VOCs high-throughput assay confirmed the strong inhibition by *Pseudomonas chlororaphis* strains despite the modifications in growth conditions. Different letters represent significant differences between respective mean values (ANOVA, Tukey-HSD, $P \leq 0.05$).

S. epidermidis could not be inhibited by all *Pseudomonas chlororaphis* strains after the incubation (Fig. 3.23), while *S. maltophilia* showed a decreased growth rate

after co-incubation with all tested strains (Fig. 3.24). It has to be mentioned that the inhibition was very strain specific.

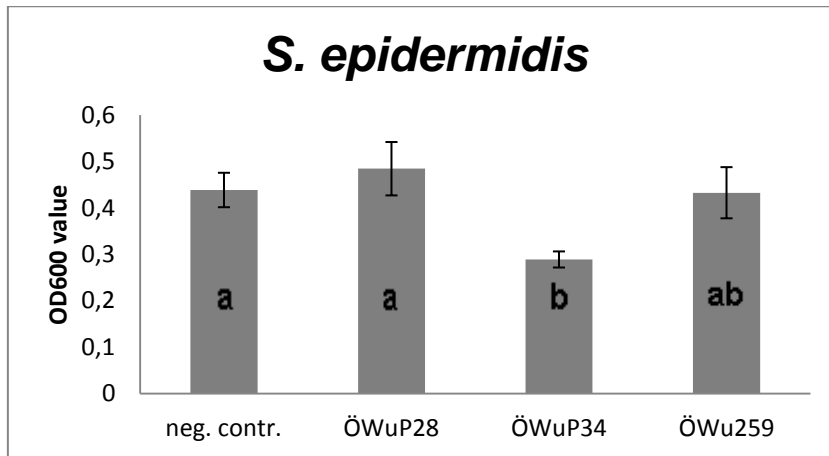


Figure 3.23 – *Pseudomonas chlororaphis* OeWuP28 and *Pseudomonas chlororaphis* OeWu259 did not affect the growth of *S. epidermidis*, though it was significantly decreased by *Pseudomonas chlororaphis* OeWuP34. Different letters represent significant differences between respective mean values (ANOVA, Tukey-HSD, $P \leq 0.05$).

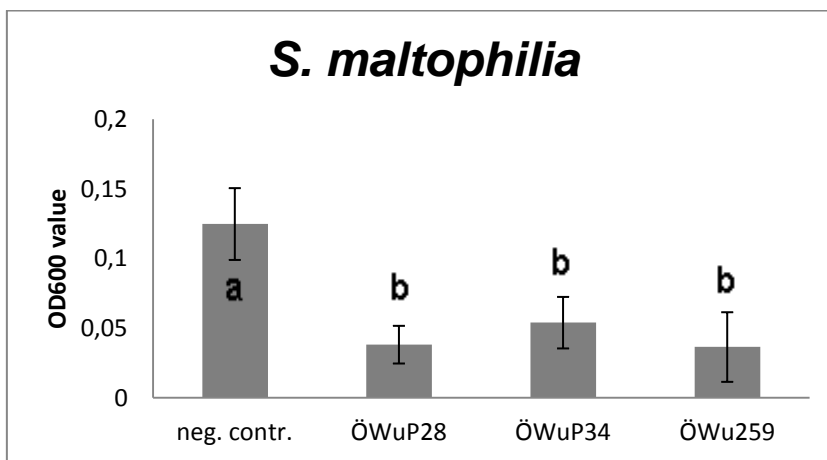


Figure 3.24 – All *Pseudomonas chlororaphis* strains inhibited the growth of *S. maltophilia* significantly. Different letters represent significant differences between respective mean values (ANOVA, Tukey-HSD, $P \leq 0.05$).

Several *Pseudomonas chlororaphis* strains inhibited the growth of *K. pneumoniae* and *C. albicans* with differing severity (Fig. 3.24 and Fig. 3.25). Again the pathogen inhibition showed to be very strain specific with high differences in the observable efficacy.

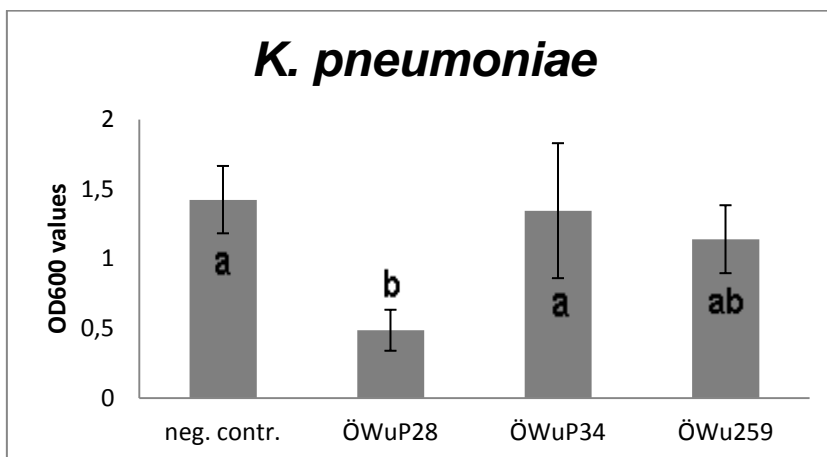


Figure 3.25 – *Pseudomonas chlororaphis* OeWuP34 didn't affect the growth of *K. pneumoniae*, though it was significantly decreased by *Pseudomonas chlororaphis* OeWuP28 and *Pseudomonas chlororaphis* OeWu259. Different letters represent significant differences between respective mean values (ANOVA, Tukey-HSD, $P \leq 0.05$).

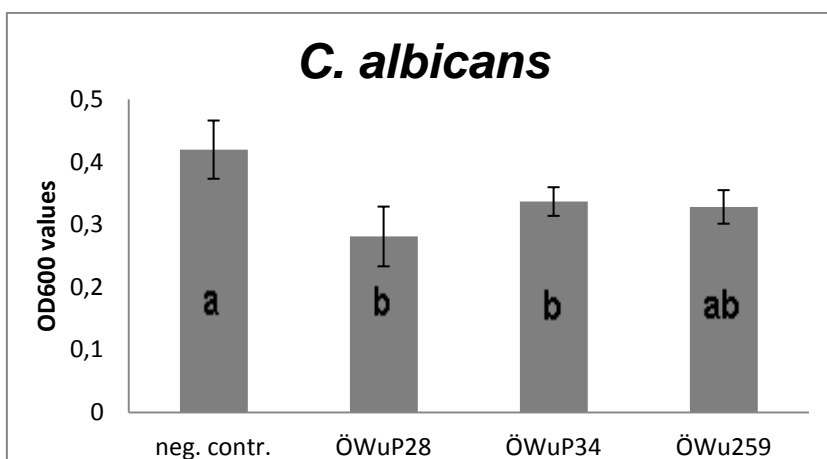


Figure 3.26 – *C. albicans* was inhibited by all *Pseudomonas chlororaphis* strains. The strongest inhibition could be observed with *Pseudomonas chlororaphis* OeWuP28. Different letters represent significant differences between respective mean values (ANOVA, Tukey-HSD, $P \leq 0.05$).

3.2.2 *Paenibacillus polymyxa* strains

Paenibacillus polymyxa strains proved to inhibit certain opportunistic pathogens by VOCs production, while other clean room and hospital related pathogens were not affected. *S. aureus* could not be inhibited efficiently in two different approaches. Interestingly both attempts resulted in a better viability of *S. aureus* which was not dependent on the growth conditions (Fig. 3.27 and Fig. 3.28).

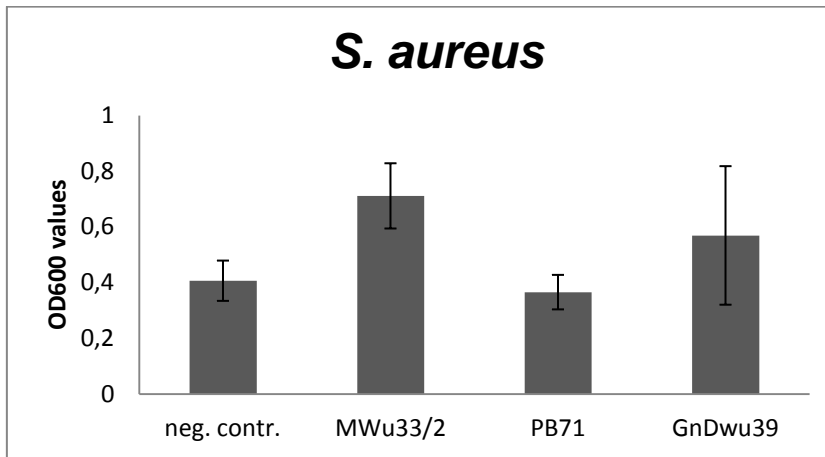


Figure 3.27 – *S. aureus* showed a thoroughly high viability after incubation in the VOCs assay with different *Paenibacillus polymyxa* strains. Error bars indicate the standard deviation of respective mean values.

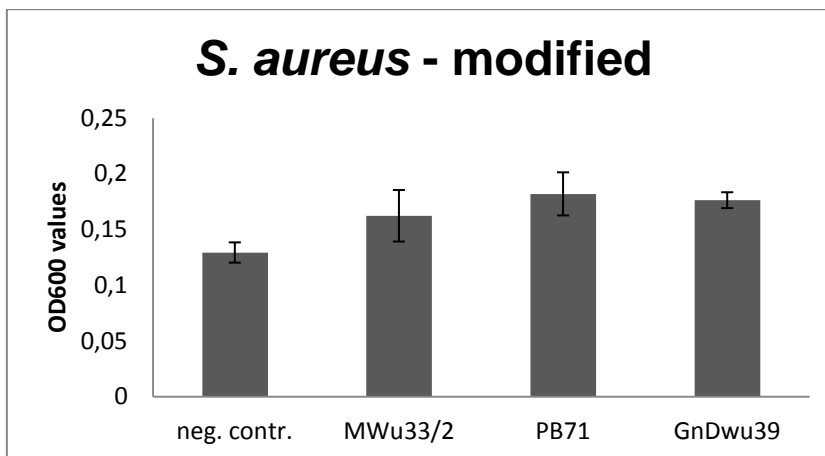


Figure 3.28 – The modified approach with media limitations confirmed the increased viability of *S. aureus* after incubation with different *Paenibacillus polymyxa* strains. Error bars indicate the standard deviation of respective mean values.

S. epidermidis was not affected by the antagonistic *Paenibacillus polymyxa* isolates through the gas phase. The viability remained stable irrespective the particular strains (Fig. 3.29). In contrast *S. maltophilia* showed a decreased viability after the treatment. The observed amplitude of growth reduction was strain specific (Fig. 3.30).

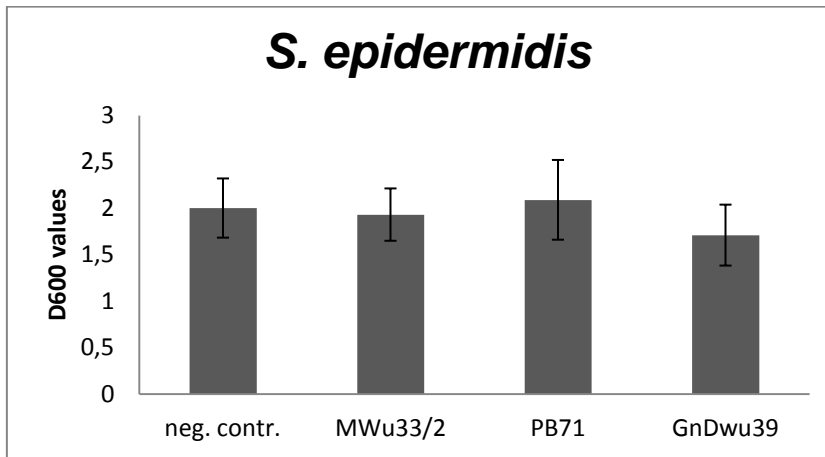


Figure 3.29 – None of the tested *Paenibacillus polymyxa* strains could inhibit the growth of *S. epidermidis* significantly in the VOCs assay. Error bars indicate the standard deviation of respective mean values.

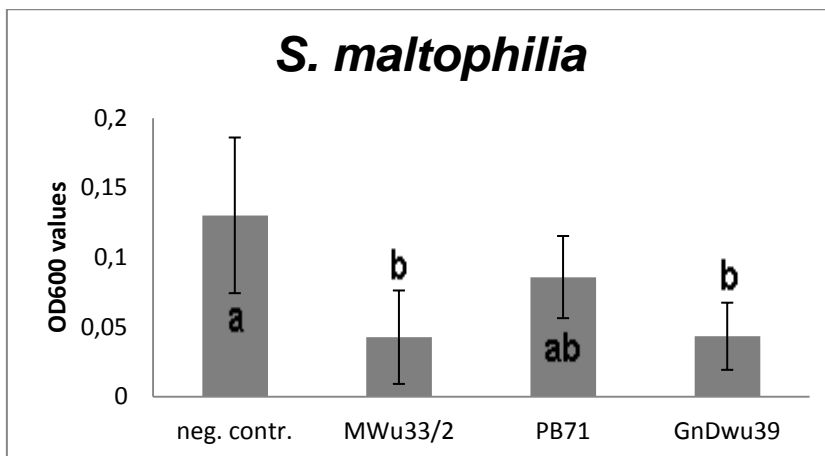


Figure 3.30 – All *Paenibacillus polymyxa* strains reduced the growth of *S. maltophilia*. The highest reduction was observed after incubation with *Paenibacillus polymyxa* MWu33/2 and *Paenibacillus polymyxa* GnDWu39. Different letters represent significant differences between respective mean values (ANOVA, Tukey-HSD, $P \leq 0.05$).

Incubation of *K. pneumoniae* with three different *Paenibacillus polymyxa* strains did not result in a significant growth reduction. The overall pathogen viability was increased in comparison to the negative control (Fig. 3.31). In contrast assays with *C. albicans* showed that two different *Paenibacillus polymyxa* strains were able to reduce the cell viability (Fig. 3.32).

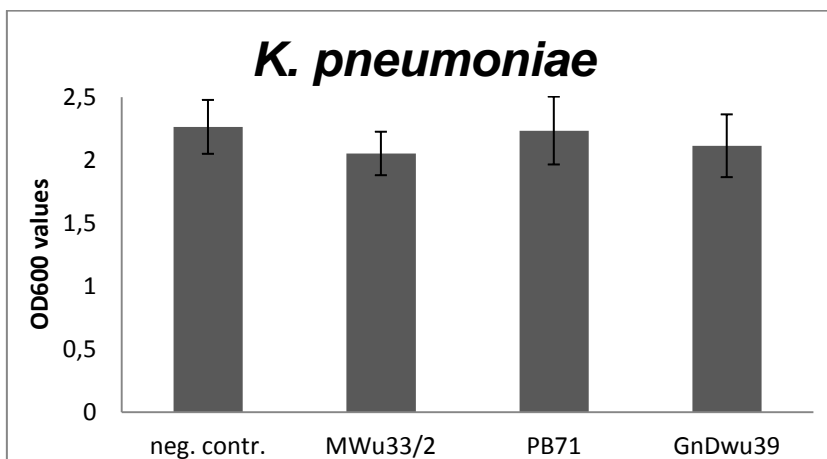


Figure 3.31 – The pathogen viability was not reduced by any of the tested *Paenibacillus polymyxa* strains in this approach. Error bars indicate the standard deviation of respective mean values.

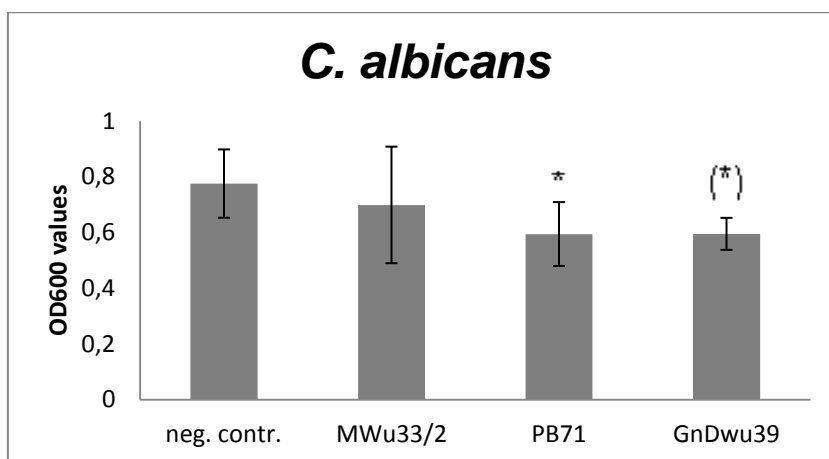


Figure 3.32 - *Paenibacillus polymyxa* PB71 and *Paenibacillus polymyxa* GnDWu39 resulted in a significantly lower viability of *C. albicans* compared to the negative control. A T-test was used to determine the significance with *P=0.037 and (*)P=0.016.

3.2.3 Synthetic pyrazines I

Synthetic 5-sec-butyl-2,3-dimethylpyrazine was used to evaluate possible effects on two different Gram-negative bacteria. *S. aureus* and *S. epidermidis* were not influenced by the volatile fraction of this pyrazine after an incubation of 48 hours (Fig. 3.33 and Fig. 3.34).

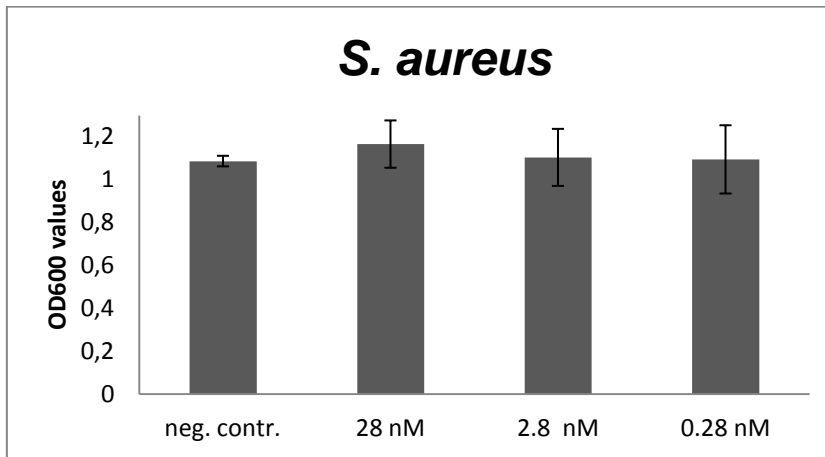


Figure 3.33 – *S. aureus* was not affected by 5-sec-butyl-2,3-dimethylpyrazine compared to the negative control. Even undiluted pyrazine (28 nM) did not decrease the pathogen viability. Error bars indicate the standard deviation of respective mean values.

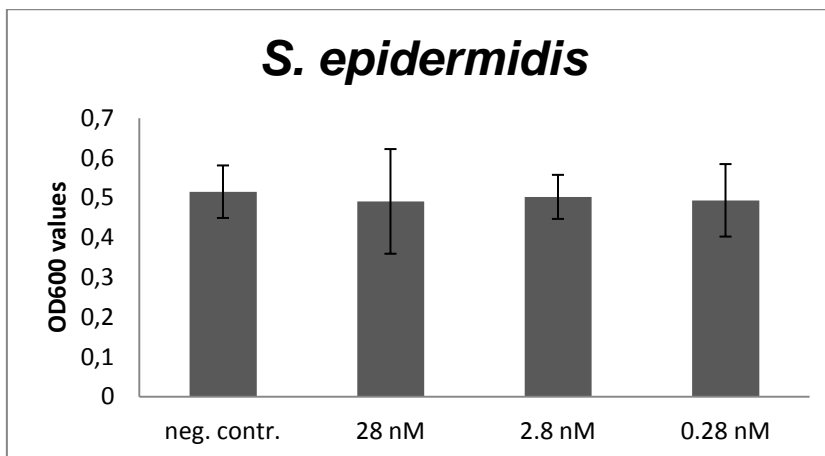


Figure 3.34 – The viability of *S. epidermidis* remained unaltered after exposure to different 5-sec-butyl-2,3-dimethylpyrazine dilutions. Error bars indicate the standard deviation of respective mean values.

The Gram-positive bacterium *S. maltophilia* was strongly inhibited by 5-sec-butyl-2,3-dimethylpyrazine in the related assays. A growth reduction was observable without an OD₆₀₀ determination in 12-well plates (Fig. 3.35). Additionally a viability test confirmed the high growth reduction by the synthetic pyrazine (Fig. 3.36). A second approach was done to identify the lowest pyrazine concentration to have an effect on the selected strains. The results give evidence that even very low VOCs concentrations resulting from 5 nL (0.028 nM) fluid pyrazine in one well of a standard 12-well plate can inhibit *S. maltophilia* significantly (Fig. 3.37).

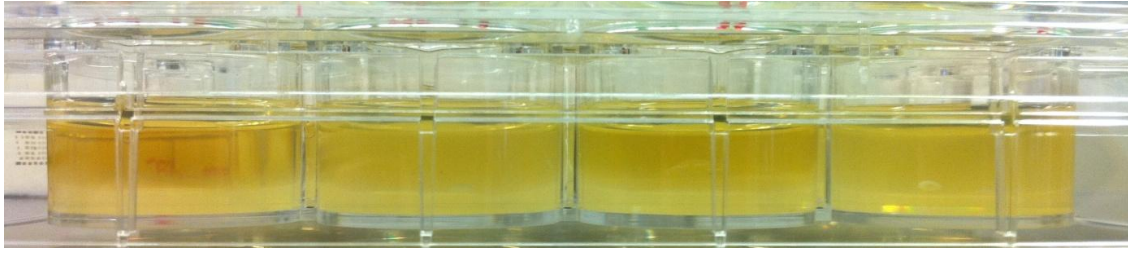


Figure 3.35 - The viability test demonstrated the antimicrobial effect of 5-sec-butyl-2,3-dimethylpyrazine on *S. maltophilia*. 28 nM pyrazine (left well) reduces bacterial viability drastically, while 0.28 nM pyrazine (right well) shows less effect on it. The negative control (second well from left) shows the highest bacterial growth indicated by intense clouding of the media.

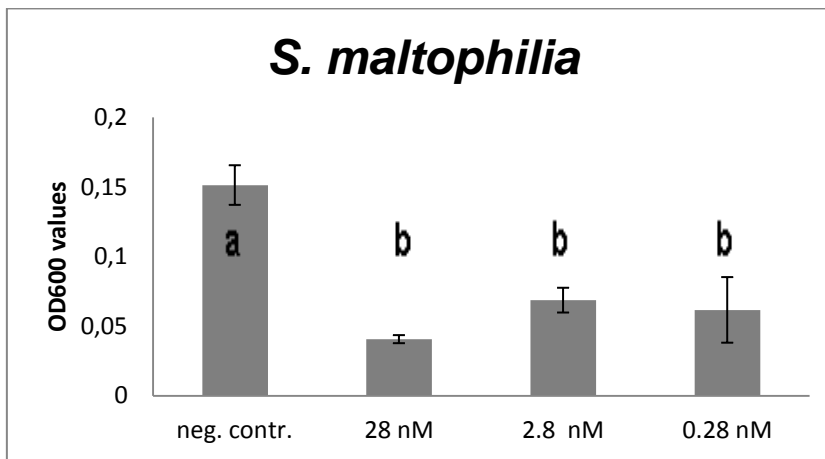


Figure 3.36 – All applied pyrazine concentrations reduced the viability of *S. maltophilia*. Low concentrations showed still a high impact on cell growth. Different letters represent significant differences between respective mean values (ANOVA, Tukey-HSD, $P \leq 0.05$).

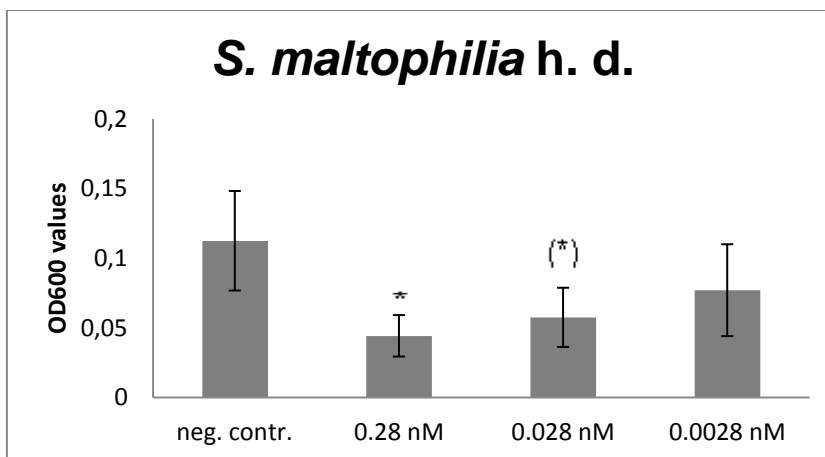


Figure 3.37 – The lowest pyrazine concentration that inhibited *S. maltophilia* growth significantly compared to the negative control was 0.028 nM. A T-test was used to determine the significance with * $P=0.023$ and (*) $P=0.053$.

The second Gram-positive bacterium *K. pneumoniae* was inhibited by 5-sec-butyl-2,3-dimethylpyrazine at high concentrations. A constantly decreasing efficiency was observed at higher dilutions (Fig. 3.38). Furthermore the fungal microorganism *C. albicans* was not inhibited by the applied pyrazine; the viability after incubation was comparable with the negative control (Fig. 3.39).

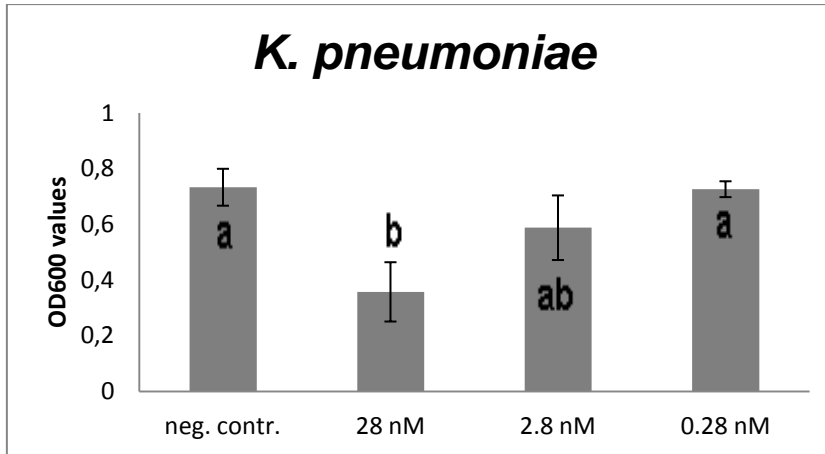


Figure 3.38 – Inhibition of *K. pneumoniae* was observed with 28 nM and 2.8 nM 5-sec-butyl-2,3-dimethylpyrazine. Different letters represent significant differences between respective mean values (ANOVA, Tukey-HSD, $P \leq 0.05$).

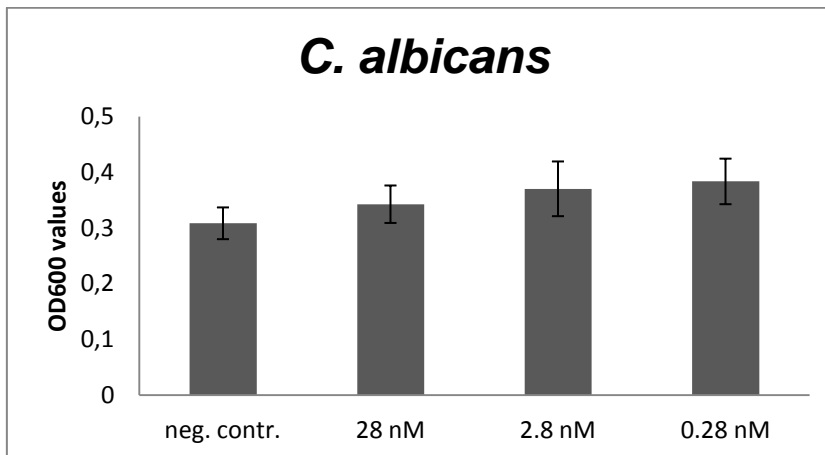


Figure 3.39 – The viability of *C. albicans* was not decreased by 5-sec-butyl-2,3-dimethylpyrazine in the VOCs assay. Error bars indicate the standard deviation of respective mean values.

3.2.4 Synthetic pyrazines II

Three opportunistic pathogens that have either shown to be inhibited by *Paenibacillus polymyxa* isolates or by 5-sec-butyl-2,3-dimethylpyrazine were incubated with an isomeric pyrazine derivative under the same conditions. The growth of *S. maltophilia* was highly reduced and the viability test confirmed an inhibition by 5-isobutyl-2,3-dimethylpyrazine (Fig. 3.40).

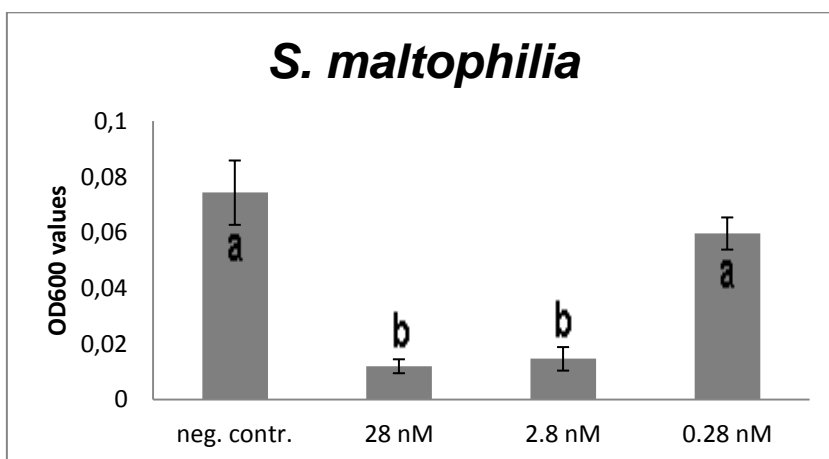


Figure 3.40 – The growth of *S. maltophilia* was significantly decreased after incubation with 5-isobutyl-2,3-dimethylpyrazine. Different letters represent significant differences between respective mean values (ANOVA, Tukey-HSD, $P \leq 0.05$).

Undiluted 5-isobutyl-2,3-dimethylpyrazine reduced the growth of *K. pneumoniae* and *C. albicans* while higher dilutions did not show a significant decrease of living pathogens (Fig. 3.41 and Fig. 3.42).

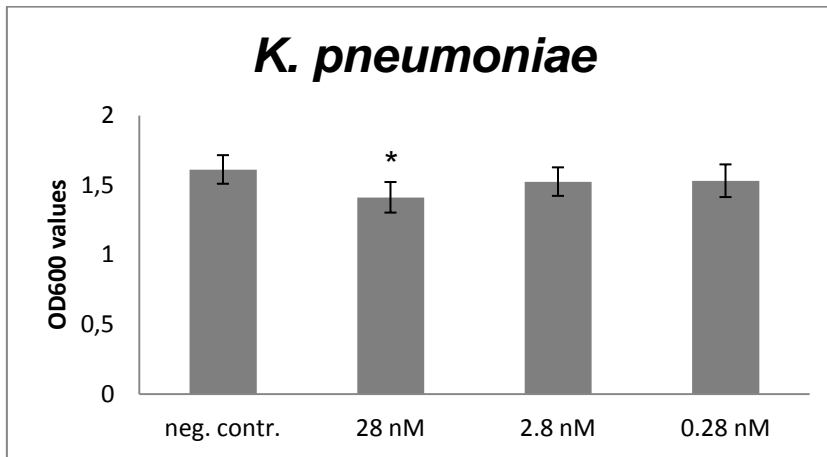


Figure 3.41 – Undiluted 5-isobutyl-2,3-dimethylpyrazine inhibited the growth of *K. pneumoniae* significantly, while 2.8 nM and 0.28 nM concentrations did not affect the living-cell concentration compared to the negative control. A T-test was used to determine the significance with *P=0.028.

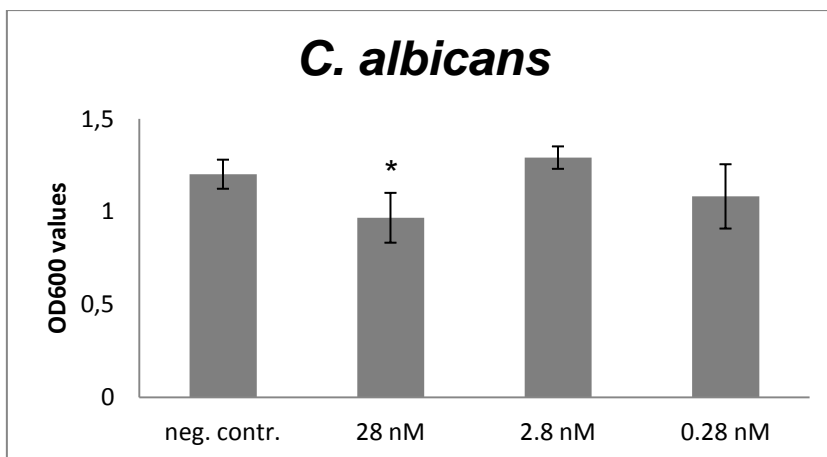


Figure 3.42 – *C. albicans* was inhibited by 28 nM pyrazine significantly, while higher dilutions did not decrease bacterial growth. A T-test was used to determine the significance with *P=0.046.

3.3 GC-MS identification and characterization of bacterial VOCs

An adapted GC-MS headspace SPME method was utilized to identify all occurring VOCs in the gas phase of different *Pseudomonas chlororaphis* and *Paenibacillus polymyxa* strains. For this reason some adjustments were done to ensure the most suitable method and hardware for an ideal identification. Furthermore the pyrazine production of different *Paenibacillus polymyxa* isolates was quantified using synthetic standards. All isolates were ranked by their relative pyrazine production in a supplementary approach. In the final step a new experimental design was utilized to study contact-free antagonist-pathogen interaction in the gas phase.

3.3.1 Comparison of different GC-MS headspace SPME fibers and methods

The first approaches were based on a 2 cm SPME headspace fiber and a 1:20 split injection. Most VOCs with a low abundance were masked by the background signal and therefore hardly to detect (Fig. 3.43). Later a 1 cm SPME headspace fiber with a different material composition was tested using a 1:20 split injection. The achieved results allowed an enhanced identification of bacterial VOCs (Fig. 3.44). Nevertheless the best results were achieved with a 1 cm SPME headspace fiber combined with a splitless method. Profiles recorded with this hardware and settings were suitable to cover the identification of most present bacterial VOCs.

Results

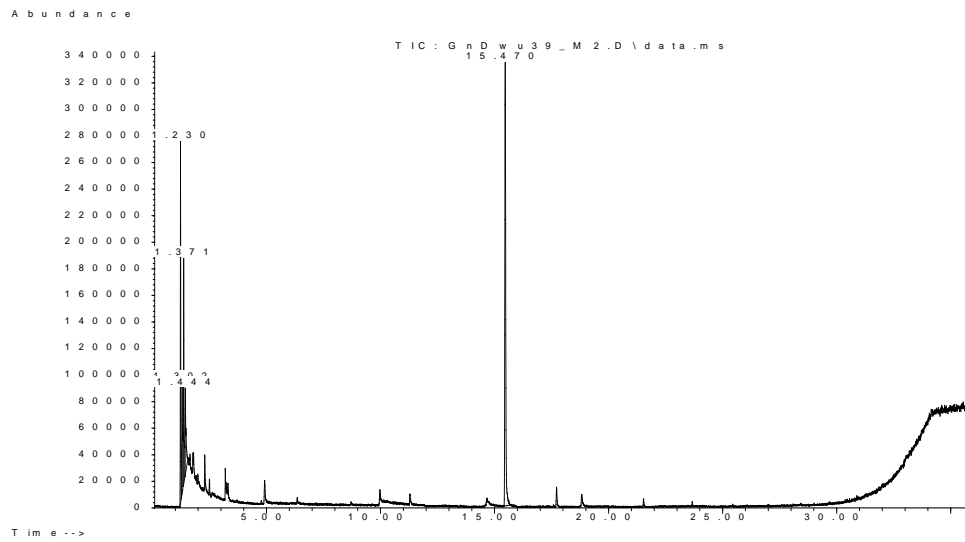


Figure 3.43 – The *Paenibacillus polymyxa* GndWu39 VOCs profile was achieved with a 50/30 μm Divinylbenzen/CarboxenTM/Polydimethylsiloxane (PDMS) 2 cm Stableflex/SS SPME headspace fiber and a 1:20 split injection.

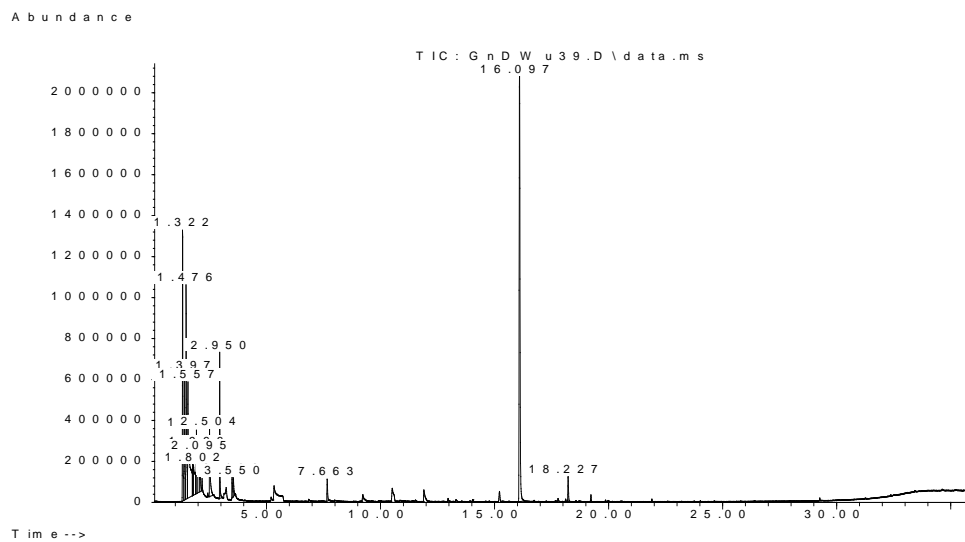


Figure 3.44 – An improved *Paenibacillus polymyxa* GndWu39 VOCs profile was achieved with an 85 μm CarboxenTM/Polydimethylsiloxane (PDMS) 1 cm Stableflex/SS SPME headspace fiber and a 1:20 split injection.

Results

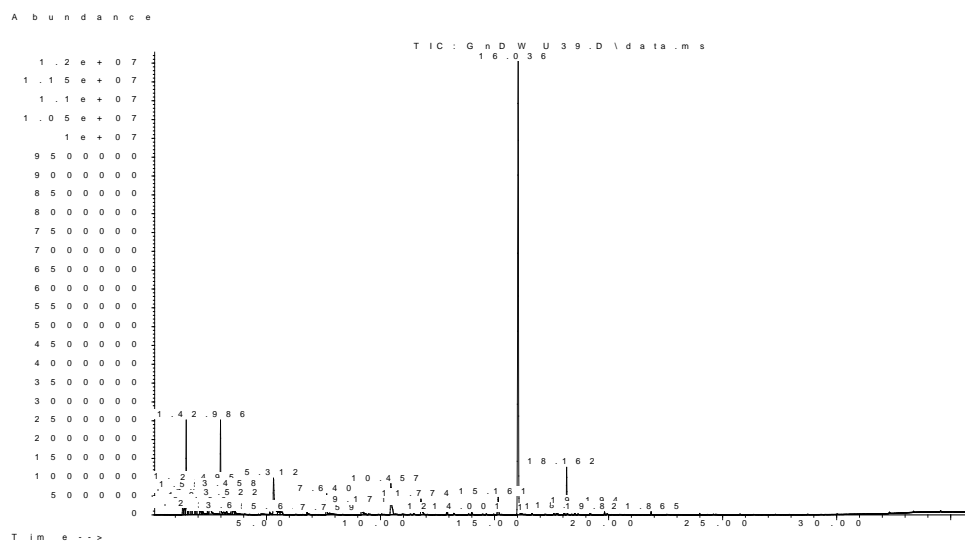


Figure 3.45 – The highest performance was achieved with a 50/30 μm Divinylbenzen/CarboxenTM/Polydimethylsiloxane (PDMS) 1 cm Stableflex/SS SPME headspace fiber and a splitless injection.

3.3.2 Identification of VOCs originating from LB-agar and GC-column

The gas phase above LB-agar contains specific VOCs that are formed without the presence of microorganisms. Therefore it was necessary to subtract them from bacterial profiles. Several chromatograms resulting from tempered LB-agar were used to identify those compounds (Fig. 3.46). Further all methylated siloxane compounds were listed that originate from the GC-column (Table 3.1).

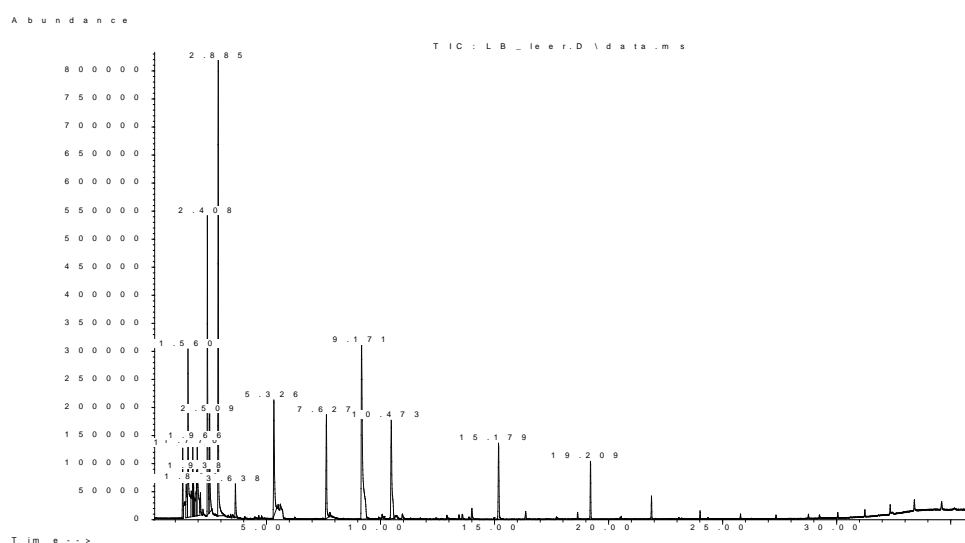


Figure 3.46 – VOCs from tempered LB-agar result in a specific chromatogram.

Table 3.1 – All detectable volatile substances are listed by their specific retention time. Siloxane compounds originate from the GC-column, other compounds like acetone originate from tempered LB-agar.

Volatile Compounds in LB-agar	
RT [min.]	Compound
1,323	Carbon dioxide
1,478	Hydroxyurea
1,562	Acetone
1,767	Propanal, 2-methyl-
1,8	Silanol, trimethyl-
1,935	Butanal
1,967	Ethene, ethoxy-
2,102	Trichloromethane
2,411	Butanal, 3-methyl-
2,508	Butanal, 2-methyl-
2,875	Silenediol, dimethyl-
5,333	Cyclotrisiloxane, hexamethyl-
7,631	Oxime-, methoxy-phenyl-
9,182	Benzaldehyde
10,483	Cyclotetrasiloxane, octamethyl-
15,188	Cyclopentasiloxane, decamethyl-
19,217	Cyclohexasiloxane, dodecamethyl-

3.3.3 Identification of VOCs from *Pseudomonas chlororaphis* strains

The adapted GC-MS method was used to evaluate VOCs production of different *Pseudomonas chlororaphis* strains. Profiles of *Pseudomonas chlororaphis* OeWuP28, *Pseudomonas chlororaphis* OeWuP34 and *Pseudomonas chlororaphis* OeWu259 were generated. All utilized strains showed similar chromatograms with analog abundances (Fig. 3.47). Remarkably a production of various sulfur containing substances could be observed. Additionally two alkenes appeared at higher retention times (Tab. 3.2). Both of these substance groups are classified as highly toxic or at least irritating.

Results

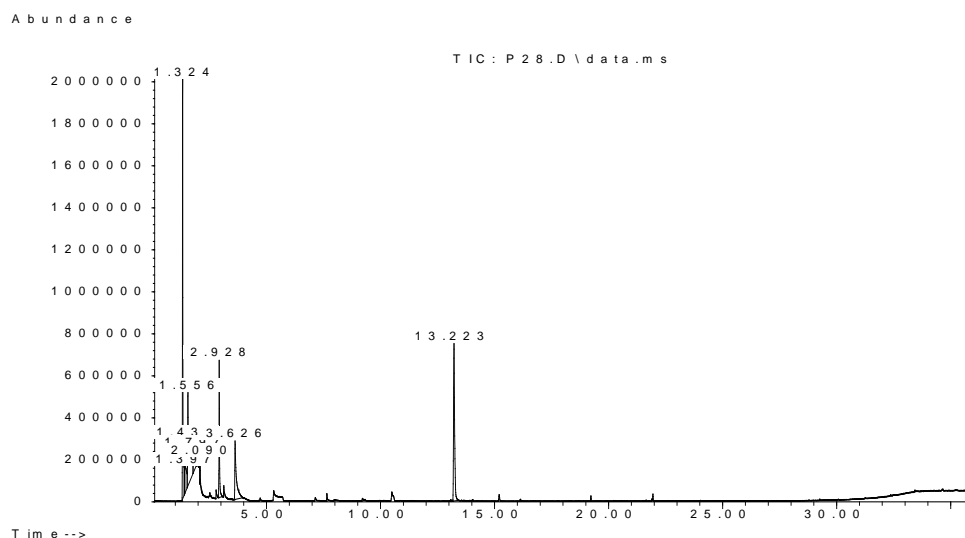


Figure 3.47 – Profiles of *Pseudomonas chlororaphis* strains contain a specific 1-undecene peak at RT 13.2 min.

Table 3.2 – VOCs produced by different *Pseudomonas chlororaphis* strains are shown. Compounds with a non-bacterial origin are indicated separately.

<i>Pseudomonas chlororaphis</i>		
RT [min.]	Substance name	Source
1,433	Methanethiol	Bacterial
1,793	Hydrazinecarboxamide	Bacterial
2,907	Mercaptoacetone	Bacterial
3,126	Thiocyanic acid, methyl ester	Bacterial
3,628	Disulfide, dimethyl-	Bacterial
7,142	1-Nonene	Bacterial
13,212	1-Undecene	Bacterial
1,323	Carbon dioxide	Partly Bacterial
1,555	Acetone	LB-agar
1,961	Ethene, ethoxy-	LB-agar
5,314	Cyclotrisiloxane, hexamethyl-	Column/Fiber
2,089	Trichloromethane	Column/Inlet
2,926	Silenediol, dimethyl-	Column/Fiber
10,483	Cyclotetrasiloxane, octamethyl-	Column/Fiber
15,188	Cyclopentasiloxane, decamethyl-	Column/Fiber
19,217	Cyclohexasiloxane, dodecamethyl-	Column/Fiber

3.3.4 Identification of VOCs from *Paenibacillus polymyxa* strains

Paenibacillus polymyxa profiles showed specific patterns with peaks of variable abundances (Fig. 3.48). The production of various volatile alcohols and aldehydes by the investigated strains was observed. Furthermore three different pyrazines could be identified in the gas phase of all strains (Tab. 3.3). The identification of 2-methyl-5-(1-methylethyl)-pyrazine and 2-(2-Methylpropyl)-3-(1-methylethyl)-pyrazine was unambiguous, while 2,3,4-trimethyl-5-propyl-pyrazine had to be confirmed within a process of elimination. *Paenibacillus polymyxa* was first streaked out together with synthetic 5-isobutyl-2,3-dimethylpyrazine (Fig. 3.49) and then with synthetic 5-sec-butyl-2,3-dimethylpyrazine (Fig. 3.50). Both attempts resulted in additional peaks with a distinctive retention time. Therefore the final identification was done by spectral comparison with the NIST08 database. Notably the overall amount of identified VOCs was high compared to other bacteria.

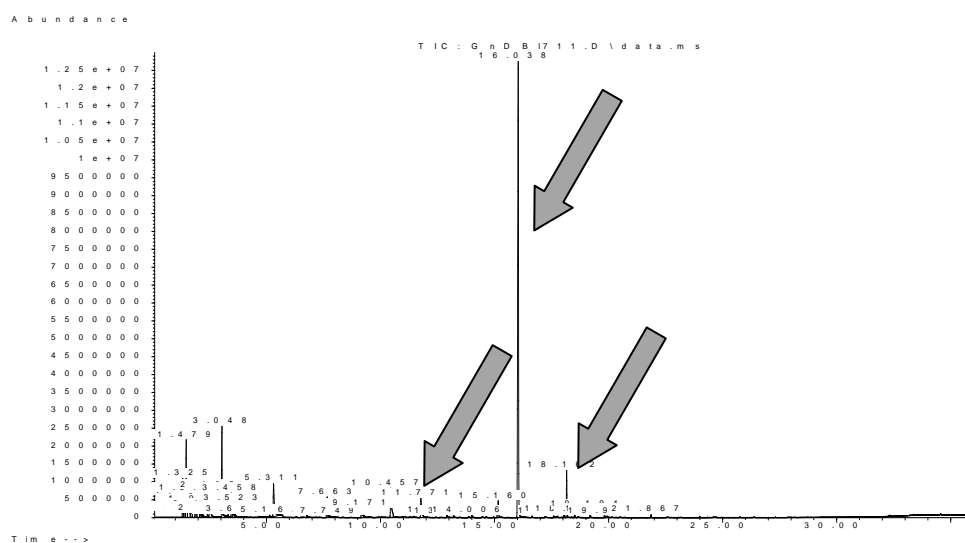


Figure 3.48 – A typical *Paenibacillus polymyxa* profile recorded with strain PB71. Three detected pyrazine peaks are indicated with arrows.

Results

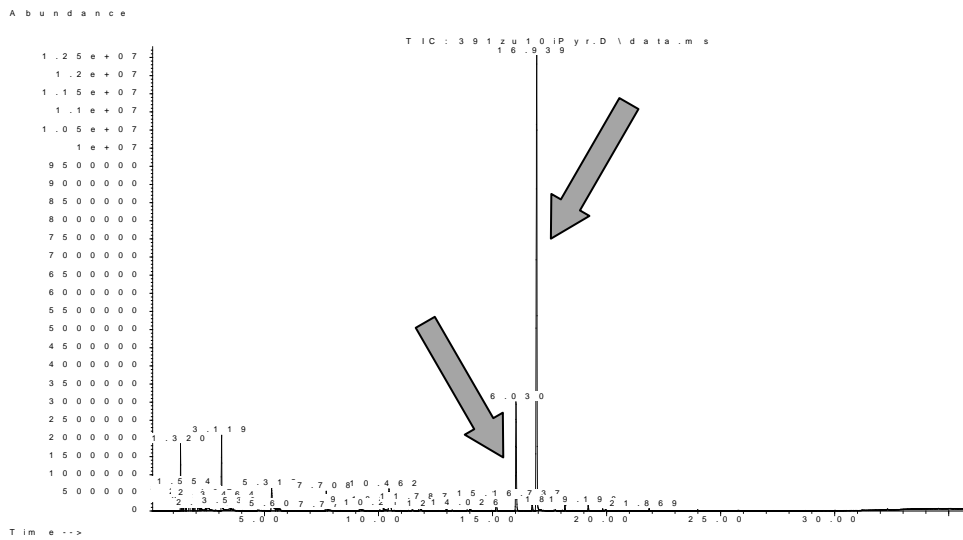


Figure 3.49 – 5-isobutyl-2,3-dimethylpyrazine addition to *Paenibacillus polymyxa* GndWu39 did not result in an overlay of the relating peaks. Two distinct pyrazine peaks are indicated with arrows. The peaks do not derive from the same substance.

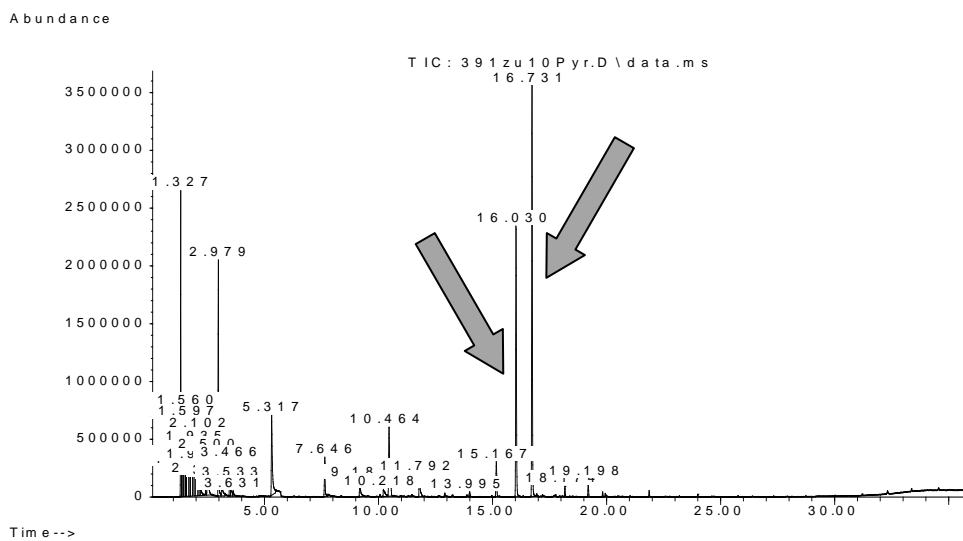


Figure 3.50 - *Paenibacillus polymyxa* GndWu39 together with 0.5 µL of synthetic 5-isobutyl-2,3-dimethylpyrazine resulted in two distinct peaks. The indicated peaks did not derive from the same substance.

Table 3.3 – A broad range of different VOCs was identified in the gas phase of *Paenibacillus polymyxa* strains. Compounds with a non-bacterial origin are indicated separately.

<i>Paenibacillus polymyxa</i>		
RT [min.]	Substance name	Source
1,400	Acetaldehyde	Bacterial
1,478	Ethanol	Bacterial
1,697	Hydroxyurea	Bacterial
1,767	Cycloserine	Bacterial
1,799	Glycine	Bacterial
1,935	Butanal	Bacterial
1,967	Ethene, etoxy-	Bacterial
2,173	1-Propanol, 2-methyl-	Bacterial
2,501	1-Butanol	Bacterial
3,145	2-Butanone, 3-hydroxy-	Bacterial
3,473	1-Butanol, 2-ethyl-	Bacterial
3,537	1-Butanol, 2-methyl-	Bacterial
7,631	Oxime-, methoxy-phenyl-	Bacterial
9,202	Benzaldehyde	Bacterial
11,815	Pyrazine, 2-methyl-5-(1-methylethyl)-	Bacterial
16,076	Pyrazine, 2,3,4-trimethyl-5-propyl-	Bacterial
18,194	Pyrazine, 2-(2-Methylpropyl)-3-(1-methylethyl)-	Bacterial
1,317	Carbon dioxide	Partly bacterial
1,561	Acetone	LB-agar
2,102	Trichloromethane	Column/Inlet
2,874	Silanediol, dimethyl-	Column/Fiber
5,333	Cyclotrisiloxane, hexamethyl-	Column/Fiber
10,489	Cyclotetrasiloxane, octamethyl-	Column/Fiber
15,194	Cyclopentasiloxane, decamethyl-	Column/Fiber
19,217	Cyclohexasiloxane, dodecamethyl-	Column/Fiber

Additional *Paenibacillus* species described by Cardinale et al. (2006) were analyzed with the established GC-MS headspace SPME method. *Paenibacillus pabuli* Bint1 and *Paenibacillus amylyticus* Eint1a produced the same volatile pyrazines that were observed with *Paenibacillus polymyxa* strains.

3.3.5 Comparison of pyrazine production between different *Paenibacillus* spp.

Pyrazine emission is both species-specific and strain-specific. *Paenibacillus polymyxa* isolates from different habitats showed to produce distinctive amounts of volatile pyrazines. All available species and strains were analyzed with an adapted GC-MS headspace SPME method and the peak areas were recorded. Absolute peak area values of pyrazines were divided with the corresponding carbon dioxide area values to get relative values in each case. Isolates from the desert soil, *Paenibacillus kribbensis* Sb3-1 and *Paenibacillus brasilensis* Mc2-9 produced significantly higher pyrazine amounts than *Paenibacillus polymyxa* GnDWu39 and *Paenibacillus polymyxa* PB71 from moderate agricultural crop lands in Styria (Figure 3.51).

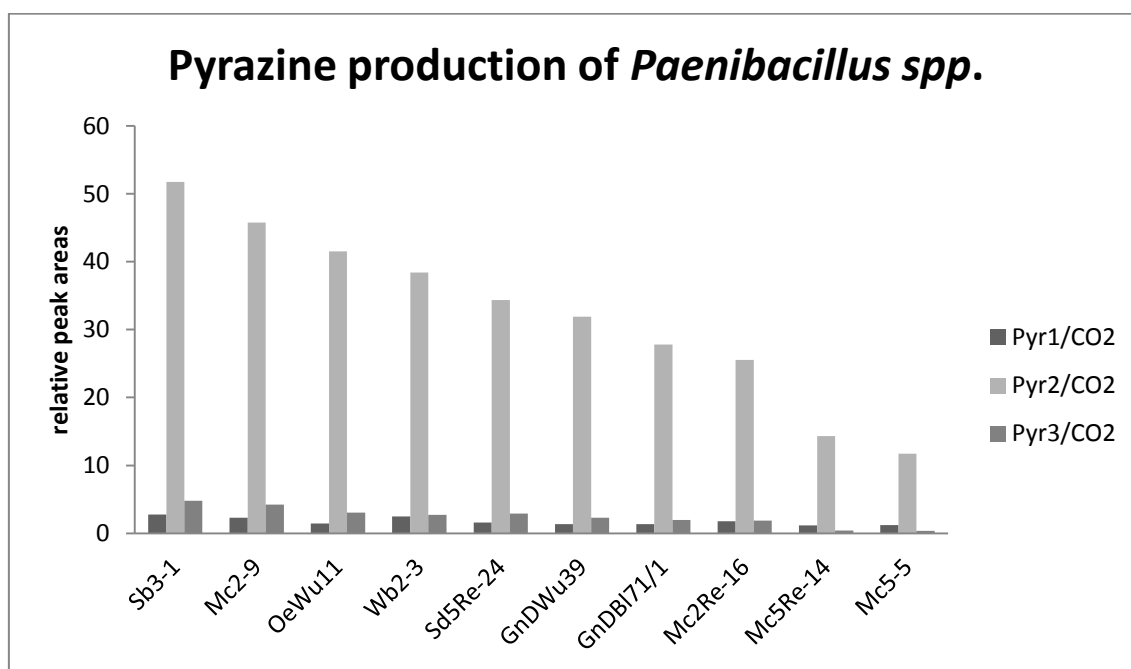


Figure 3.51 – *Paenibacillus* species were sorted regarding to their relative pyrazine production. The highest amounts were produced by a *Paenibacillus kribbensis* strain.

Pyr1 = 2-methyl-5-(1-methylethyl)-pyrazine

Pyr2 = 2,3,4-trimethyl-5-propyl-pyrazine

Pyr3 = 2-(2-Methylpropyl)-3-(1-methylethyl)-pyrazine

3.3.6 GC-MS quantification of volatile pyrazines

Synthetic 5-sec-butyl-2,3-dimethylpyrazine was used as a standard to enable bacterial pyrazine quantification with the utilized GC-MS headspace SPME method. Peak areas of different dilutions were recorded within three separate repeats (Tab. 3.4). The achieved data was used to construct a calibration curve (Fig. 3.52). This allowed a quantification of pyrazines produced by different *Paenibacillus* species and *Paenibacillus polymyxa* strains.

Table 3.4 – Different 5-sec-butyl-2,3-dimethylpyrazine dilutions were used to determine the corresponding peak areas.

1st GC-MS analysis		2nd GC-MS analysis		3rd GC-MS analysis	
Dilution	Peak Area	Dilution	Peak Area	Dilution	Peak Area
1:100	375388615	1:100	517514121	1:100	409489220
1:1000	34184407	1:1000	14292250	1:1000	38081950
1:10000	2392747	1:10000	1121814	1:10000	3075631
1:100000	158398	1:100000	102067	1:100000	52148
1:1000000	29237	1:1000000	34147	1:1000000	25570

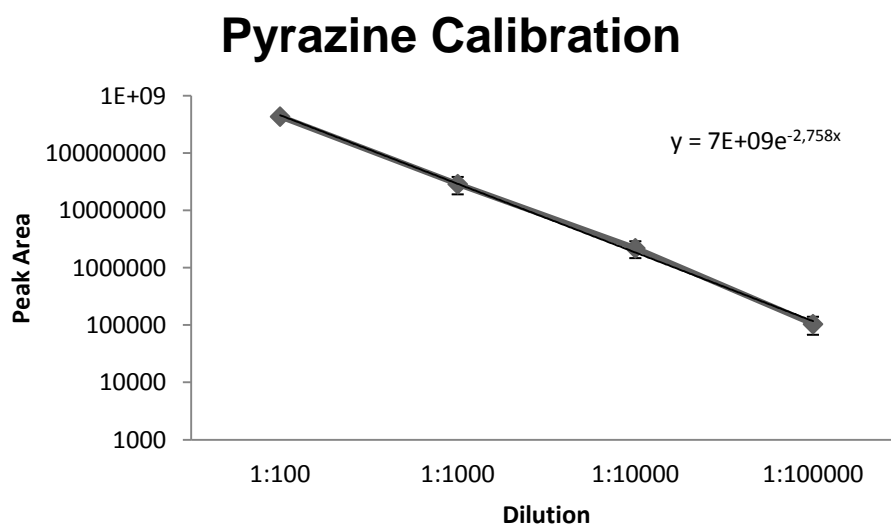


Figure 3.52 – A calibration curve was constructed with mean values of 3 different data sets. The data points were log-transformed for a better display.

The resulting formula of the pyrazine calibration was used to calculate the amount of produced pyrazines by different *Paenibacillus spp.* isolates. Determined pyrazine concentrations were in the range of 0.4 ng and 8.2 ng per cm² growth media (Tab. 3.5).

Table 3.5 – The concentrations were calculated by using the calibration curve created with a 5-sec-butyl-2,3-dimethylpyrazine standard.

Strain	Pyrazine concentration [ng/cm ²]		
	Pyr1	Pyr2	Pyr3
Sb3-1	0.8	8.2	1
Mc2-9	0.6	6.8	0.8
OeWu11	0.6	7	0.7
Wb2-3	0.9	8.6	0.9
Sd5Re-24	0.7	7.4	0.8
GnDWu39	0.6	3.3	0.7
PB71	0.6	6.6	0.7
Mc2Re-16	0.7	5.6	0.7
Mc5Re-14	0.5	1.7	0.4
Mc5-5	0.5	1.4	0.4

Pyr1 = 2-methyl-5-(1-methylethyl)-pyrazine

Pyr2 = 2,3,4-trimethyl-5-propyl-pyrazine

Pyr3 = 2-(2-Methylpropyl)-3-(1-methylethyl)-pyrazine

3.3.7 Co-cultivation experiments with *Paenibacillus polymyxa* GnDWu39

The effect of VOCs on different pathogens, which were grown together with an antagonist in the same gas phase, was studied with *Paenibacillus polymyxa* GnDWu39. An increase of 2,3,4-trimethyl-5-propyl-pyrazine production was observed with *Staphylococcus aureus*, *Stenotrophomonas maltophilia* and *Candida albicans*. The utilized *Paenibacillus polymyxa* strain produced 10% more of this distinct pyrazine compared to the negative control where no pathogens were present in the gas phase (Fig. 3.53).

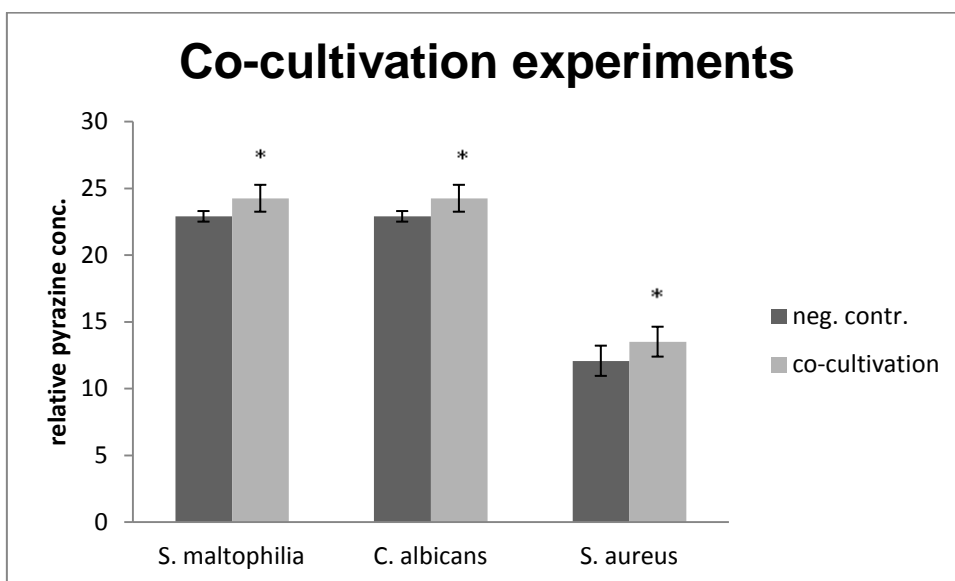


Figure 3.53 – An increase of 2,3,4-trimethyl-5-propyl-pyrazine production was observed after pathogen exposition in the gas phase of *Paenibacillus polymyxa* GnDWu39. The error bars indicate a confidence interval within * $P \leq 0.05$.

3.4 Random mutagenesis of *Pseudomonas chlororaphis* P28

The Gram-negative isolate exhibited a notable VOCs-derived antagonistic potential against various opportunistic pathogens. Therefore different strategies were developed to enable identification of effective substances. Mutants with deficiencies in random gene regions could serve as indicators for essential gene products. A Kanamycin-resistance gene was randomly inserted into the genome of *Pseudomonas chlororaphis* P28 by using an EZ-Tn5TM <KAN-2>Tnp TransposomeTM Kit. Insertion mutants were selected with LB-agar containing 25 $\mu\text{g}/\text{mL}$ Kanamycin. A negative control with wild type *Pseudomonas chlororaphis* P28 was carried out to show that growth is restricted on the selective medium. Both, the growth rate and morphological appearance of the mutants were comparable to the wild type strain grown on LB-agar. The yield of mutants was higher than 10^3 cfu/mL and therefore suitable for further experiments (Fig. 3.54).

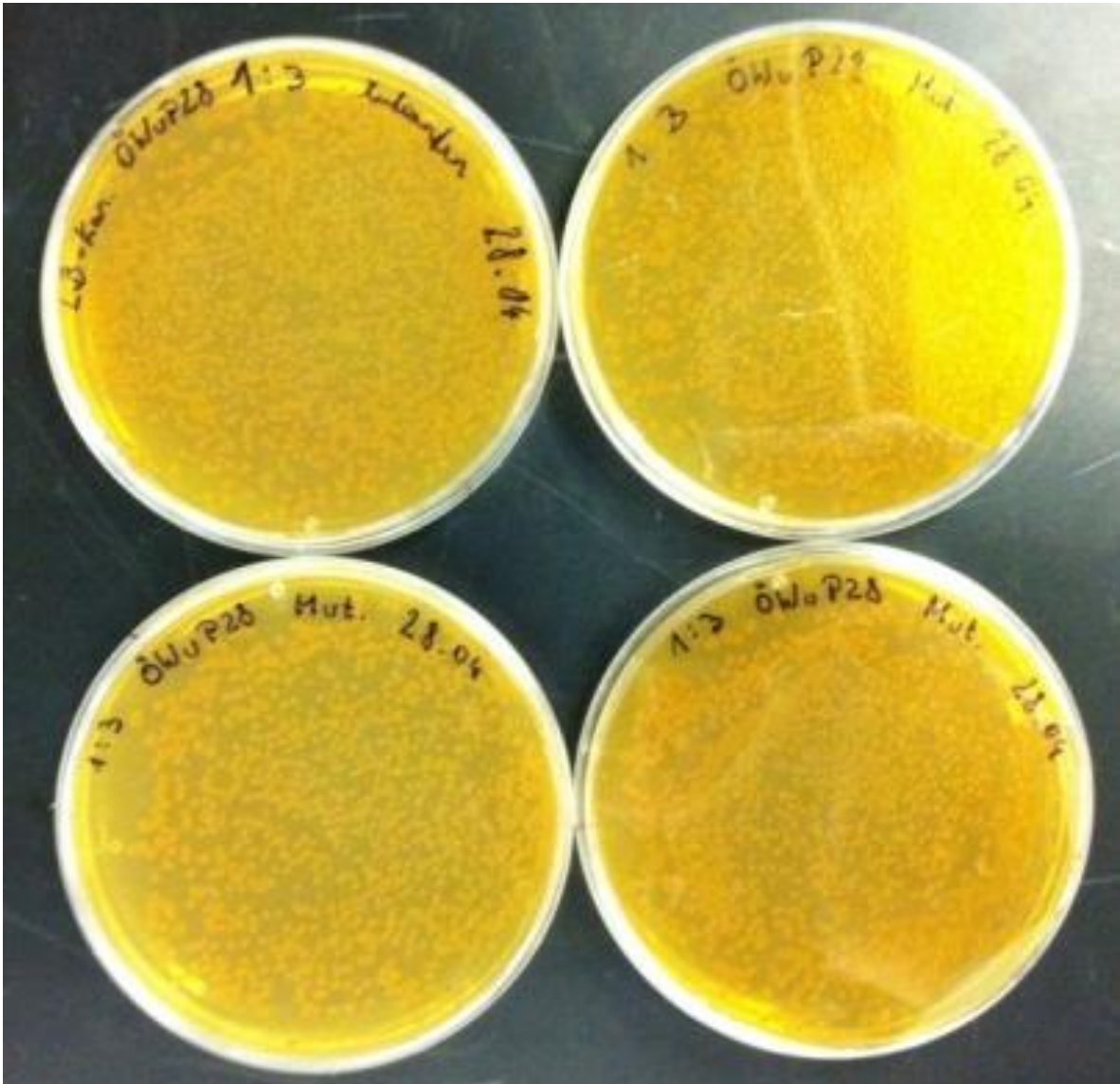


Figure 3.54 – Several selective LB-agar plates were obtained with a mutant growth density higher than 10^3 cfu/mL.

4 Discussion

4.1 First evaluation of antagonistic efficacy in microscopy approaches

The broad spectrum of pathogen inhibition by *Pseudomonas chlororaphis* OeWuP28 in VOCs dual-culture tests correlates with previous observations (Liebminger et al. 2011). However *S. epidermidis* was not affected by volatiles produced by this *Pseudomonas chlororaphis* strain. This could be explained by an attachment of pathogen cells to notches of the polyester fibers where the accessibility of VOCs is lowered. Liebminger et al. (2011) demonstrated this occurrence with gfp-tagged *S. epidermidis* 1457 and ION-NOSTAT VI.2 fabrics. Furthermore the time-dependent VOCs dual-culture test has proved a strong and fast developing inhibition of *S. aureus*, which could be advantageous in biocontrol approaches.

Paenibacillus polymyxa GnDWu39 presented a lower antagonistic potential compared to *Pseudomonas chlororaphis* OeWuP28. The cell growth of *S. maltophilia* and *C. albicans* was reduced while no effects were observable with other opportunistic pathogens. This might be the result of specific inhibition by *Paenibacillus polymyxa* derived VOCs. An inhibition of *S. aureus* was not given in the VOCs dual-culture tests and in the time-dependent experiment. The observations indicate that *S. aureus* is resistant toward emitted volatiles originating from *Paenibacillus polymyxa*. However earlier studies could show that diffusible antibiotics derived from this species can inhibit *S. aureus* growth (Seldin et al., 1999).

Lysobacter sp. MWu228 presented the lowest VOCs-based antagonistic potential in VOCs dual-culture tests. A time-consuming cultivation together with intense biofilm formation makes this strain less suitable for biocontrol attempts in non-agricultural fields. We decided for this reason to proceed with further experiments without utilization of *Lysobacter* sp. isolates.

4.2 Re-evaluation of antagonistic activity

Results from high-throughput VOCs assays confirmed the inhibitory effects that were already observed in VOCs dual-culture test and additionally allowed qualification of these results. Furthermore a strain-specificity regarding the severity of pathogen inhibition could be demonstrated. Both studies were not accessible with VOCs dual-culture tests only. A complementary adapted high-throughput VOCs assay with nutrient limitation was used to explore the growth inhibition of *S. aureus* under harsh conditions. *S. aureus* is known to have a good adaption ability which allows persistence in hostile environments (Hall-Stoodley et al., 2004). Nutrient limitation was proposed to either make the pathogen more susceptible to antagonistic VOCs or contrariwise induce a more persistent status by e.g. biofilm formation. The results obtained from modified VOCs high-throughput assays suggest that a change in the inhibition accessibility is not given compared to standard VOCs high-throughput assays. Such assays may present more similar growth conditions for opportunistic pathogens to clean room environments and could be therefore more suitable for such simulations.

4.3 Identification of novel bacteria-derived VOCs

The coating material of headspace SPME fibers has considerable influence on the adsorption of volatile compounds in the sample. Different materials with similar specifications are available on the market. We have compared three different headspace SPME fibers and two different sampling methods. Obtained bacterial profiles could demonstrate that 50/30 μm Divinylbenzen/CarboxenTM/Polydimethylsiloxane (PDMS) 1 cm Stableflex/SS SPME headspace fibers together with a splitless injection result in the best performance. The preliminary applied 1:20 split prevented a sufficient saturation of the GC-MS and the detection limit was not reached for less abundant VOCs.

VOCs profiles obtained with pure LB-agar revealed that different volatile substances are formed within 48 h of incubation. These substances interfere with bacterial VOCs and had to be subtracted manually for this reason. Additionally the GC column produced distinct molecules due to thermal processes. They can be

recognized by prominent silanol and siloxane residues. Furthermore trichloromethane, also known as chloroform, with unknown origin was detected in irrespective samples. The most feasible explanation is prior utilization as solvent in experiments and that it remained as residue in the GC column or inlet.

Pseudomonas chlororaphis strains produced different sulfur containing volatiles, but also 1-nonene as well as 1-undecen. This was already observed in earlier studies (Kai et al., 2006). Specific antimicrobial substances like phenazines, lipopeptides and phloroglucinols could not be detected in the gas phase conditioned by their high molecular weight. Therefore the observed antagonistic potential of *Pseudomonas chlororaphis* strains carried out through VOCs is suggested to be unspecific.

VOCs profiles gained with different *Paenibacillus polymyxa* strains contained different small organic molecules, mostly alcohols and aldehydes. Additionally three different pyrazines were also detected in the gas phase. 2,3,4-trimethyl-5-propyl- pyrazine had to be identified within a process of elimination, because of limiting spectra in the NIST08 database. Although it is known that *Paenibacillus polymyxa* can produce different pyrazines (Beck et al., 2003), we could show that just a small fraction is detectable in the gas phase. This results either from concentrations below the detection limit of the developed headspace SPME method or from higher molecular weights due to long side chains. The availability of these three pyrazines indicated a possible specific antagonistic potential. Two different approaches were used to compare the pyrazine production by different *Paenibacillus* isolates. Relative pyrazine abundances were divided by the metabolic rate, expressed by the carbon dioxide concentration. This resulted in normalized values which are not growth dependent. In the other approach a calibration curve was used to determine pyrazine concentrations per cm² growth media. The results did not correlate completely although we could show that isolates from Sekem/Egypt produced higher pyrazine amounts in both cases. More interestingly we demonstrated that various pathogens induce an increase of pyrazine production. This can be interpreted as a responding ability of different *Paenibacillus* species to different signals from the environment.

4.4 Antimicrobial effects of synthetic pyrazines

The antimicrobial effect of two different synthetic pyrazines was demonstrated with VOCs high-throughput assays. VOCs resulting from fluid pyrazines applied in different concentrations inhibited the growth of two different Gram-negative bacteria and one fungal species with varying severity. The mechanism is unknown although we demonstrated that higher concentrations are more effective. Inhibition of *S. maltophilia* was equal with both pyrazines, while 5-sec-butyl-2,3-dimethylpyrazine had a higher impact on *K. pneumoniae*. Interestingly only 5-isobutyl-2,3-dimethylpyrazine inhibited the growth of *C. albicans*. The results indicate that isomeric pyrazine derivatives express varying antimicrobial efficacy. *Paenibacillus* species may harbor even more effective pyrazine metabolites which need to be identified.

4.5 High efficiency *Pseudomonas chlororaphis* P28 mutation

An additional strategy was developed to identify antimicrobial VOCs from *Pseudomonas chlororaphis* strains. Gene-knockout mutants which are deficient in production of antimicrobial VOCs can be compared with wild type strains. Furthermore a process of elimination could be useful to determine which certain VOCs are most efficient. Several plates with mutants of *Pseudomonas chlororaphis* P28 were prepared, although utilization was not necessary since the GC-MS headspace SPME method allowed identification of all occurring VOCs.

5 Conclusions

Two different plant-associated bacterial genera with antagonistic properties were successfully investigated regarding their VOCs production. Various volatile substances were identified in both cases, with either specific or unspecific antibacterial and antifungal properties. *Pseudomonas chlororaphis* and different *Paenibacillus* species are interesting candidates for novel approaches in clean room management. Their utilization should be further investigated regarding application of whole-cell systems. Encapsulated bacteria or bacterial spores could be introduced in model clean rooms coupled with a time-dependent monitoring and a final evaluation of the efficacy. Furthermore a group of synthetic pyrazines expressing antibacterial and antifungal properties was found. However their applicability in large-scale utilization needs to be evaluated in further experiments. Application of these substances in clean room environments would require additional investigations to ensure their harmlessness toward personnel in such areas.

6 References

Adams TB, Doull J, Feron VJ, Goodman JI, Marnett LJ, Munro IC, Newberne PM, Portoghese PS, Smith RL, Waddell WJ, Wagner BM (2003), *The FEMA GRAS assessment of pyrazine derivatives used as flavor ingredients*, *Food and Chemical Toxicology*, Volume 40, Issue 4, 429–451

Anand R, Hegde SG, Rao BS, Gopinath CS (2002), *Catalytic Synthesis of 2-Methyl Pyrazine Over Zn-Modified Zeolites*, *Catalysis Letters*, Volume 84, Numbers 3-4, 265-272, DOI: 10.1023/A:1021400624969

Barbosa TM and Levy SB (2000), *The impact of antibiotic use on resistance development and persistence*, *Drug Resistance Updates* 3, 303–311, DOI: 10.1054/drup.2000.0167

Beck HC, Hansen AM and Lauritsen FR (2003), *Novel pyrazine metabolites found in polymyxin biosynthesis by Paenibacillus polymyxa*, *FEMS Microbiology Letters*, Volume 220, Issue 1, 67–73

Berg G (2009), *Plant–microbe interactions promoting plant growth and health: perspectives for controlled use of microorganisms in agriculture*, *Applied Microbiology and Biotechnology*, Volume 84, Number 1, 11-18, DOI: 10.1007/s00253-009-2092-7

Berg G, Eberl L and Hartmann A (2005), *The rhizosphere as a reservoir for opportunistic human pathogenic bacteria*, *Environmental Microbiology* Volume 7, Issue 11, 1673–1685, DOI: 10.1111/j.1462-2920.2005.00891.x

Berg G, Roskot N and Smalla K (1999), *Genotypic and Phenotypic Relationships between Clinical and Environmental Isolates of Stenotrophomonas maltophilia*, *Journal of Clinical Microbiology*, Volume 37, no. 11, 3594-3600

Boswell TC and Fox PC (2006), *Reduction in MRSA environmental contamination with a portable HEPA-filtration unit*, *Journal of Hospital Infection*, Volume 63, Issue 1, 47–54

Brencic A and Winans SC (2005), *Detection of and Response to Signals Involved in Host-Microbe Interactions by Plant-Associated Bacteria*, *Microbiology and Molecular Biology Reviews*, Volume 69, no. 1, 155-194, DOI: 10.1128/MMBR.69.1.155-194.2005

Burdock GA and Carabin IG (2008), *Safety assessment of 2-ethyl-3,(5 or 6) dimethylpyrazine as a food ingredient*, *Regulatory Toxicology and Pharmacology*, Volume 50, Issue 3, 303–312

Burwen DR, Banerjee SN and Gaynes RP (1994), *Ceftazidime resistance among selected gram-negative bacilli in the United States*, *Journal of Infectious Disease* 170 (6), 1622-1625, DOI: 10.1093/infdis/170.6.1622

Cardinale M, Puglia AM and Grube M (2006), *Molecular analysis of lichen-associated bacterial communities*, *FEMS Microbiology Ecology*, Volume 57, Issue 3, 484–495, DOI: 10.1111/j.1574-6941.2006.00133.x

Cha C, Gao P, Chen YC, Shaw PD, Farrand SK (1998), *Production of Acyl-Homoserine Lactone Quorum-Sensing Signals by Gram-Negative Plant-Associated Bacteria*, *Molecular Plant-Microbe Interactions*, Volume 11, Number 11, 1119-1129

Cheng TB, Reineccius GA, Bjorklund JA, Leete E (1991), *Biosynthesis of 2-methoxy-3-isopropylpyrazine in Pseudomonas perolens*, *Journal of Agricultural and Food Chemistry*, 39 (5), 1009–1012, DOI: 10.1021/jf00005a042

Chin-A-Woeng TFC, Bloemberg GV, Van der Bij AJ, Van der Drift KMGM, Schripsema J, Kroon B, Scheffer RJ, Keel C, Bakker PAHM, Tichy HV, De Bruijn FJ, Thomas-Oates JE, Lugtenberg BJJ (1998), *Biocontrol by Phenazine-1-carboxamide-Producing Pseudomonas chlororaphis PCL1391 of Tomato Root Rot Caused by Fusarium oxysporum f. sp. radicle-lycopersici*, *Molecular Plant-Microbe Interactions*, Volume 11, Number 11, 1069-1077

Christensen GD, Bisno AL, Parisi JT, McLaughlin B, Hester MG, Luther RW (1982), *Nosocomial Septicemia due to Multiply Antibiotic-Resistant Staphylococcus epidermidis*, *Annals of internal medicine*, Volume 96, 1-10

Costacurta A and Vanderleyden J (1995), *Synthesis of Phytohormones by Plant-Associated Bacteria*, *Critical Reviews in Microbiology*, Volume 21, no. 1, 1-18, DOI:10.3109/10408419509113531

Cross JH, Byler RC, Ravid U, Silverstein RM, Robinson SW, Baker PM, Oliveira JS, Jutsum AR, Cherrett JM (1979), *The major component of the trail pheromone of the leaf-cutting ant, *Atta sexdens rubropilosa* forel*, *Journal of Chemical Ecology*, Volume 5, Number 2, 187-203, DOI: 10.1007/BF00988234

Danhorn T and Fuqua C (2007), *Biofilm Formation by Plant-Associated Bacteria*, *Annual Review of Microbiology*, Volume 61, 401-422, DOI: 10.1146/annurev.micro.61.080706.093316

Demain AL, Jackson M and Trenner NR (1967), *Thiamine-dependent Accumulation of Tetramethylpyrazine Accompanying a Mutation in the Isoleucine-Valine Pathway*, *Journal of Bacteriology*, Volume 94, no. 2, 323-326

Dharan S and Pittet D (2002), *Environmental controls in operating theatres*, *Journal of Hospital Infection*, Volume 51, Issue 2, 79–84

Dickschat JS, Wickel S, Bolten CJ, Nawrath T, Schulz S, Wittmann C (2010), *Pyrazine Biosynthesis in *Corynebacterium glutamicum**, *European Journal of Organic Chemistry*, Volume 2010, Issue 14, 2687–2695, DOI: 10.1002/ejoc.201000155

Dilantha Fernando WG, Ramarathnam R, Krishnamoorthy AS, Savchuk SC (2005), *Identification and use of potential bacterial organic antifungal volatiles in biocontrol*, *Soil Biology & Biochemistry* 37, 955–964

Dossey AT, Gottardo M, Whitaker JM, Roush WR, and Edison AS (2009), *Alkyldimethylpyrazines in the Defensive Spray of *Phyllium westwoodii*: A First for Order Phasmatodea*, *Journal of Chemical Ecology*, Volume 35, Number 8, 861-870, DOI: 10.1007/s10886-009-9666-9

Emmert EAB and Handelsman J (1999), *Biocontrol of plant disease: a (Gram-) positive perspective*, *FEMS Microbiology Letters*, Volume 171, Issue 1, 1–9, DOI: 10.1111/j.1574-6968.1999.tb13405.x

Fürnkranz M, Lukesch B, Müller H, Huss H, Grube M, Berg G (2011), *Microbial Diversity Inside Pumpkins: Microhabitat-Specific Communities Display a High Antagonistic Potential Against Phytopathogens*, *Microbial Ecology* Volume 63, Number 2, 418-428, DOI: 10.1007/s00248-011-9942-4

Golfinopoulos SK, Lekkas TD and Nikolaou AD (2001), *Comparison of methods for determination of volatile organic compounds in drinking water*, *Chemosphere*, Volume 45, Issue 3, 275–284

Götz F (2002), *Staphylococcus and biofilms*, *Molecular Microbiology*, Volume 43, Issue 6, 1367–1378, DOI: 10.1046/j.1365-2958.2002.02827.x

Haas D and Keel C (2003), *Regulation of Antibiotic Production in Root-Colonizing Pseudomonas Spp. and Relevance for Biological Control of Plant Disease*, *Annual Review of Phytopathology*, Volume 41, 117-153, DOI: 10.1146/annurev.phyto.41.052002.095656

Hall-Stoodley L, William Costerton J and Stoodley P (1999), *Bacterial biofilms: from the Natural environment to infectious diseases*, *Nature Reviews Microbiology* 2, 95-108, DOI: 10.1038/nrmicro821

Hayward AC, Fegan N, Fegan M, Stirling GR (2010), *Stenotrophomonas and Lysobacter*. ubiquitous plant-associated *gamma*-proteobacteria of developing significance in applied microbiology, *Journal of Applied Microbiology* Volume 108, Issue 3, 756–770, DOI: 10.1111/j.1365-2672.2009.04471.x

Ji GH, Wie LF, He YQ, Wu YP, Bai XH (2008), *Biological control of rice bacterial blight by Lysobacter antibioticus strain 13-1*, *Biological Control*, Volume 45, Issue 3, 288–296

Jochum CC, Osborne LE and Yuen GY (2006), *Fusarium head blight biological control with Lysobacter enzymogenes strain C3*, *Biological Control*, Volume 39, Issue 3, 336–344

Johnsson L, Hökeberg M and Gerhardson B (1998), *Performance of the Pseudomonas chlororaphis biocontrol agent MA 342 against cereal seed-borne diseases in field experiments*, *European Journal of Plant Pathology*, Volume 104, Number 7, 701-711, DOI: 10.1023/A:1008632102747

Kai M, Effmert U, Berg G, Piechulla B (2006), *Volatiles of bacterial antagonists inhibit mycelial growth of the plant pathogen Rhizoctonia solani*, Archives of Microbiology, Volume 187, Number 5, 351-360, DOI: 10.1007/s00203-006-0199-0

Köberl M, Müller H, Ramadan EM, Berg G (2011), *Desert Farming Benefits from Microbial Potential in Arid Soils and Promotes Diversity and Plant Health*, Plos One, Volume 6, Issue 9, e24452

La Duc MT, Dekas A, Osman S, Moissi C, Newcombe D and Venkateswaran K (2007), *Isolation and Characterization of Bacteria Capable of Tolerating the Extreme Conditions of Clean Room Environments*, Applied Environmental Microbiology, Volume 73, no. 8, 2600-2611

Larsen TO and Frisvad JC (1995), *Comparison of different methods for collection of volatile chemical markers from fungi*, Journal of Microbiological Methods, Volume 24, Issue 2, 135-144

Lemar KM, Muller CT, Plummer S, Lloyd D (2003), *Cell Death Mechanisms in the Human Opportunistic Pathogen Candida albicans*, The Journal of Eukaryotic Microbiology, Volume 50, Issue Supplement s1, 685-686, DOI: 10.1111/j.1550-7408.2003.tb00687.x

Liebminger S, Aichner M, Oberauner L, Fürnkranz M, Cardinale M, Berg G (2011), *A new textile-based approach to assess the antimicrobial activity of volatiles*, Textile Research Journal, Volume 82, no. 5, 484-491, DOI: 10.1177/0040517511429607

Liu WW, Mu W, Zhu BY, Du YC, Liu F (2008), *Antagonistic Activities of Volatiles from Four Strains of Bacillus spp. and Paenibacillus spp. Against Soil-Borne Plant Pathogens*, Agricultural Sciences in China, Volume 7, Issue 9, 1104-1114

MacArthur RD, Miller M, Albertson T, Panacek E, Johnson D, Teoh L, Barchuk W (2003), *Adequacy of Early Empiric Antibiotic Treatment and Survival in Severe Sepsis: Experience from the MONARCS Trial*, Clinical Infectious Diseases, Volume 38, Issue 2, 284-288

Mageshwaran V, Walia S and Annapurna K (2010), *Isolation and partial characterization of antibacterial lipopeptide produced by Paenibacillus polymyxa HKA-15 against phytopathogen Xanthomonas campestris pv. phaseoli M-5*, World Journal of Microbiology and Biotechnology, Volume 28, Number 3, 909-917, DOI: 10.1007/s11274-011-0888-y

Masuda H and Mihara S (1986), *Synthesis of alkoxy-, (alkylthio)-, phenoxy-, and (phenylthio)pyrazines and their olfactive properties*, Journal of Agricultural and Food Chemistry, 34 (2), 377–381, DOI: 10.1021/jf00068a057

Murray KE, Shipton J and Whitfield FB (1970), *2-methoxypyrazines and the flavour of green peas (Pisum sativum)*, Chemistry & Industry, Volume 27, 897-898

Naghmouchi K, Paterson L, Forster B, McAllister T, Ohene-Adjei S, Drider D, Teather, Baah J (2011), *Paenibacillus polymyxa JB05-01-1 and its perspectives for food conservation and medical applications*, Archives of Microbiology, Volume 193, Number 3, 169-177, DOI: 10.1007/s00203-010-0654-9

Niu B, Rueckert C, Blom J, Wang Q, Borriss R (2011), *The genome of the plant growth-promoting rhizobacterium Paenibacillus polymyxa M-1 contains nine sites dedicated to nonribosomal synthesis of lipopeptides and polyketides*, Journal of Bacteriology, 193(20), 5862-3

Oliveira DC, Tomasz A and De Lencastre H (2002), *Secrets of success of a human pathogen: molecular evolution of pandemic clones of methicillin-resistant Staphylococcus aureus*, Lancet Infectious Diseases 2002; 2, 180–89

Pawley JB (2006), *Handbook of Biological Confocal Microscopy*, ISBN-13: 978-0387259215

Percival SL, Bowler PG and Russell D (2005), *Bacterial resistance to silver in wound care*, Journal of Hospital Infection, Volume 60, Issue 1, 1–7

Pierson III LS, Wood DW and Pierson EA (1998), *Homoserine Lactone-Mediated Gene Regulation in Plant-Associated Bacteria*, Annual Review of Phytopathology, Volume 36, 207-225, DOI: 10.1146/annurev.phyto.36.1.207

Postma J, Stevens LH, Wieggers GL, Davelaar E, Nijhuis EH (2009), *Biological control of Pythium aphanidermatum in cucumber with a combined application of Lysobacter enzymogenes strain 3.1T8 and chitosan*, *Biological Control*, Volume 48, Issue 3, 301–309

Quinn JP (1998), *Clinical Problems Posed by Multiresistant Nonfermenting Gram-Negative Pathogens*, *Clinical Infectious Diseases* 27, Supplement 1, 117–124, DOI: 10.1086/514912

Radovic BS, Careri M, Mangia A, Musci M, Gerboles M, Anklam E (2001), *Contribution of dynamic headspace GC-MS analysis of aroma compounds to authenticity testing of honey*, *Food Chemistry* 72, 511-520

Raio A, Puopolo G, Cimmino A, Danti R, Della Rocca G, Evidente A (2011), *Biocontrol of cypress canker by the phenazine producer Pseudomonas chlororaphis subsp. aureofaciens strain M71*, *Biological Control*, Volume 58, Issue 2, 133–138

Rogul M and Brendle JJ (1974), *A Metabolic Inquiry into the Iridescent Lysis of Agar Lawns of Pseudomonas aeruginosa Strain 227*, *The Journal of Infectious Diseases* 130 (Supplement), S103-S109 DOI: 10.1093/infdis/130.Supplement.S103

Rosenthal VD, Maki DG, Jamulitrat S, Medeiros EA, Todi SK, Gomez DY, Leblebicioglu H, Khader IA, Novales MGM María, Berba R, Wong FMR, Barkat A, Pino OR, Dueñas L, Mitrev Z, Bijie H, Gurskis V, Kanj SS, Mapp T, Hidalgo RF, Jaballah NB, Raka L, Gikas A, Ahmed A, Thu LTA, Guzmán Siritt ME, INICC Members (2009), *International Nosocomial Infection Control Consortium (INICC) report, data summary for 2003-2008, issued June 2009*, *American Journal of Infection Control*, Volume 38, Issue 2, 95–104

Schulz S and Dickschat JS (2007), *Bacterial volatiles: the smell of small organisms*, *Natural Product Reports*, Volume 24, Issue 4, 814-842, DOI: 10.1039/B507392H

Seldin L, Silva De Azevedo F, Alviano DS, Alviano CS, De Freire Bastos MC (1999), *Inhibitory activity of Paenibacillus polymyxa SCE2 against human pathogenic micro-organisms*, *Letters in Applied Microbiology*, Volume 28, Issue 6, 423–427

Sirota-Madi A, Olender T, Helman Y, Ingham C, Brainis I, Roth D, Hagi E, Brodsky L, Leshkowitz D, Galatenko V, Nikolaev V, Mugasimangalam RC, Bransburg-Zabary S, Gutnick DL, Lancet D, Ben-Jacob E (2010), *Genome sequence of the pattern forming Paenibacillus vortex bacterium reveals potential for thriving in complex environments*, BMC Genomics, 11:710 DOI:10.1186/1471-2164-11-710

Tombolini R, Van der Gaag DJ, Gerhardson B, Jansson JK (1999), *Colonization Pattern of the Biocontrol Strain Pseudomonas chlororaphis MA 342 on Barley Seeds Visualized by Using Green Fluorescent Protein*, Applied and Environmental Microbiology, Volume 65, no. 8, 3674-3680

Verginer M, Leitner E and Berg G (2010), *Production of Volatile Metabolites by Grape-Associated Microorganisms*, Journal of Agricultural and Food Chemistry, 58 (14), 8344–8350, DOI: 10.1021/jf100393w

Weller DM (2007), *Pseudomonas biocontrol agents of soilborne pathogens: Looking back over 30 years*, Phytopathology 97, 250-256.

Wheatley RE (2002), *The consequences of volatile organic compound mediated bacterial and fungal interactions*, Antonie Van Leeuwenhoek, Volume 81, Numbers 1-4, 357-364, DOI: 10.1023/A:1020592802234

Yeşilel OZ, Mutlu A, Darcan C, Büyükgüngör O (2010), *Syntheses, structural characterization and antimicrobial activities of novel cobalt-pyrazine-2,3-dicarboxylate complexes with N-donor ligands*, Journal of Molecular Structure, Volume 964, Issues 1–3, 39–46

Zhang Z and Pawliszyn J (1993), *Analysis of Organic Compounds in Environmental Samples by Headspace Solid Phase Microextraction*, Journal of High Resolution Chromatography, Volume 16, Issue 12, 689–692

Zhang Z, Wie T, Hou J, Li G, Yu S, Xin W (2003), *Tetramethylpyrazine scavenges superoxide anion and decreases nitric oxide production in human polymorphonuclear leukocytes*, Life Sciences, Volume 72, Issue 22, 2465–2472

Zhao LJ, Yang XN, Li XY, Mu W, Liu F (2011), *Antifungal, Insecticidal and Herbicidal Properties of Volatile Components from Paenibacillus polymyxa Strain BMP-11*, Agricultural Sciences in China, Volume 10, Issue 5, 728–736

7 List of abbreviations

°C	degree centigrade
cfu	colony forming unit
CLSM	confocal laser scanning microscopy
cm	centimeter
ddH ₂ O	double distilled water
e.g.	exempli gratia
et al.	et alteri
Fig.	figure
h	hour
H ₂ O	water
KCl	potassium chloride
KH ₂ PO ₄	potassium dihydrogen phosphate
L	liter
LB	lysogeny broth
μ	micro
m	milli
M	molar
MgCl ₂	magnesium chloride
MgSO ₄	magnesium sulfate
min	minute
MRSA	methicillin-resistant <i>Staphylococcus aureus</i>
n	nano
Na ₂ HPO ₄	disodium hydrogen phosphate
NaCl	sodium chloride
ONC	overnight culture
PBS	phosphate-buffered saline
PCR	polymerase chain reaction
%	percentage
pH	pondus hydrogenii
rpm	rounds per minute
SSCP	single-strand conformation polymorphism

Tab.	table
TSB	tryptic soy broth
TY	trypton yeast
UV	ultraviolet
VOCs	volatile organic compounds

8 List of figures

Figure 1.1 – Pyrazine compounds always contain a heterocyclic aromatic ring as main building block. The four carbon atoms can be substituted with a great variety of side chains. Source: www.sigmaaldrich.com.....	6
Figure 2.1 – The molecular structure of 2,3-dimethyl-5-(1-methylpropyl)-pyrazine is shown. One common synonym used for this structure is 5-sec-butyl-2,3-dimethylpyrazine. Source: www.sigmaaldrich.com.....	12
Figure 2.2 – The molecular structure of 2,3-dimethyl-5-(2-methylpropyl)-pyrazine is shown. One common synonym used for this structure is 5-isobutyl-2,3-dimethylpyrazine. Source: www.sigmaaldrich.com.....	12
Figure 2.3 - Specifications of the used ION-NOSTAT VI.2 textile are shown above.....	14
Figure 2.4 – Visual analysis of all pathogen inoculated textiles was performed with an adapted evaluation scale. The effects have been classified in strong inhibition, significant inhibition and negligible inhibition like shown above.....	16
Figure 2.5 - The particular steps of the VOCs assay assembly are shown together with important components. A perforated silicone foil serves as seal between nearby wells and therefore only allows VOCs exchange between joining wells. Ordinary clamps were utilized to hold two multi-well plates together.	21
Figure 2.6 – The diagram shows the adjusted temperature gradient in the GC oven. Additionally the carrier gas (Helium) flow is shown, which remains constant while the pressure rises conditioned by the temperature changes.	22
Figure 2.7 – The assembly of the GC-MS co-cultivation experiment allows VOCs detection from antagonists that were sharing the same gas phase with particular pathogens. It is important to avoid contamination of the solid media (15% LB-agar) with the applied pathogen.	23
Figure 3.1 – CLSM pictures of two different fabrics stained with LIVE/DEAD® Bacterial Viability Kit. The samples were not inoculated with bacteria. White ION-NOSTAT VI.2 fabrics showed better applicability for VOCs dual-culture tests. The differences in the SYTO® 9 channel were negligible while the blue textile showed a high unspecific signal in the propidium iodide channel.	27
Figure 3.2 – CLSM pictures of <i>C. albicans</i> negative control and VOCs dual-culture test with antagonist after 44-48 h co-incubation. BacLight™ staining allows visualization of living cells (green) and dead cells (red). A decrease in growth of <i>C. albicans</i> and increase of dead cells can be observed after incubation with <i>Paenibacillus polymyxa</i> GnDWu39.....	28

Figure 3.3 – CLSM pictures of <i>C. albicans</i> negative control and VOCs dual-culture test with antagonist after 44-48 h co-incubation. BacLight™ staining allows visualization of living cells (green) and dead cells (red). The growth inhibiting effect of <i>Lysobacter</i> sp. MWu228 on <i>C. albicans</i> was negligible expressed by the number of dead cells.....	28
Figure 3.4 – CLSM pictures of <i>C. albicans</i> negative control and VOCs dual-culture test with antagonist after 44-48 h co-incubation. BacLight™ staining allows visualization of living cells (green) and dead cells (red). <i>Pseudomonas chlororaphis</i> OeWuP28 reduced the growth of <i>C. albicans</i> and led to a high number of dead cells simultaneously.	29
Figure 3.5 – CLSM pictures of <i>P. aeruginosa</i> negative control and VOCs dual-culture test with antagonist after 44-48 h co-incubation. BacLight™ staining allows visualization of living cells (green) and dead cells (red). The growth of <i>P. aeruginosa</i> was not affected by <i>Paenibacillus polymyxa</i> GnDWU39 and there was no difference in the amount of dead cells compared to the negative control.	30
Figure 3.6 – CLSM pictures of <i>P. aeruginosa</i> negative control and VOCs dual-culture test with antagonist after 44-48 h co-incubation. BacLight™ staining allows visualization of living cells (green) and dead cells (red). <i>Lysobacter</i> sp. MWu227 did not show a reduction of viable pathogens and a low number of dead <i>P. aeruginosa</i> cells.	30
Figure 3.7 – CLSM pictures of <i>P. aeruginosa</i> negative control and VOCs dual-culture test with antagonist after 44-48 h co-incubation. BacLight™ staining allows visualization of living cells (green) and dead cells (red). <i>Pseudomonas chlororaphis</i> OeWuP28 showed a decrease of viable <i>P. aeruginosa</i> cells together with a high amount of dead cells in the propidium iodide channel.	31
Figure 3.8 – CLSM pictures of <i>S. aureus</i> negative control and VOCs dual-culture test with antagonist after 44-48 h co-incubation. BacLight™ staining allows visualization of living cells (green) and dead cells (red). A growth inhibiting effect of <i>Paenibacillus polymyxa</i> GnDWu39 on <i>S. aureus</i> was not given. Therefore no dead cells could be detected after incubation.	32
Figure 3.9 – CLSM pictures of <i>S. aureus</i> negative control and VOCs dual-culture test with antagonist after 44-48 h co-incubation. BacLight™ staining allows visualization of living cells (green) and dead cells (red). <i>S. aureus</i> could not be inhibited after incubation with <i>Lysobacter</i> sp. MWu228 in the dual-culture test.....	32
Figure 3.10 – CLSM pictures of <i>S. aureus</i> negative control and VOCs dual-culture test with antagonist after 44-48 h co-incubation. BacLight™ staining allows visualization of living cells (green) and dead cells (red). The growth of <i>S. aureus</i> was reduced by <i>Pseudomonas chlororaphis</i> OeWuP28 expressed by an increase of dead pathogens.....	33
Figure 3.11 – CLSM pictures of <i>S. epidermidis</i> negative control and VOCs dual-culture test with antagonist after 44-48 h co-incubation. BacLight™ staining allows visualization of living cells	

(green) and dead cells (red). <i>S. epidermidis</i> was not affected by <i>Paenibacillus polymyxa</i> GnDWu39, no growth inhibiting effect could be observed after the incubation.....	34
Figure 3.12 – CLSM pictures of <i>S. epidermidis</i> negative control and VOCs dual-culture test with antagonist after 44-48 h co-incubation. BacLight™ staining allows visualization of living cells (green) and dead cells (red). <i>Lysobacter</i> sp. Mwu228 did not affect the growth of <i>S. epidermidis</i> expressed by the number of dead cells.	34
Figure 3.13 – CLSM pictures of <i>S. epidermidis</i> negative control and VOCs dual-culture test with antagonist after 44-48 h co-incubation. BacLight™ staining allows visualization of living cells (green) and dead cells (red). A growth inhibiting effect of <i>Pseudomonas chlororaphis</i> OEWuP28 on <i>S. epidermidis</i> was not detectable after incubation in the dual-culture test.	35
Figure 3.14 – CLSM pictures of <i>S. maltophilia</i> negative control and VOCs dual-culture test with antagonist after 44-48 h co-incubation. BacLight™ staining allows visualization of living cells (green) and dead cells (red). <i>S. maltophilia</i> was significantly inhibited by <i>Paenibacillus polymyxa</i> GnDWu39. The pathogen growth was decreased while the number of dead cells increased.	36
Figure 3.15 – CLSM pictures of <i>S. maltophilia</i> negative control and VOCs dual-culture test with antagonist after 44-48 h co-incubation. BacLight™ staining allows visualization of living cells (green) and dead cells (red). <i>Lysobacter</i> sp. MWu228 reduced the growth of <i>S. maltophilia</i> significantly, but an increase of dead pathogens could not be observed.	36
Figure 3.16 – CLSM pictures of <i>S. maltophilia</i> negative control and VOCs dual-culture test with antagonist after 44-48 h co-incubation. BacLight™ staining allows visualization of living cells (green) and dead cells (red). The growth of <i>S. maltophilia</i> was reduced by <i>Pseudomonas chlororaphis</i> OeWuP28, while a gain of dead cells was not observed.	37
Figure 3.17 – CLSM pictures of negative controls 13 h, 17 h and 21 h after incubation of <i>S. aureus</i> on ION-NOSTAT VI.2 textile without antagonist. BacLight™ staining allows visualization of living cells (green) and dead cells (red). Constant bacterial growth was observed on the textile surface during the whole experiment.	38
Figure 3.18 – CLSM pictures of <i>S. aureus</i> co-incubated on ION-NOSTAT VI.2 textile with <i>Paenibacillus polymyxa</i> GnDWu39. Samples were taken after 13 h, 17 h and 21 h incubation. BacLight™ staining allows visualization of living cells (green) and dead cells (red). The growth process was not significantly hindered and an occurrence of dead cells could not be observed during the whole experiment.	39
Figure 3.19 – CLSM pictures of <i>S. aureus</i> co-incubated on ION-NOSTAT VI.2 textile with <i>Pseudomonas chlororaphis</i> OeWuP28. Samples were taken after 13 h, 17 h and 21 h incubation. BacLight™ staining allows visualization of living cells (green) and dead cells (red). A growth	

deficiency was observed at early growth stages and the first dead cells appeared after 21 h incubation.	40
Figure 3.20 – Treatment of <i>S. aureus</i> with <i>Pseudomonas chlororaphis</i> OeWuP34 resulted in clear spots (C), while the negative controls became milky and nontransparent (M).	41
Figure 3.21 – All <i>Pseudomonas chlororaphis</i> strains inhibited the growth of <i>S. aureus</i> in the standard VOCs high-throughput assay. Different letters represent significant differences between respective mean values (ANOVA, Tukey-HSD, $P \leq 0.05$).	42
Figure 3.22 – The modified VOCs high-throughput assay confirmed the strong inhibition by <i>Pseudomonas chlororaphis</i> strains despite the modifications in growth conditions. Different letters represent significant differences between respective mean values (ANOVA, Tukey-HSD, $P \leq 0.05$).	42
Figure 3.23 – <i>Pseudomonas chlororaphis</i> OeWuP28 and <i>Pseudomonas chlororaphis</i> OeWu259 did not affect the growth of <i>S. epidermidis</i> , though it was significantly decreased by <i>Pseudomonas chlororaphis</i> OeWuP34. Different letters represent significant differences between respective mean values (ANOVA, Tukey-HSD, $P \leq 0.05$).	43
Figure 3. 24 – All <i>Pseudomonas chlororaphis</i> strains inhibited the growth of <i>S. maltophilia</i> significantly. Different letters represent significant differences between respective mean values (ANOVA, Tukey-HSD, $P \leq 0.05$).	43
Figure 3.25 – <i>Pseudomonas chlororaphis</i> OeWuP34 didn't affect the growth of <i>K. pneumoniae</i> , though it was significantly decreased by <i>Pseudomonas chlororaphis</i> OeWuP28 and <i>Pseudomonas chlororaphis</i> OeWu259. Different letters represent significant differences between respective mean values (ANOVA, Tukey-HSD, $P \leq 0.05$).	44
Figure 3.26 – <i>C. albicans</i> was inhibited by all <i>Pseudomonas chlororaphis</i> strains. The strongest inhibition could be observed with <i>Pseudomonas chlororaphis</i> OeWuP28. Different letters represent significant differences between respective mean values (ANOVA, Tukey-HSD, $P \leq 0.05$).	44
Figure 3.27 – <i>S. aureus</i> showed a thoroughly high viability after incubation in the VOCs assay with different <i>Paenibacillus polymyxa</i> strains. Error bars indicate the standard deviation of respective mean values.	45
Figure 3.28 – The modified approach with media limitations confirmed the increased viability of <i>S. aureus</i> after incubation with different <i>Paenibacillus polymyxa</i> strains. Error bars indicate the standard deviation of respective mean values.	45
Figure 3.29 – None of the tested <i>Paenibacillus polymyxa</i> strains could inhibit the growth of <i>S. epidermidis</i> significantly in the VOCs assay. Error bars indicate the standard deviation of respective mean values.	46

Figure 3.30 – All <i>Paenibacillus polymyxa</i> strains reduced the growth of <i>S. maltophilia</i> . The highest reduction was observed after incubation with <i>Paenibacillus polymyxa</i> MWu33/2 and <i>Paenibacillus polymyxa</i> GnDWu39. Different letters represent significant differences between respective mean values (ANOVA, Tukey-HSD, $P \leq 0.05$).....	46
Figure 3.31 – The pathogen viability was not reduced by any of the tested <i>Paenibacillus polymyxa</i> strains in this approach. Error bars indicate the standard deviation of respective mean values. ..	47
Figure 3.32 - <i>Paenibacillus polymyxa</i> PB71 and <i>Paenibacillus polymyxa</i> GnDWu39 resulted in a significantly lower viability of <i>C. albicans</i> compared to the negative control. A T-test was used to determine the significance with $*P=0.037$ and $(*)P=0.016$	47
Figure 3.33 – <i>S. aureus</i> was not affected by 5-sec-butyl-2,3-dimethylpyrazine compared to the negative control. Even undiluted pyrazine (28 nM) did not decrease the pathogen viability. Error bars indicate the standard deviation of respective mean values.	48
Figure 3.34 – The viability of <i>S. epidermidis</i> remained unaltered after exposure to different 5-sec-butyl-2,3-dimethylpyrazine dilutions. Error bars indicate the standard deviation of respective mean values.	48
Figure 3.35 - The viability test demonstrated the antimicrobial effect of 5-sec-butyl-2,3-dimethylpyrazine on <i>S. maltophilia</i> . 28 nM pyrazine (left well) reduces bacterial viability drastically, while 0.28 nM pyrazine (right well) shows less effect on it. The negative control (second well from left) shows the highest bacterial growth indicated by intense clouding of the media.....	49
Figure 3.36 – All applied pyrazine concentrations reduced the viability of <i>S. maltophilia</i> . Low concentrations showed still a high impact on cell growth. Different letters represent significant differences between respective mean values (ANOVA, Tukey-HSD, $P \leq 0.05$).....	49
Figure 3.37 – The lowest pyrazine concentration that inhibited <i>S. maltophilia</i> growth significantly compared to the negative control was 0.028 nM. A T-test was used to determine the significance with $*P=0.023$ and $(*)P=0.053$	49
Figure 3.38 – Inhibition of <i>K. pneumoniae</i> was observed with 28 nM and 2.8 nM 5-sec-butyl-2,3-dimethylpyrazine. Different letters represent significant differences between respective mean values (ANOVA, Tukey-HSD, $P \leq 0.05$).....	50
Figure 3.39 – The viability of <i>C. albicans</i> was not decreased by 5-sec-butyl-2,3-dimethylpyrazine in the VOCs assay. Error bars indicate the standard deviation of respective mean values.....	50
Figure 3.40 – The growth of <i>S. maltophilia</i> was significantly decreased after incubation with 5-isobutyl-2,3-dimethylpyrazine. Different letters represent significant differences between respective mean values (ANOVA, Tukey-HSD, $P \leq 0.05$).....	51

Figure 3.41 – Undiluted 5-isobutyl-2,3-dimethylpyrazine inhibited the growth of *K. pneumoniae* significantly, while 2.8 nM and 0.28 nM concentrations did not affect the living-cell concentration compared to the negative control. A T-test was used to determine the significance with *P=0.028. 52

Figure 3.42 – *C. albicans* was inhibited by 28 nM pyrazine significantly, while higher dilutions did not decrease bacterial growth. A T-test was used to determine the significance with *P=0.046. . 52

Figure 3.43 – The *Paenibacillus polymyxa* GndWu39 VOCs profile was achieved with a 50/30 µm Divinylbenzen/Carboxen™/Polydimethylsiloxane (PDMS) 2 cm Stableflex/SS SPME headspace fiber and a 1:20 split injection..... 54

Figure 3.44 – An improved *Paenibacillus polymyxa* GndWu39 VOCs profile was achieved with an 85 µm Carboxen™/Polydimethylsiloxane (PDMS) 1 cm Stableflex/SS SPME headspace fiber and a 1:20 split injection..... 54

Figure 3.45 – The highest performance was achieved with a 50/30 µm Divinylbenzen/Carboxen™/Polydimethylsiloxane (PDMS) 1 cm Stableflex/SS SPME headspace fiber and a splitless injection..... 55

Figure 3.46 – VOCs from tempered LB-agar result in a specific chromatogram. 55

Figure 3.47 – Profiles of *Pseudomonas chlororaphis* strains contain a specific 1-undecene peak at RT 13.2 min..... 57

Figure 3.48 – A typical *Paenibacillus polymyxa* profile recorded with strain PB71. Three detected pyrazine peaks are indicated with arrows. 58

Figure 3.49 – 5-isobutyl-2,3-dimethylpyrazine addition to *Paenibacillus polymyxa* GndWu39 did not result in an overlay of the relating peaks. Two distinct pyrazine peaks are indicated with arrows. The peaks do not derive from the same substance..... 59

Figure 3.50 - *Paenibacillus polymyxa* GndWu39 together with 0.5 µL of synthetic 5-sec-butyl-2,3-dimethylpyrazine resulted in two distinct peaks. The indicated peaks did not derive from the same substance..... 59

Figure 3.51 – *Paenibacillus* species were sorted regarding to their relative pyrazine production. The highest amounts were produced by a *Paenibacillus kribbensis* strain. 61

Figure 3.52 – A calibration curve was constructed with mean values of 3 different data sets. The data points were log-transformed for a better display. 62

Figure 3.53 – An increase of 2,3,4-trimethyl-5-propyl-pyrazine production was observed after pathogen exposition in the gas phase of *Paenibacillus polymyxa* GndWu39. The error bars indicate a confidence interval within *P≤0.05..... 64

Figure 3.54 – Several selective LB-agar plates were obtained with a mutant growth density higher than 10³ cfu/mL..... 65

9 List of tables

Table 3.1 – All detectable volatile substances are listed by their specific retention time. Siloxane compounds originate from the GC-column, other compounds like acetone originate from tempered LB-agar.....	56
Table 3.2 – VOCs produced by different <i>Pseudomonas chlororaphis</i> strains are shown. Compounds with a non-bacterial origin are indicated separately.	57
Table 3.3 – A broad range of different VOCs was identified in the gas phase of <i>Paenibacillus polymyxa</i> strains. Compounds with a non-bacterial origin are indicated separately.....	60
Table 3.4 – Different 5-sec-butyl-2,3-dimethylpyrazine dilutions were used to determine the corresponding peak areas.....	62
Table 3.5 – The concentrations were calculated by using the calibration curve created with a 5-sec-butyl-2,3-dimethylpyrazine standard.	63